OVERLAND FLOW UNDER RAINFALL:

SOME ASPECTS RELATED TO MODELLING AND CONDITIONING FACTORS

Promotor: dr. ir. W.H. van der Molen
oud-hoogleraar in de agrohydrologie

Co-promotor: dr. ir. R.W.R. Koopmans
universitair hoofddocent bij de vakgroep Hydrologie,
Bodemnatuurkunde en Hydraulica

J.L.M.P. de Lima

OVERLAND FLOW UNDER RAINFALL:

SOME ASPECTS RELATED TO MODELLING AND CONDITIONING FACTORS

Proefschrift
ter verkrijging van de graad van
doctor in de landbouwwetenschappen,
op gezag van de rector magnificus,
dr. H.C. van der Plas,
in het openbaar te verdedigen
op vrijdag 8 december 1989
des namiddags te vier uur in de aula
van de Landbouwuniversiteit te Wageningen

To Isabel and Rui

STATEMENTS

1. Raindrop splash anisotropy is a factor affecting splash erosion. Slope, wind and overland flow velocity are the factors contributing to that anisotropy.

This thesis, Section 7.4.

2. At the hillslope scale, wind action should be considered in the modelling of overland flow.

This thesis, Sections 7.1 to 7.3.

3. The morphological factors affecting overland flow on slopes are: slope gradient, slope length, slope shape, and slope exposure to prevailing rain-bringing winds.

This thesis, Chapter 6.

4. The processes of overland flow and infiltration occur simultaneously in nature during and after the occurrence of rainfall. What is required in overland flow modelling is a combined study of these two processes.

R.E. Smith and D.A. Woolhiser, Water Resources Research 7 (1971): 899-913.
This thesis, Chapter 5.

5. Depression storage as a result of tillage is of considerable importance in the assessment of water erosion.

This thesis, Chapter 4.

6. Kinematic wave solutions of the overland flow process have been shown to give very accurate results for most hydrologically relevant situations.

D.A. Woolhiser and J.A. Liggett, Water Resources Research 3 (1967): 753-771.
This thesis, Chapter 2, 4, 5 and 7.

7. In contrast with the classical approaches in studies on overland flow, physically-based models are presently being used to model the overland flow process. However, the application of these models to field situations often fails due to specific processes or conditions generally not taken into account.

8. Wind effects on overland flow should be taken into consideration in the design of roads and highways with respect to aquaplane phenomenon.

9. Widespread agreement exists that water erosion has severely impaired land productivity in many parts of the world. Yet, reliable data on the amount of human-induced erosion and its impact on permanent soil productivity is nearly nonexistent. There is a need for standardizing metodologies to increase reliability and accuracy of data on soil erosion.

10. Nomographs have not lost their usefulness in the computer age. As a consequence nomography should still be included in the curriculum of practical courses such as the agricultural and civil engineering.

11. Better scientific and technological cooperation between universities and industry could be achieved by a regular interchange of scientific staff. Further, particular demands for specific profiles of engineers should be contemplated when defining or reviewing the curricula of both technical and university courses.

12. Indiscriminate budget cuts at universities may result in a rapid decline of research potential and quality of those departments that are mainly relying on the public sector.

13. Begin at the beginning, and go on till you come to the end; then stop.

Lewis Carroll, Alice's Adventure in Wonderland (1865).

J.L.M.P. de Lima
Overland flow under rainfall:
some aspects related to modelling and conditioning factors.
Wageningen, 8th December 1989

ABSTRACT

Lima, J.L.M.P. de, 1989. Overland flow under rainfall: some aspects related to modelling and conditioning factors. Doctoral thesis, Agricultural University Wageningen, Wageningen, The Netherlands, (XII) + 160 p., 60 Figures, 8 Photographs and 2 Tables (Summary and Conclusions in English, Portuguese and Dutch).

This study concerns the theory and some practical aspects of overland flow under rainfall. Of the conditioning factors and processes which govern the generation of overland flow, the following were studied: depression storage, infiltration, morphology and wind. Special attention was paid to wind-driven rain and its effect on raindrops, raindrop splash and wind induced shear stress on the water-air boundary in relation to overland flow.

The study was carried out by means of laboratory experiments and mathematical modelling, both numerical and analytical. The laboratory experiments included the use of two rainfall simulators and a wind tunnel. Impermeable surfaces (concrete, plastic, plywood and Perspex) and pervious surfaces (loess from Limburg, the Netherlands, and a clay loam from Alentejo, Portugal) were used. A photographic set-up was also used for the assessment of the factors affecting raindrop splash anisotropy.

In the modelling of the overland flow process, the kinematic wave approach (along with linear and nonlinear assumptions) was used, both for the numerical and analytical solutions. Two numerical models were developed: model KININF for overland flow on an infiltrating surface, and model WROF for overland flow under wind-driven rain. An analytical solution was derived for the rising limb of overland flow over infiltrating surfaces of parabolic shape. The upper boundary conditions used on overland flow studies were also discussed, both with and without wind effects.

Free descriptors: Overland flow; sheet flow; hillslope hydrology; kinematic-wave; finite difference schemes; water erosion; sheet erosion; splash erosion; depression storage; infiltration; rainfall simulation; soil flume; wind action.

The author would like to express his gratitude to Prof. Dr. W.H. van der Molen (Wageningen Agricultural University) for giving him the opportunity to carry out the present studies under his supervision and guidance. He very much appreciated his continued encouragement and his valuable criticism and corrections of the text.

The author expresses his gratitude to Dr. R.W.R. Koopmans and Ir. P.M.M. Warmerdam for the stimulating discussions during the various stages of this work. He further wishes to thank the staff of the Department of Hydrology, Soil Physics and Hydraulics (formerly the Department of Land and Water Use and Department of Hydraulics and Catchment Hydrology) for their kind and continued cooperation.

The present study was carried out while on leave from the University of Coimbra (Portugal) and financially supported by "Comissão Permanente INVOTAN" of Portugal. Both are gratefully acknowledged. The author wants also to express his gratitude to Prof. Dr. V.M. Graveto, who kindly made the necessary arrangements to temporarily relieve him of his teaching activities at the University of Coimbra.

The author tried to make acknowledgments as specific as possible in the body of the text. To all the specific contributions the author is very grateful. Any omission on his part has been entirely inadvertent. The drawings were made by A. van't Veer whose work was most worthwhile.

João Luis Mendes Pedroso de Lima was born in Coimbra (Portugal) on October 26th, 1959. He received his degree in Civil Engineering (specialization Hydraulics) at the Faculty of Science and Technology of the University of Coimbra in 1982. In November 1982 he joined the Department of Civil Engineering of the University of Coimbra were he taught courses in Hydraulics, Hydrology and Applied Hydraulics.

He undertook several trainings: Delta Works (Rijkswaterstaat), The Netherlands in August-September 1982, and Villarino Fall (Iberduero), Spain in July-August 1983. From August to December 1983 he attended the 22nd International Course on Land Drainage, held in Wageningen and organized by the International Institute for Land Reclamation and Improvement (ILRI) and the International Agricultural Centre (IAC).

He entered the Agricultural University Wageningen in August 1985, and received the degree of Master of Science in Soil Science and Water Management, specializations Agrohydrology and Drainage, in June 1987. During the subsequent two and a half years he has been working on the present research with Prof. Dr. W.H. van der Molen, in joint co-operation between the Department of Land and Water Use and the Department of Hydraulics and Catchment Hydrology of the Agricultural University Wageningen. Since the 1st of October 1989 these two Departments, together with the Soil Physics group (of the Soil Science Department), merged into the Department of Hydrology, Soil Physics and Hydraulics.

His present address is: Departamento de Engenharia Civil,
Faculdade de Ciências e Tecnologia,
Universidade de Coimbra,
3049 Coimbra Codex,
Portugal.

CONTENTS

INTRODUCTION

Among the planets, Earth is characterized by an abundance of liquid water. The hydrologic cycle is a major force in reshaping the surface of the Earth. Within this cycle, overland flow is defined as the movement of water over the land surface before it concentrates into recognizable channels. Overland flow is a key process within the hydrologic cycle and a subject of great importance for people and their environment. Practical applications are found in the design of hydraulic structures, in irrigation, drainage, flood control, erosion and sediment control, waste water treatment, environment and wildlife protection, to mention only some of the most important fields of interest.

The physical system investigated is schematically illustrated in Fig.1.

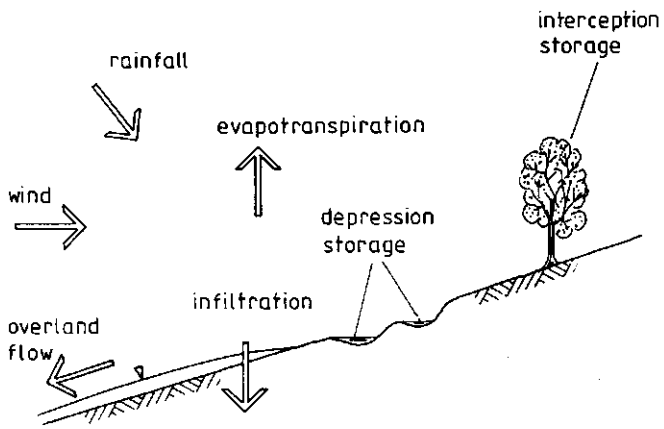

Fig. 1 The physical system under investigation.

Not all rain reaching the surface is removed by overland flow because part of it is involved in other processes such as infiltration into the soil, interception by vegetation, accumulation of water in depression storage and evapotranspiration. As a consequence of these losses, rainfall often causes no direct surface runoff. Overland flow can be significant in cases where the rainfall is heavy, the vegetation sparse, and a major fraction of the surface is relatively impermeable or nearly saturated with water.

Although many relevant topics like water quality, sediment transport, rainfall-runoff processes in large drainage basins, losses of water through transpiration and evaporation of both intercepted and soil water, etc. are closely related to the overland flow process, they are excluded from discussion here.

The research described in this thesis was mostly phenomenologic. Overland flow under rainfall was studied from a physical point of view. The primary motivation was therefore the study of the physical phenomena and their interrelations.A practical approach was adopted by illustrating the theory with examples and laboratory results.

The subject matter of this thesis is divided into three parts. The first part presents general concepts perceived to be background information for the understanding of Parts II and III. Overland flow is defined in Section 1.1 and the conditioning factors are reported in Section 1.2. Overland flow in relation to (agro)hydrology, water erosion, water quality, wastewater treatment, and surface irrigation and drainage are dealt with in Sections 1.3 to 1.7, respectively.

Part II deals with the mathematical modelling of overland flow under rainfall. Using the kinematic wave theory an analytical solution for the rising limb of overland flow over infiltrating surfaces, with longitudinal section of parabolic shape (concave and convex surfaces), is presented in Section 2.4. Chapter 3 discusses the upper boundary conditions for overland flow under rainfall.

Part III concentrates on some aspects related to conditioning factors, namely depression storage, infiltration, morphology and wind. A method of predicting a spatial average value for depression storage of tilled surfaces is proposed in Chapter 4. In Chapter 5 a combined study of infiltration and overland flow is undertaken. A detailed analysis of the different morphological factors affecting overland flow under rainfall on slopes is presented in Chapter 6.

Wind effects are generally not considered in overland flow and rainfall erosion studies. Chapter 7 is devoted to the overland flow process under wind-driven rain. In Sections 7.1 and 7.2, the effects of inclined rainfall and the wind induced shear-stress on overland flow have been investigated in an experimental study. These processes have been simulated in a wind tunnel with a variable slope. In Section 7.3 the effect of oblique rain on inclined surfaces is studied and a nomograph is presented for the rain-gauge correction factor. Finally, Section 7.4 emphasises the importance of raindrop splash anisotropy as a factor affecting splash erosion.

In this work the numbering of figures is done by Sections. The symbols used are defined throughout the text (see also "Notation").

1. OVERLAND FLOW

1.1 WHAT IS OVERLAND FLOW ?

1.1.1 Introduction

Many conflicting opinions and numerous terminologies have been proposed regarding overland flow processes. A simple but precise definition could be: the flow of water over the land surface before becoming channelized. Horton (1933) described overland flow as follows: "Neglecting interception by vegetation, surface runoff is that part of the rainfall that is not absorbed by the soil by infiltration". Horton considered overland flow to take the form of a sheet flow. Combined with overland flow there is depression storage in surface hollows, and surface detention storage proportional to the depth of the overland flow itself.

Figure 1 is an attempt to give a hydrologic classification of the terms concerned. This scheme is solely based on the actual form of water flow over the surface. Overland flow may be divided into the relatively frequent, low magnitude sheet flow, and the less frequent sheet flood of higher magnitude (Hogg, 1982).

Nearly all surface runoff starts as overland flow in the upper reaches of a catchment, and travels at least a short distance before it reaches a rill or a channel (Emmett, 1970). On natural surfaces overland flow may occur with a great variety of flow depths within a small area. It is both unsteady and spatially varied. Under certain conditions the flow may become unstable and may give rise to the formation of roll waves. In that case, the assumptions behind the analytical or numerical models used should be carefully examined. The actions of raindrop impact and wind on the sheet of flowing water further complicate the overland flow problem. On vegetated surfaces these influences are less, but the hydraulic resistance of plants and plant debris should be taken into account.

The hydraulic characteristics of overland flow are basically described by its Reynolds and Froude numbers. The Reynolds number is an

index of the turbulence of the flow. However, Reynolds number does not fully describe the degree of turbulence of overland flow which is also influenced by raindrop impact and topographic irregularities (i.e., obstacles such as grass stems, pebbles and crop ridges) inducing flow disturbances. The Froude number differentiates a subcritical from a supercritical flow (Chow, 1959).

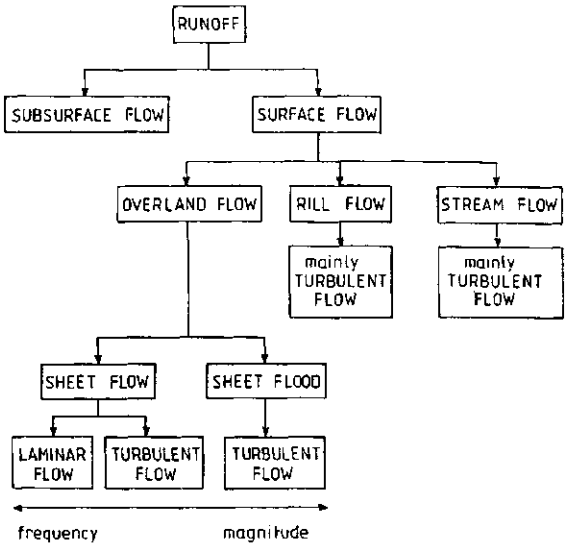

Fig. 1 Hydrologic classification of the overland flow process (modified from Hogg, 1982)

1.1.2 Types of overland flow

Four major types of overland flow can be distinguished, as shown in Fig. 2:

(1) Hortonian overland flow occurs when rainfall intensity exceeds the infiltration rate (Dunne and Leopold, 1978). Usually this happens only in that part of a catchment where the initial soil moisture content is high or the surface is relatively impermeable. Thus it is applicable for impervious surfaces in urban areas, and for natural surfaces with low infiltration capacity.

(2) Delayed Hortonian overland flow occurs when rainfall intensity exceeds the infiltration rate only after some delay, during which changes in the soil occur under the influence of wetting or raindrop

impact. This is typical for swelling clays, where infiltration is very high in dry conditions (existence of cracks) but very low in wet conditions. It also occurs in soils which are liable to form crusts (Bergsma, 1983).

(3) Topsoil saturation overland flow takes place on soils where a relatively permeable topsoil layer overlies less permeable material. This is the case of ploughpans, shallow profiles over bedrock, sand and gravel overlying layers of compact structure, etc (Bergsma, 1983). When the topography is suitable, there may even be a return flow from the soil to the surface, thus creating or increasing overland flow.

(4) Saturation overland flow (Kirkby and Chorley, 1967; Dunne and Black, 1970) is produced when the storage capacity of the soil is completely filled, so that all subsequent additions of water at the surface, irrespective of their rate of application, are forced to flow over the surface (Kirkby, 1988). This frequently occurs when soils become saturated at the surface, from below, by rising water tables.

The knowledge of these four types of overland flow mechanisms is an important step in understanding runoff response from hillslopes and drainage basins. The incorporation of these concepts into forecasting models is still in progress (Kirkby, 1988). Of these mechanisms, the Hortonian mechanism has been most widely used. All these different types of overland flow can occur concurrently and merge into one another in a given drainage basin (Singh, 1988).

From a hydraulic point of view, overland flow may be either laminar, turbulent or transitional. Most researchers agree that all three forms are encountered. Generally, flow changes from laminar to turbulent and back to laminar through the rise and recession of a hydrograph. Many researchers feel that the raindrop impact increases the hydraulic roughness and results in flow being turbulent at lower Reynolds numbers (Yoon and Wenzel, 1971).

1.2 CONDITIONING FACTORS

The generation of overland flow reflects the influence of relief, geology, climate, soil type, land use and the application of control measures. It is greatly influenced by both natural and human activities (e.g. morphological factors like shape, length, steepness and exposure of slopes, type of drainage basins, and others like rainfall frequency and intensity, resistance to soil erosion, structure of agricultural lands, soil cover of natural vegetation and tilled crops, wind, etc).

During the process of overland flow generation under rainfall the major factors to consider are: a) surface storage (interception and depression), b) surface sealing, c) infiltration, d) depth of less permeable layers, e) antecedent soil moisture conditions, and f) lateral moisture supply (return flow). Return flow occurs when

subsurface water is constrained to flow out of the soil, overland, in areas of topographic concavity, or where soil thickness and/or permeability are decreasing downslope.

Fig. 3 summarizes the main inputs, conditioning phenomena and hazards that should be kept in mind when studying the overland flow phenomena. Some of the conditioning factors mentioned here will be dealt with in detail in Part II and III of this thesis, namely depression storage (Chapter 4), infiltration (Chapter 5), morphological factors (Chapter 6), and wind (Chapter 7).

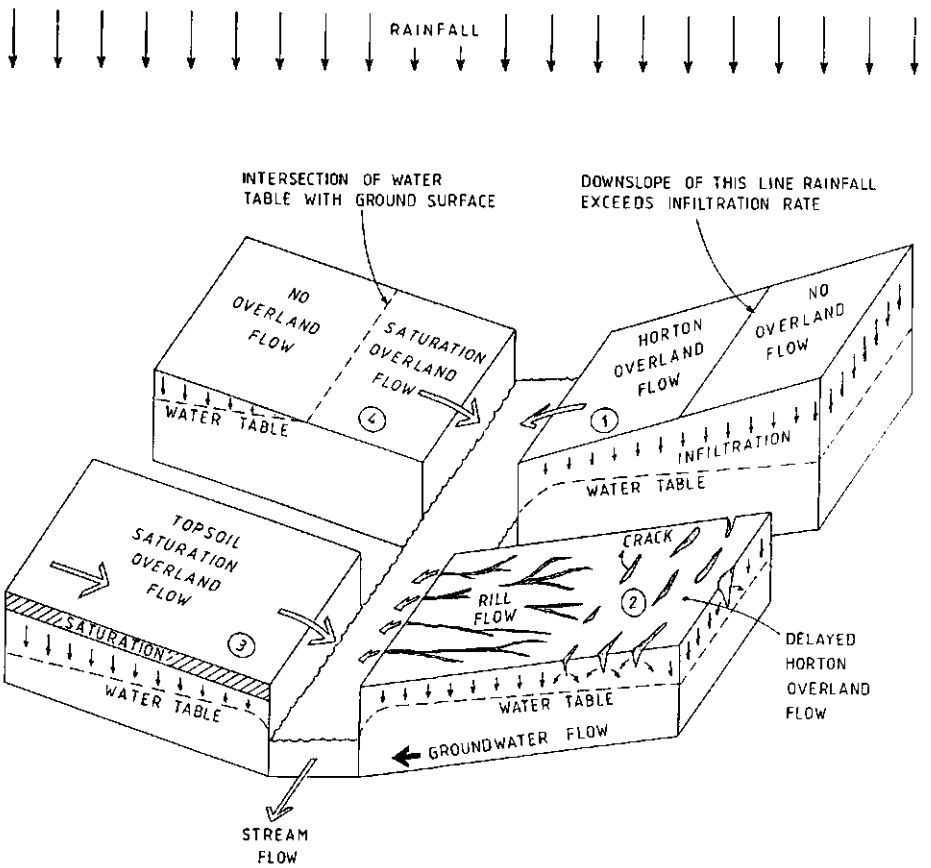

Fig. 2 Types of overland flow: (1) Hortonian overland flow, (2) delayed Hortonian overland flow, (3) topsoil saturation overland flow, and (4) saturation overland flow.

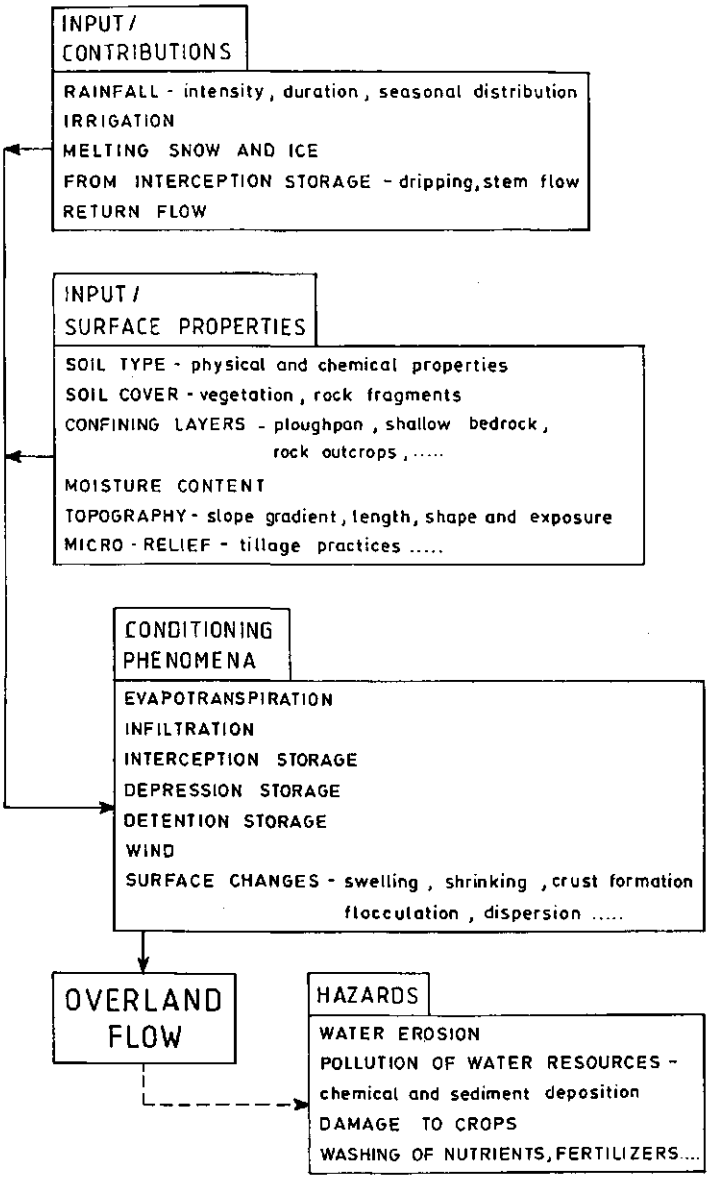

Fig. 3 Aspects related to overland flow studies.

1.3 OVERLAND FLOW AND (AGRO)HYDROLOGY

Overland flow has attracted considerable attention in the past because of its (agro)hydrologic significance.

The dynamic relationship between rainfall and overland flow in natural, rural, and urban areas is a central problem in hydrology. It is of importance to workers in a wide spectrum of disciplines such as hydrologists, sedimentologists, and civil, agricultural and environmental engineers. Mathematical modelling of this relationship is often based on a so-called black-box approach. This means that no explicit assumptions are made regarding the physical structure of the process. This approach is understandable due to the complexity of the hydrologic system. However, there is a continuous interest within the field of hydrology in the development and application of rainfall-runoff models with a theoretical structure based on physical laws.

Most quantitative hydrologic models can be classified as deterministic, statistical, or a combination of these. The division between these types of models is not always clear. One can think of models as being made up of some combination of components, each of which represents a point on a continuous spectrum of model "types", ranging from completely deterministic on the one hand to completely stochastic on the other (Haan, 1977).

According to Fleming (1975), the statistical models can be divided into three subdivisions: regression and correlation techniques, probabilistic methods, and stochastic models. Deterministic models describe the behaviour of the hydrologic cycle in terms of mathematical relationships outlining the interactions of various phases of the hydrologic cycle. No attempt is made to represent random processes. Another group of deterministic models are the component models, that seek to describe each part of the whole hydrologic sequence mathematically by means of appropriate equations (Shaw, 1983). Notable advances have been made related to component models in the last decades.

In this thesis, overland flow is treated in a component and conceptual way, by attempting to represent the time and space variant interaction between the different processes involved and to give physical relevance to the parameters used.

1.4 OVERLAND FLOW AND WATER EROSION

Soil erosion has been a major environmental force in all times; however, because of the increasing intensity of land use, erosion and sedimentation pose a world wide threat to sustainable agriculture and the overall stability and quality of the environment (Lal, 1988).

There are two major types of erosion: natural erosion and accelerated erosion. As a consequence of the hydrologic cycle, water has been acting on the surface of the continents since its beginning.

Such action of water, together with the actions of wind, temperature, gravity and glaciers, determines natural erosion, which in the broadest sense is an established process within the environment and has been responsible for the cause of present land surface features, such as hills, mountains, canyons, plateaus, deltas and stream channels. Accelerated erosion results, for example, when man uses land for the production of food, over-exploits forest resources, constructs buildings, industrial plants and transport facilities. Failure to distinguish between natural and accelerated erosion has often resulted in not recognizing the seriousness of man-made erosion damage (Horning and Reese, 1970). Photographs 1 and 2 give two examples of accelerated erosion in Alentejo, Portugal (further information on that region is given in Appendix C).

Soil erosion is a two-phase process consisting of the detachment of individual particles from the soil mass and their transport by erosive agents such as overland flow. When sufficient energy is no longer available to transport the particles a third phase, deposition, occurs. The severity of erosion depends upon the quantity of material supplied by detachment and the capacity of the eroding agents to transport it (Morgan, 1986).

Raindrop splash is the most important detaching agent. As a result of raindrops striking a bare soil surface, soil particles may be thrown through the air over distances of more than one meter. Continuous exposure to intense rainstorms considerably weakens the soil. Flowing water and wind are further contributors to the detachment of soil particles. Section 7.4 of this thesis emphasizes the importance of raindrop splash anisotropy as a factor affecting splash erosion. Slope, wind and overland flow velocity were found to be factors contributing to the anisotropy of the splash.

The transporting agents comprise those which act areally and contribute to the removal of a relatively uniform soil layer sheets and those which concentrate their action in channels (Morgan, 1986). The first group consists of raindrop splash, overland flow, and wind. The second group covers water flow in rills and in larger features such as gullies and rivers.

The interrelations between erosion and its harmful effects are manifold. Most directly affected are soil and water as natural resources. The soils are destroyed by water erosion and reduced in their value for production in agriculture, animal husbandry and forestry. In addition, soil fertilizers and pesticides carried away by water erosion, act as pollutants of water resources. Loss of soil cover and soil, indirectly affect water resources by increasing floods and droughts. All these factors have a considerable number of secondary effects, such as encroachment of deserts, salt water intrusion, reduction of irrigation, and flooding of agricultural land, to mention only some of the effects important for agriculture (Horning and Reese, 1970).

Photo 1 Water erosion in Alentejo (Portugal)

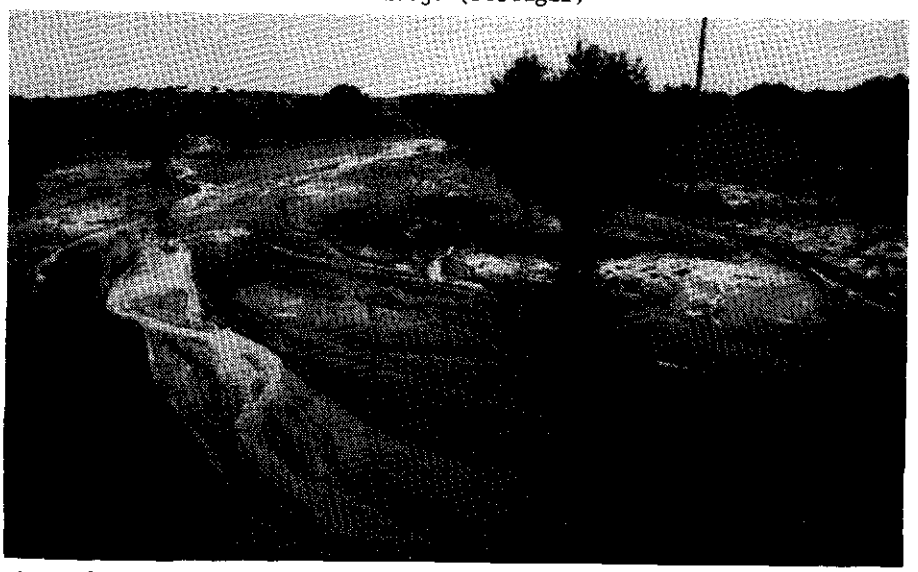

Photo 2 Deposition of eroded material after heavy shower in Alentejo (By R. Ferreira)

1.5 OVERLAND FLOW AND WATER QUALITY

1.5.1 Introduction

In the past rainfall water was considered to be clean. Now that we have learned that precipitation is polluted in many aspects, overland flow water has fallen under suspicion as well. The precipitation itself is contaminated by air pollution. Air pollution, originating from natural sources (like the sea), from industrial and domestic sources and traffic, appears as solid particles, aerosols and in gaseous form. The pollutants, present in the air, may reach the Earth again in dry periods (dry deposition) and in wet periods (rainfall) (Uunk, 1985).

Following the precipitation on its way to the canals and rivers, significant water quality changes can be observed. During overland flow the water can pick up or lose pollutants. The nature of the collected and lost pollutants depends on the characteristics of both the rainfall and runoff, and the surfaces involved.

1.5.2 Urban runoff and water pollution

Now it is quite clear that runoff is polluted in many ways. Many of the substances discharged with the runoff can affect the quality of the aquatic environment.

The quality of the runoff from urban surfaces depends on the type of surface (roof, street, sidewalks, etc.) and the incoming load of pollution, its accumulation and removal (Dam et al., 1986). Runoff from a city motorway is heavily polluted by traffic.

The most important sources of pollution for both covered and uncovered surfaces are wet and dry depositions, traffic, animal excrements, corrosion and organic waste from litter, leaves, etc. Some pollutants will be removed by adsorption to the soil, by street sweeping and cleaning the gullypots and manholes.

The excess rainfall on an urban area flows off by way of roofs, pavements, streets, gullypots, etc. into the sewer system. In case of separate sewer systems, for rainwater and for wastewater, the rain-sewers convey the runoff directly to the receiving surface water. The basic idea behind this system is that stormwater is "clean" and direct discharge into open water allowed. When a combined sewer system is used, in principle, all water is led to a treatment plant.

1.5.3 Agricultural runoff and water pollution

Crop production practices have changed greatly during this century with the introduction of large-scale machinery, increased fertilizer

use, chemical pest control methods, and conversion from pasture and hay to row crops. These production changes have created new problems associated with runoff and soil erosion, including pollution of water resources. Until recently there has been little consideration of the influence of agricultural chemicals or agricultural nutrients and animal waste upon water quality.

Many kinds of land use offer a source or origin for sediments, although agricultural land and disturbed or denuded lands afford more opportunity to supply translated sediment than more natural areas. Sediment with respect to water quality is a pollutant (the number one pollutant on a volume basis in agricultural runoff). Its pollutional aspect can be conveniently thought of in two categories. Firstly, there is the direct effect of its presence in water and its negative interference with the desired water use. Secondly, the sediment will serve as an electro-chemical carrier for entraining or transporting other pollutants. The major portion of harmful chemicals is usually adsorbed to sediments, although the dissolved portion has the most direct effect on water quality. The large portion carried on sediments may not be directly important for water quality, but it may furnish a long-lasting supply of chemicals to the receiving body of water.

1.6 OVERLAND FLOW AS A SYSTEM OF TREATMENT OF WASTEWATER

In some cases the overland flow process is used as a form of treatment in which wastewater is supplied to the upper parts of carefully graded, grass-covered slopes usually having soils or subsoils of low permeability. Wastewater undergoes treatment through a variety of mechanisms as it flows in a thin film over the slope surface. Typically, 40 to 80 percent of the applied effluent runs off. The remainder is lost to percolation and evapotranspiration (Tchobanoglous, 1979). Renovation is accomplished by physical, chemical, and biological means (Tchobanoglous, 1979). Treated effluent is collected as surface runoff in ditches at the bottom of the slope.

Perennial grasses with long growing seasons, high moisture tolerance and extensive root formation are best suited to overland flow treatment. Biological oxidation, sedimentation and grass filtration are the primary removal mechanisms for organic and suspended solids. Nitrogen removal is attributed primarily to nitrification/denitrification and plant uptake (Vernick and Walker, 1981). Slope gradients must be steep enough to prevent ponding, yet mild enough to prevent erosion and provide sufficient detention time for the wastewater on the slope. Slopes must be free from rills and gullies to prevent channeling and allow uniform distribution of overland flow over the surface.

Overland flow has been demonstrated to be a reliable method of treatment for municipal as well as some industrial wastewaters. In the past decade the technology of overland flow has been advanced considerably through publication of research studies and design guidelines (Culp, 1978, Tchobanoglous, 1979, Vernick and Walker, 1981). Rainfall

affects the performance of an overland flow wastewater treatment system (Figueiredo et al., 1984).

Detailed studies on the overland flow treatment of wastewater are excluded from the present thesis.

1.7 OVERLAND FLOW AND SURFACE IRRIGATION AND DRAINAGE

1.7.1 Overland flow and surface irrigation

Surface irrigation is the irrigation method most widely applied; it is used on some 200 million ha., representing almost 90% of the world's irrigated area. Surface irrigation is accomplished on flat fields by ponding water on the soil surface (check irrigation) and on sloping fields by maintaining for some time a flow of water over the soil surface (flow irrigation). Surface irrigation methods include basin, border and furrow irrigation.

The physical purpose of irrigation is in case of "wet" crops (e.g. rice) to maintain or to restore the water layer on the field, and in case of "dry" crops to increase the moisture content of the soil in the root zone of the crop. In the latter case, water is supplied to the field and flows (overland) with flow diminishing as water advances over the soil surface whilst infiltrating (Roscher, 1988).

The research described in this thesis concerns solely overland flow under rainfall and overland flow under surface irrigation will not be further dealt with.

1.7.2 Overland flow and surface drainage

Surface drainage is the evacuation of excess water over the ground surface to an open drainage system with an adequate outlet (Concaret, 1981). Surface drainage as a field drainage technique has existed in one form or another for centuries. For many years it has been considered a local art. In flat areas the main problem is the timely removal of stagnant water and in sloping areas it is usually the removal of excess water without causing erosion (Raadsma and Schulze, 1980). Surface drainage will bring usually three types of benefits: direct and indirect yield increase; increased efficiency of machinery; and increased efficiency in the use of fertilizers (Coote and Zwerman, 1970). Indirect yield increase may result from earlier planting, for example.

The need for surface drainage is a result of a combination of certain climatic, hydrologic, and soil conditions, and of topography and land use (Raadsma and Schulze, 1980). Soil types which may benefit from surface drainage are slowly permeable soils, or shallow soils over a restricting layer in combination with an unfavourable topographic

position.

Another aspect of surface drainage is urban drainage. Human occupation of a land area causes a change in the nature of the land surface. The natural permeable soil surface into which rainfall water is able to infiltrate at varying rates, is replaced by a range of more or less impervious surfaces. An increase in the impermeable surface area has two immediate consequences (Colyer and Pethick, 1976). Firstly, the volume of overland flow is increased; and secondly, runoff is concentrated. Furthermore flow over a paved impermeable surface is much more rapid than over natural soil, especially if vegetated.

In the construction of roads and highways, surface drainage is one of the most essential elements to be considered. A sheet of water over the pavement creates a hazard to driving, which is aggravated if freezing occurs.

Urban and highway drainage, and field drainage techniques, like land forming, grading, levelling and bedding, will not be dealt with in this thesis, although the mechanics of surface drainage, i.e. of the removal of rainfall excess water from pervious and paved surfaces by overland flow, is implicit in many Chapters.

ACKNOWLEDGEMENTS

The author wishes to thank Prof. Dr. W.H. van der Molen and Dr. R.W.R. Koopmans (Department of Land and Water Use), and Ir. K. Roscher (Department of Irrigation and Civil Engineering) for their constructive criticism of the draft of Chapter 1.

REFERENCES

Bergsma, E., 1983. Rainfall erosion surveys for conservation planning. ITC Journal no. 1983-2, 166-174.

Bergsma, E., 1986. Aspects of mapping units in the rain erosion hazard catchment survey. ILRI publ. no. 40, 84-104.

Chow, V.T., 1959. Open channel hydraulics. McGraw Hill, New York, 680 p.

Chow, V.T., D.R. Maidment and L.M. Mays, 1988. Applied hydrology. McGraw-Hill, New York, 527 p.

Colyer, P.J. and R.W. Pethick, 1976. Storm drainage design methods: a literature review. Report no. INT 154, Hydraulics Research Station, Wallingford, 85 p.

Concaret, J. (Ed.), 1981. Drainage Agricole: Théorie et pratique. Chambre Régionale d'Agriculture de Bourgogne, France, 509 p.

Coote, D.R. and P.J. Zwerman, 1970. Surface drainage of flat lands in the Eastern United States. New York College of Agriculture, Cornell University, Extension Bulletin 1224, 48 p.

Culp, R.L., G.M. Wesner and G.L. Culp, 1978. Handbook of advanced wastewater treatment. Van Nostrand Reinhold Company, New York, 632 p.

Dam, C.H. van, M. Scholten and F.H.M. van de Ven, 1986. Urban water quality in Lelystad: rainfall and runoff from selected surfaces. In: Urban storm water quality and effects upon receiving waters. International Conference, Wageningen, The Netherlands, 25-37.

Dunne, T. and R.D. Black, 1970. An experimental investigation of runoff prediction in permeable soils. Water Resources Research, 6(2): 478-490.

Emmett, W.W., 1970. The hydraulics of overland flow on hillslopes. Geological Survey Professional Paper no. 662-a, U.S. Dep. of the Interior, 68 p.

Figueiredo, R.F. de, R.G. Smith and E.D. Schroeder, 1884. Rainfall and overland flow performance. J. of Environmental Engineering, 110(3): 678-694.

Fleming, G., 1975. Computer simulation techniques in hydrology. Elsevier, New York.

Haan, C.T., 1977. Statistical methods in hydrology. Ames: Iowa State University Press, 378 p.

Hogg, S.E., 1982. Sheetflood, sheetwash, or...? Earth-Sciences Reviews. 18: 59-76.

Horning, H.M. and W.E. Reese, 1970. Water as it affects agriculture. Proc. ICID International Water Erosion Symposium, Praha.

Horton, R.E., 1933. The role of infiltration in the hydrologic cycle. Am. Geophys. Union, Transcripts, 446-460.

Kirkby, M. J., 1988. Hillslope runoff processes and models. J. of Hydrology, 100: 315-339.

Kirkby, M.J. and R.J. Chorley, 1967. Throughflow, overland flow and erosion. Bull. Intern. Assoc. Sci. Hydrology, 12: 5-21.

Lal, R. (Ed.), 1988. Soil erosion research methods. Soil and Water Conservation Society, Wageningen, The Netherlands, 244 p.

Menzel, R.G., 1977. Agricultural chemicals/sediment interaction. In: Agricultural and silvicultural nonpoint source water pollution in Texas. Proc. 208 Planning for Texas Conference, Texas, 118-125.

Morgan, R.P.C., 1986. Soil erosion and conservation. Longman Scientific & Technical, 298 p.

Raadsma, S. and F.E. Schulze, 1980. Surface field drainage systems. Drainage principles and applications, International Institute for Land Reclamation and Improvement, Wageningen, The Netherlands, Publ. 16 (Vol. IV), 470 p.

Roscher, K., 1988. Surface irrigation, characteristics, design and performance. Department of Irrigation and Civil Engineering, Agricultural University Wageningen, The Netherland, 90 p.

Shaw, E.M., 1983. Hydrology in practice. Van Nostrand Reinhold Co. (UK), 569 p.

Singh, V.P., 1988. Hydrology systems: Rainfall-runoff modeling (Vol. 1). Prentice Hall, Englewood Cliffs, New Jersey, USA, 480 p.

Tchobanoglous, G., 1979. Wastewater Engineering: treatment, disposal, reuse (second Edition) Metcalf & Eddy, Inc, McGraw-Hill Book Company, New York, 920 p.

Uunk, E.J.B., 1985. Urban stormwater runoff pollution. In: Water in urban areas. Proc. of technical meeting 42 (proc. and information TNO committee on hydrological research no.33), The Netherlands, 77-98.

Vernick, A.S. and E.C. Walker, 1981. Handbook of wastewater processes. Marcel Dekker, Inc., New York, 255 p.

Ven, F.H.M. van de, 1985. From rainfall to sewer inflow: a process with consequences. In: Water in urban areas. Proc. of technical meeting 42 (proc. and information TNO committee on hydrological research no.33), The Netherlands, 47-75.

Vittetoe, G.C., 1977. Status of sediment problems in Texas. In: Agricultural and silvicultural nonpoint source water pollution in Texas, Proc. 208 Planning for Texas Conference, Texas, USA, 118-125.

Yoon, Y.N. and H.G. Wenzel, 1971. Mechanics of sheet flow under simulated rainfall. Journal of the Hydraulic Division, ASCE, 97: 1367-1386.

2. MATHEMATICAL MODELLING OF THE OVERLAND FLOW PROCESS

2.1. INTRODUCTION

The objective of this Chapter is to give a short introduction on the possibilities for the mathematical modelling of the overland flow process. Further applications are presented in part III of this thesis.

Overland flow under rainfall is an example of gradually varied, unsteady, nonuniform, free surface flow and is governed by the laws of conservation of mass and momentum (Chow, 1959). These laws give rise to equations of continuity and momentum which are often referred to as Saint-Venant equations (Barre de Saint-Venant, 1871) or simply equations of motion. The derivation of the one-dimensional form of these equations has appeared in text books and scientific articles (e.g. Lai, 1986; Stephenson and Meadows, 1986; Chow et al., 1988).

These equations can either be solved in their full form or, in many cases, be approximated by the diffusion and kinematic wave equations. The conditions under which various approximations are valid are reviewed by, among others, Morris and Woolhiser (1980), Morris (1981) and Vieira (1983). Many general overland flow modelling problems do not require the use of the full Saint-Venant equations.

The models described in this thesis made use of the kinematic wave theory (Sections 2.2 and 2.3). In Section 2.4, an analytical solution for the rising limb of overland flow over infiltrating surfaces, with longitudinal sections of parabolic shape, was derived.

2.2. KINEMATIC WAVE MODELLING

Owing to its simplicity, the kinematic wave approach has been frequently used to solve unsteady flow problems. The Rational method and Unit hydrograph methods are easy to apply but limited in accuracy and versatility. Kinematic wave modelling is the next logical step in sophistication before the full hydrodynamic equations are resorted to (Stephenson and Meadows, 1986). Also the kinematic wave equations have an important advantage over the hydrodynamic equations for describing overland flow; analytical solutions are possible for simple surface

geometries. A great insight into the phenomenon of overland flow can be gained by studying these analytical solutions.

The term kinematic refers to movement where accelerations and water level slope are negligible and friction slope equals the bed slope, i.e. acceleration and pressure terms in the momentum equation are assumed zero. An explicit mathematical exposition of basic hypotheses of kinematic wave formulation was first presented by Lighthill and Whitham, in 1955, to describe flood movement in long rivers (Singh, 1978). However, for overland flow, this method of calculation is attributed to Henderson and Wooding (1964) while a more complete analysis was given by Woolhiser and Liggett (1967). Since then, analytical solutions have been obtained for overland flow hydrographs during steady rainfall on surfaces of simple geometric shape. Numerical models have also been developed for application to more complex surfaces and unsteady rainfall.

Kinematic wave solutions have been shown to give very accurate results for most hydrologically significant overland flow situations (Woolhiser and Liggett, 1967; Morris and Woolhiser, 1980; Vieira, 1983; Hromadka II et al., 1987, and others). In this thesis the kinematic wave approach was used for both the numerical and analytical models without any further attempt to verify its validity. The basic kinematic equations are presented in several Chapters and will not be repeated here.

Solutions of the kinematic wave equations have usually been obtained numerically, using explicit and implicit finite difference schemes (Brakensiek, 1967; Kibler and Woolhiser, 1970 and 1972; Singh, 1976; Rovey et al., 1977; Constantinides, 1981; Stephenson and Meadows, 1986; among others). A comparison of numerical models of overland flow has been made recently by Hromadka et al. (1987), Hall et al. (1989), Bell et al. (1989) and Wheater et al. (1989). Also the method of characteristics has been used frequently (Eagleson, 1970; Kibler and Woolhiser, 1970; Stephenson and Meadows, 1986). Analytical solutions are also available (Parlange et al., 1981; Rose et al., 1983; Zarmi et al., 1983; Leu and Liu, 1988; and others).

The following recent works give detailed literature surveys on dynamic and kinematic wave models: Singh (1976, 1978 and 1988), Lai (1986), Hromadka II et al. (1987), Kirkby (1988), and Chow et al. (1988).

2.3. NUMERICAL SOLUTIONS OF THE KINEMATIC WAVE EQUATIONS

The numerical solutions of the kinematic wave equations are more flexible than the analytical solutions. They can handle more easily variation in the surface properties, rainfall rates and initial and boundary conditions. For the numerical solution of the kinematic wave equations it is necessary to discretisize both in space and time. This is accomplished by dividing the overland flow surface into elementary sections and dividing the time into time steps. There are various

numerical methods available for solving the kinematic wave equations which include finite difference and finite element techniques.

Two numerical models of overland flow will be described, in detail, in Part III of this thesis: (a) model KININF for overland flow on an infiltrating surface (Chapter 5); (b) model WROF for overland flow under wind-driven rain (Sections 7.1 and 7.2, and Appendices A and B). Both of these models make use of the kinematic wave approach for the overland flow process and a second order explicit finite difference scheme.

Explicit finite difference schemes have been used to solve the kinematic wave equations, but the size of time step is severely limited by the Courant condition for stability. The major problems accompanying these schemes are those of stability and accuracy. However, they have been found to be economical and efficient by many researchers (e.g. Woolhiser and Liggett, 1967; Kibler and Woolhiser, 1970; Freeze, 1978; Constantinides, 1981). Stability problems may be avoided by using implicit approximations.

The explicit finite difference scheme, the second order single step Lax-Wendroff scheme, used in the numerical models presented in Chapter 5 and Sections 7.1 and 7.2, was shown to be stable and accurate, and to produce less numerical distortion in peak discharge rates than other finite difference schemes (Kibler and Woolhiser, 1970). This finite difference scheme has been used successfully by Kibler and Woolhiser (1970 and 1972), Lane et al. (1975), Rovey at al. (1977), Freeze (1978), Wu et al. (1978), Lima (1987), among others.

2.4 AN ANALYTICAL KINEMATIC MODEL FOR THE RISING LIMB OF OVERLAND FLOW ON INFILTRATING PARABOLIC SHAPED SURFACES

Published in: Journal of Hydrology, Elsevier Science Publishers B.V., Amsterdam, 104 (1988): 363-370.

Journal of Hydrology, 104 (1988) 363-370
Elsevier Science Publishers B.V., Amsterdam — Printed in The Netherlands

Technical Note

[5]

AN ANALYTICAL KINEMATIC MODEL FOR THE RISING LIMB OF OVERLAND FLOW ON INFILTRATING PARABOLIC SHAPED SURFACES

J.L.M.P. DE LIMA and W.H. VAN DER MOLEN

Department of Land and Water Use, Agricultural University, Nieuwe Kanaal 11, 6709 PA, Wageningen (The Netherlands)

(Received and accepted for publication May 11, 1988)

ABSTRACT

De Lima, J.L.M.P. and Van der Molen, W.H., 1988. An analytical kinematic model for the rising limb of overland flow on infiltrating parabolic shaped surfaces. J. Hydrol., 104: 363 370.

Using the kinematic wave theory and Zarmi's hypothesis, an analytical solution for overland flow over an infiltrating, parabolic shaped surface (concave or convex surfaces, that may be represented by a quadratic equation) is presented. The velocity of the water flow is assumed to be independent of time. The analytical solution developed is easier to utilize than numerical simulation and can be used to calibrate numerical methods devised for more complicated cases. An illustration is presented.

INTRODUCTION

For a realistic simulation of overland flow it is necessary to attempt simulation on surfaces that are not restricted to a plane of fixed slope. The overland flow process is strongly affected by the shape of the slopes.

Using the kinematic wave theory in combination with Zarmi's hypothesis (Zarmi et al., 1983) for the flow equation, an analytical solution for overland flow over an infiltrating, parabolic shaped surface (concave or convex surfaces, that may be represented by a quadratic equation) is presented.

One of the major topics in geomorphology is the evolution of hillslope profiles through time. The model formulated can be used to analyse the effect of that evolution on the overland flow processes.

This model is an extension to curved surfaces of the theory of Zarmi et al., 1983.

THEORY

The equation of continuity for shallow water flow may be written as:

$$\delta h/\delta t + \delta q/\delta x = p - i(t) \quad (1)$$

0022-1694/88/$03.50

where: h = flow depth at time t, and position x (m); x = space axis along the direction of flow (m); q = volumetric water flux per unit plane width ($m^2 s^{-1}$); p = rainfall rate, assumed to be a constant ($m s^{-1}$); and $i(t)$ = infiltration rate, assumed to be a function of time only ($m s^{-1}$).

By assuming that the bed slope equals the friction slope (kinematic wave assumption) and by using existing open-channel flow friction equations we can express the discharge at any point and time as a function of the water depth only, as follows:

$$q = \alpha h^m \tag{2}$$

where: m = parameter for the type of flow; and α = hydraulic coefficient.

The shape of the surface is assumed to be represented by a quadratic equation:

$$y = a_1 x_1^2 + b x_1 + c \quad \text{with: } b > 0,\ a_1 > -b/2L \text{ and } a_1 \neq 0 \tag{3}$$

where: x_1 = space axis along the horizontal direction (m); y = space axis along the vertical direction (m); a_1, b, c = parameters; and L = length of the surface in the horizontal direction (m).

For gentle slopes $x_1 \approx x$, and consequently, the slope gradient $S(x)$ becomes:

$$S(x) = dy/dx = 2 a_1 x + b \tag{4}$$

For the infiltration process use is made of a Horton type equation (Morin and Benyamini, 1977):

$$i(t) = f_c + (f_0 - f_c)\, e^{-at}, \quad \text{with } f_c < p \leqslant f_0 \tag{5}$$

where: a = parameter (s^{-1}); f_0 = initial infiltration rate of the soil ($m s^{-1}$); and f_c = final infiltration rate of the soil ($m s^{-1}$).

The parameter α in eqn. (2) is usually given a physical or quasiphysical interpretation, reflecting the effects of surface slope and hydraulic roughness on the depth of flow. For example for the Darcy–Weisbach equation:

$$\alpha = \sqrt{8gS/f}, \qquad \text{for } m = 3/2 \tag{6}$$

where: g = acceleration due to gravity ($m s^{-2}$); S = bed slope; and f = Darcy–Weisbach friction coefficient. For the Manning–Strickler equation:

$$\alpha = \sqrt{S}/n, \qquad \text{for } m = 5/3 \tag{7}$$

where: n = Manning–Strickler coefficient. ($m^{-1/3} s$).

It has been suggested that runoff can be represented by a linear kinematic approximation to the momentum equation (Zarmi et al., 1983):

$$q = \alpha h \tag{8}$$

The value of α (the water flow velocity for $m = 1$) was then considered constant, independent of time and position. In the formulation of the model for the curved surface it is assumed that α is independent of time but dependent of the position along the surface, given by:

$$\alpha(x) = k \sqrt{S(x)} \tag{9}$$

where k can be estimated by measuring the flow velocity and slope or using eqns. like (6) and (7).

With these assumptions:

$$\alpha(x) = \sqrt{B + Cx}$$

with:

$$B = bk^2 > 0;\ C = 2a_1k^2 > -B/L;\ \text{and}\ C \neq 0. \tag{10}$$

Runoff starts when $p = i(t_c)$, where t_c is the critical time. Let us now define a new variable τ:

$$\tau = t - t_c, \qquad \text{with } t_c = \frac{1}{a} \ln \frac{(f_0 - f_c)}{(p - f_c)}; \quad f_c < p \leqslant f_0 \tag{11}$$

and

$$\begin{aligned} p - i(t) &= (p - f_c) - (f_0 - f_c)\, e^{-a\tau}\, e^{-at_c} \\ &= A - A\, e^{-a\tau}, \qquad \text{with } A = p - f_c \end{aligned} \tag{12}$$

Rewriting eqn. (1), and introducing eqns. (8), (10) and (12), gives:

$$\frac{\delta h}{\delta \tau} + \alpha(x) \frac{\delta h}{\delta x} + \Phi(x)\, h = A - A\, e^{-a\tau} \tag{13}$$

with:

$$\Phi(x) = \frac{d\alpha}{dx} = \frac{C}{2\sqrt{B + Cx}} \tag{14}$$

which is a first order differential equation. It can be solved by using Laplace transformations, with the boundary conditions:

$$\left.\begin{aligned} h(0, \tau) &= 0 \quad \text{(boundary condition)} \\ h(x, 0) &= 0 \quad \text{(initial condition)} \end{aligned}\right| \tag{15}$$

Laplace transformation of eqn. (13) with respect to τ, yields:

$$s\mathcal{L}(h) - h(x, 0) + \alpha(x) \frac{d\mathcal{L}(h)}{dx} + \Phi(x)\, \mathcal{L}(h) = \frac{A}{s} - \frac{A}{s + a} \tag{16}$$

where $\mathcal{L}(h)$ = Laplace transform of $h(x, \tau)$, and s = independent variable.

At time $\tau = 0$, $h(x, 0) = 0$ so:

$$\frac{d\mathcal{L}(h)}{dx} + \frac{s + \Phi(x)}{\alpha(x)}\, \mathcal{L}(h) = \frac{A}{s\, \alpha(x)} - \frac{A}{(s + a)\, \alpha(x)} \tag{17}$$

which is a nonhomogeneous first-order differential equation in x.

If $C \neq 0$, then the general solution of eqn. (17) is of the form:

$$\mathscr{L}(h) = \frac{\left(\frac{A}{s} - \frac{A}{s+a}\right)\left(\frac{\sqrt{B+Cx}}{s} - \frac{C}{2s^2}\right)}{\sqrt{B+Cx}} + \frac{k'}{\sqrt{B+Cx}\, e^{(2s\sqrt{B+Cx})/C}} \tag{18}$$

The constant of integration k' follows from the boundary condition $x = 0$, $h(0, \tau) = 0$, and $\mathscr{L}(h) = 0$:

$$k' = -\frac{A\sqrt{B}\, e^{2s(\sqrt{B})/C}}{s^2} + \frac{AC\, e^{2s(\sqrt{B})/C}}{2s^3} + \frac{A\sqrt{B}\, e^{2s(\sqrt{B})/C}}{s(s+a)} - \frac{AC\, e^{2s(\sqrt{B})/C}}{2s^2(s+a)} \tag{19}$$

Using the auxiliary variables:

$$T = \frac{A\sqrt{B}}{\sqrt{B+Cx}} \tag{20}$$

$$U = \frac{AC}{2\sqrt{B+Cx}} \tag{21}$$

$$V = -2(\sqrt{B} - \sqrt{B+Cx})/C \tag{22}$$

and by substituting eqn. (19) into eqn. (18), and splitting the terms with $1/[s^2(s+a)]$:

$$\mathscr{L}(h) = -\frac{U}{a^2}\frac{1}{s} + \left(A + \frac{U}{a}\right)\frac{1}{s^2} - U\frac{1}{s^3} + \frac{U}{a^2}\frac{1}{(s+a)} - A\frac{1}{s(s+a)} + \frac{U}{a^2}\frac{e^{-Vs}}{s}$$
$$- \left(T + \frac{U}{a}\right)\frac{e^{-Vs}}{s^2} + U\frac{e^{-Vs}}{s^3} - \frac{U}{a^2}\frac{e^{-Vs}}{(s+a)} + T\frac{e^{-Vs}}{s(s+a)} \tag{23}$$

Finally, the inverse transform of eqn. (23) is of the form:

$$h(x, t) = D_1 + D_2(t - t_c) + D_3(t - t_c)^2 + D_4\, e^{-a(t - t_c)}, \quad \text{if } t \leqslant t_c + V \tag{24a}$$

$$h(x, t) = D_5 + D_6(t - t_c) + D_7\, e^{-a(t - t_c)} + D_8\, e^{-a(t - t_c - V)}, \quad \text{if } t \geqslant t_c + V \tag{24b}$$

where $D_1, D_2, \ldots, D_8$ are functions of x:

$$D_1 = -\frac{U}{a^2} - \frac{A}{a} \tag{25}$$

$$D_2 = A + \frac{U}{a} \tag{26}$$

$$D_3 = -\frac{U}{2} \tag{27}$$

$$D_4 = -D_1 \tag{28}$$

$$D_5 = -\frac{A}{a} + TV + \frac{T}{a} + \frac{UV}{a} + \frac{UV^2}{2} \tag{29}$$

$$D_6 = A - T - UV \tag{30}$$

$$D_7 = -D_1 \tag{31}$$

$$D_8 = -\frac{U}{a^2} - \frac{T}{a} \tag{32}$$

EXAMPLE I — COMPARISON WITH THE MODEL OF ZARMI ET AL. (1983)

The model of Zarmi et al. (1983) for overland flow on an infiltrating plane sets $m = 1$ and assumes the slope, S, and consequently α, constant and independent of time and position. They also assumed constant rainfall rates, and infiltration to be described by eqn. (5).

For a plane, $a_1 = 0$ in eqn. (3) which leads to $\alpha = \sqrt{B}$ and $C = 0$, and consequently, from eqns. (20), (21) and (22):

$$U = 0; \quad \lim_{c \to 0} T(x) = A; \quad \lim_{c \to 0} V(x) = x/\sqrt{B} \tag{33}$$

From these, the first branch of the solution, eqn. (24a), with:

$$D_1 = -\frac{p - f_c}{a}; \quad D_2 = p - f_c; \quad D_3 = 0; \quad D_4 = \frac{p - f_c}{a} \tag{34}$$

becomes:

$$h(x, t) = (p - f_c)\left[(t - t_c) - \frac{1 - e^{-a(t - t_c)}}{a}\right], \quad \text{if } t \leqslant t_c + \frac{x}{\alpha} \tag{35}$$

which is in agreement with the model of Zarmi et al. (1983).

The second branch of the solution, eqn. (24b), with:

$$D_5 = \frac{(p - f_c)x}{\alpha}; \quad D_6 = 0; \quad D_7 = \frac{p - f_c}{a}; \quad D_8 = -\frac{p - f_c}{a} \tag{36}$$

becomes:

$$h(x, t) = (p - f_c)\left[\frac{x}{\alpha} - \frac{e^{ax/\alpha} - 1}{a} e^{-a(t - t_c)}\right], \quad \text{if } t \geqslant t_c + \frac{x}{\alpha} \tag{37}$$

which is also in agreement with the model of Zarmi et al. (1983).

EXAMPLE II — APPLICATION

Using Y and L as normalizing constants, the following dimensionless variables are defined:

$$x^* = x/L; \quad y^* = y/Y \tag{38}$$

Assuming that at $x = 0$ when $y = 0$, the dimensionless shape of the surface is:

$$y^* = \left(1 - \frac{S_0}{S_{av}}\right) x^{*2} + \frac{S_0}{S_{av}} x^*, \quad \text{with } 0 \leqslant S_0 < 2S_{av} \tag{39}$$

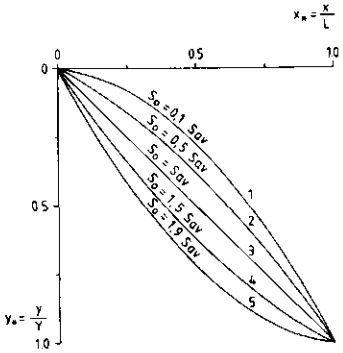

Fig. 1. Dimensionless surface profiles.

where: S_0 = slope at $x = 0$; $S_{av} = Y/L$ = average slope; $a_1 = (Y - bL)/L^2$; and $b = S_0$.

From this equation a range of possible dimensionless curves has been generated (Fig. 1).

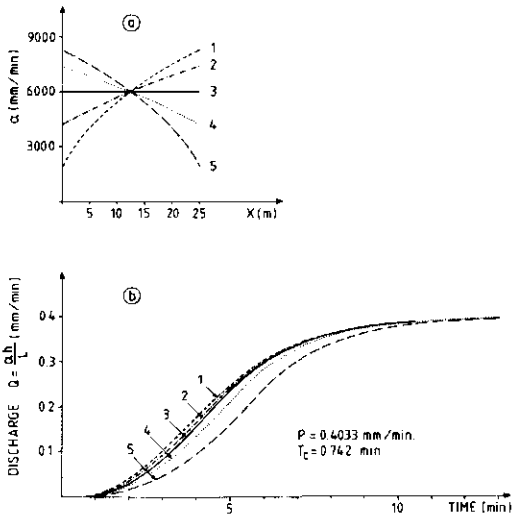

Fig. 2. (a) π as a function of position for strips of concave, plane and convex surfaces; (b) overland flow hydrographs.

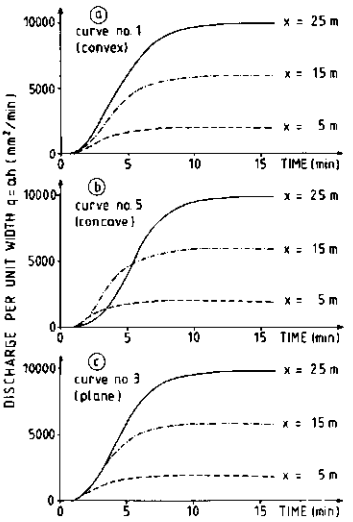

Fig. 3. Difference in response at x = 5, 15 and 25 m for the convex, concave, and plane surfaces.

The solution for unit strips of concave, convex and plane surfaces (Fig. 1) are shown in Fig. 2 for: (a) S_{av} = 1% and L = 25 m with very little surface storage; (b) loess soil with a = 0.5 min^{-1}, f_0 = 0.583 mm min^{-1}, f_c = 0.00333 mm min^{-1}; (c) constant rainfall rate of 0.4033 mm min^{-1}; and average flow velocity of 6000 mm min^{-1} which gives k = 60000 mm min^{-1}.

It is apparent from this example that, for surfaces with the same characteristics, the shape of the slope is a significant factor in determining the shape of the rising limb of the overland flow hydrograph. The difference in response in time, at three locations (x = 5, 15, and 25 m) along the slope, for the convex, concave and plane surfaces is presented in Fig. 3. Notice the relative position of the three hydrographs in each case.

CONCLUSION

An analytical solution for linearized kinematic flow on an infiltrating, parabolic shaped, surface is presented for constant rainfall rates. Thus it is possible to investigate the overland flow on different concave and convex surfaces that might be represented by a quadratic equation. The analytical solution developed is easier to utilize than numerical simulation, and can be used to calibrate numerical methods devised for more complicated cases.

ACKNOWLEDGEMENTS

Financial support of "Comissão Permanente INVOTAN" and of the University of Coimbra (Portugal) is acknowledged.

REFERENCES

Campbell, S.Y., Van der Molen, W.H., Rose, C.W. and Parlange, J.-Y., 1985. A new method for obtaining spatially averaged infiltration rate from rainfall and runoff rates. J. Hydrol., 82: 57–68.

Langford, K.J., 1975. Overland flow. In: T.G. Chapman and F.X. Dunin (Editors), Prediction in Catchment Hydrology. Aust. Acad. Sci., pp. 127–147.

Morin, J. and Benyamini, Y., 1977. Rainfall infiltration into bare soils. Water Resour. Res., 13(5): 813–817.

Parlange, J.-Y., Rose, C.W. and Sander, G., 1981. Kinematic flow approximation of runoff on a plane: an exact analytical solution. J. Hydrol., 52: 171–176.

Zarmi, Y., Asher, J.B. and Greengard, T., 1983. Constant velocity kinematic analysis of an infiltrating microcatchment hydrograph. Water Resour. Res., 19(1): 227–283.

REFERENCES

Brakensiek, D.L., 1967. Kinematic flood routing. Trans. Am. Soc. Agric. Engrs., 10(3): 340-343.

Bell, N.C., H.S. Wheater and P.M. Johnston, 1989. Evaluation of overland flow models using laboratory catchment data: II. Parameter identification of physically based (kinematic wave) models. Journal of Hydrological Sciences, 34(3): 289-317.

Constantinides, C.A., 1981. Numerical techniques for a two-dimensional kinematic overland flow model. Water SA, 7(4): 234-248.

Chow, V.T., 1959. Open channel hydraulics. McGraw Hill Book Co., New York, 680 p.

Chow, V.T., D.R. Maidment and L.W. Mays, 1988. Applied hydrology. McGraw-Hill Book Company, New York, 527 p.

Eagleson, P.S., 1970. Dynamic hydrology. McGraw-Hill Book Company, New York, 462 p.

Freeze, R.A., 1978. Mathematical models of hillslope hydrology. In: M.J. Kirkby (Ed.), Hillslope Hydrology. John Wiley & Sons, Chichester, 177-225.

Hall, M.J., P.M. Johnston and H.S. Wheater, 1989. Evaluation of overland flow models using laboratory catchment data: I. An apparatus for laboratory catchment studies. Journal of Hydrological Sciences, 34(3): 277-288.

Henderson, F.M. and R.A. Wooding, 1964. Overland flow and groundwater flow from a steady rainfall of infinite duration. J. Geophys. Res., 69: 1531-1540.

Hromadka II, T.V., R.H. McCuen and C.C. Yen, 1987. Comparison of overland flow hydrograph models. J. of Hydraulic Engineering, 113(11): 1422-1440.

Kibler, D.F. and D.A. Woolhiser, 1970. The kinematic cascade as a hydrologic model. Hydrology Paper no. 39, Colorado State University, Fort Collins, Colorado, 27 p.

Kibler, D.F. and D.A. Woolhiser, 1972. Mathematical properties of the kinematic cascade. J. of Hydrology, 13: 131-147.

Kirkby, M., 1988. Hillslope runoff processes and models. J. of Hydrology, 100: 315-339.

Lai, C., 1986. Numerical modeling of unsteady open-channel flow. In: B.C. Yen (Ed.) Advances in Hydroscience. Academic Press, Orlando, 14: 161-333.

Lane, L.J., D.A. Woolhiser and V.P. Yevjevich, 1975. Influence of simplifications in watershed geometry in simulation of surface runoff. Paper no. 81, Colorado State University, Fort Collins, Colorado, 50 p.

Leu, J.M. and C.L. Liu, 1988. Overland flow computation with the characteristics method for a kinematic catchment model. Water Resources Management 2: 269-288.

Lighthill, M.J. and Whitham, G.B., 1955. On kinematic waves: flood movement in long rivers. Proc. of the Royal Society (London), Series A, 299: 281-316.

Lima, J.L.M.P. de, 1987. Overland flow on an infiltrating surface: the model KININF. Depart. of Land & Water Use, Agricultural Univ. Wageningen, Wageningen, Internal Report No. 36, 13p.

Morris, E.M., 1981. Models of surface water flow. In: R. Lal and E.W. Russell (Eds.). Tropical Agricultural Hydrology. John Wiley & Sons, Chichester, 421-432.

Morris, E.M. and D.A. Woolhiser, 1980. Unsteady one-dimensional flow over a plane: partial equilibrium and recession hydrographs. Water Resour. Res., 16: 355-360.

Parlange, J.-Y., C.W. Rose and G.C. Sander, 1981. Kinematic flow approximation of runoff on a plane: an exact analytical solution. J. of Hydrology, 52: 171-176.

Rose, C.W., J.-Y. Parlange, G.C. Sander, S.Y. Campbell and D.A. Barry, 1983. Kinematic flow approximation of runoff on a plane: an approximate analytical solution. J. of Hydrology, 62: 363-369.

Rovey, E.W., D.A. Woolhiser and R.E. Smith, 1977. A distributed kinematic model of upland watersheds. Paper no. 93, Colorado State University, Fort Collins, Colorado, 35 p.

Saint-Venant, B. de, 1871. Theory of unsteady water flow, with application to river floods and to propagation of tides in river channels. French Academy of Science, No. 73.

Singh, V.P., 1976. Studies on rainfall-runoff modeling: 2. A distributed kinematic wave model of watershed runoff. Water Resources Research Institute, Report No. 065, New Mexico Water Resources Research Institute, New Mexico State University, La Cruces, New Mexico, 154 pp.

Singh, V.P., 1978. Mathematical modelling of watershed runoff. Int. Conf. on Water Resources Engineering (Vol. II), Asian Institute of Technology, Bangkok, Thailand, 703-726.

Singh, V.P., 1988. Hydrology systems: Rainfall-runoff modeling (Vol. 1). Prentice Hall, Englewood Cliffs, New Jersey, 480 p.

Stephenson, D. and M.E. Meadows, 1986. Kinematic hydrology and modelling. Development in Water Science, 26, Elsevier Science Publishers, Amsterdam, 250 p.

Vieira, J.H.D., 1983. Conditions governing the use of approximations for the Saint-Venant equations for shallow surface water flow. J. of Hydrology, 60: 43-58.

Wheater, H.S., N.C. Bell and P.M. Johnston, 1989. Evaluation of overland flow models using laboratory catchment data: III. Comparison of conceptual models. Journal of Hydrological Sciences, 34(3): 319-337.

Woolhiser, D.A. and J.A. Liggett, 1967. Unsteady one-dimensional flow over a plane: the rising hydrograph. Water Resour. Res. 3(3): 753-771.

Wu, Y.-H., V. Yevjevich and D.A. Woolhiser, 1978. Effects of surface roughness and its spatial distribution on runoff hydrographs. Paper no. 96, Colorado State University, Fort Collins, Colorado, 44 p.

Zarmi, Y., J.B. Asher and T. Greengard, 1983. Constant velocity kinematic analysis of an infiltration microcatchment hydrograph. Water Resources Research, 19(1): 227-283.

3 UPPER BOUNDARY CONDITIONS FOR OVERLAND FLOW

J.L.M.P. de Lima[1] and P.J.J.F Torfs[2]

[1]Assist. Lect., Dept. of Civil Engeneering, Univ. of Coimbra, Coimbra, Portugal.

[2]Lect., Dept. of Hydr. and Catchment Hydrol., Wageningen Agric. Univ., Wageningen, The Netherlands.

ABSTRACT

A laboratory experiment was done to learn more about the influence of upstream boundary conditions on the hydraulics of overland flow under rainfall. The experiment was done on an impermeable plane surface with a rainfall simulator. Results show the importance of considering upstream boundary conditions, for gentle slopes, other than the most frequently used $h(0,t)=0$ for $t\geq 0$, where $h(x,t)$ is the flow depth as a function of position x and time t.

3.1 INTRODUCTION

The solutions to equations of continuity and motion for overland flow, whether analytical or numerical, require the specification of initial and boundary conditions. The upstream boundary condition most frequently used in overland flow modelling is $h(0,t)=0$ for $t\geq 0$ (Fig. 1a), where $h(x,t)$ is the flow depth as a function of position x and time t. On watersheds with steep slopes, this condition is valid, but for moderate to gentle slopes, its validity is questionable (Singh, 1978). Mathematical tractability is perhaps one reason for its use.

The hydraulics of overland flow on smooth surfaces and the effect of simulated rainfall have been treated extensively (Yu & McNown, 1964; Yoon & Wenzel, 1971; Savat, 1977; among others). Robertson et al. (1966), Kilinc & Richardson (1973) and many other researchers, assumed an overland flow profile like the one presented in Fig. 1a. Shen & Li (1973) did experiments on overland flow over smooth surfaces caused by a constant base flow and constant rainfall rate. They studied the effect of different boundary conditions (Fig. 1b shows one of these, for a fully supercritical regime). Lima (1989a and 1989b) studied the effect of oblique rainfall on the overland flow process and verified that the impact of inclined raindrops, and the shear stress caused by wind (blowing upslope) at the water surface, can create a discharge at the upstream boundary of a plane (depending strongly on slope, rainfall

intensity, and wind speed). This implies the existence of a non-zero water depth at x=0 (Fig. 1c).

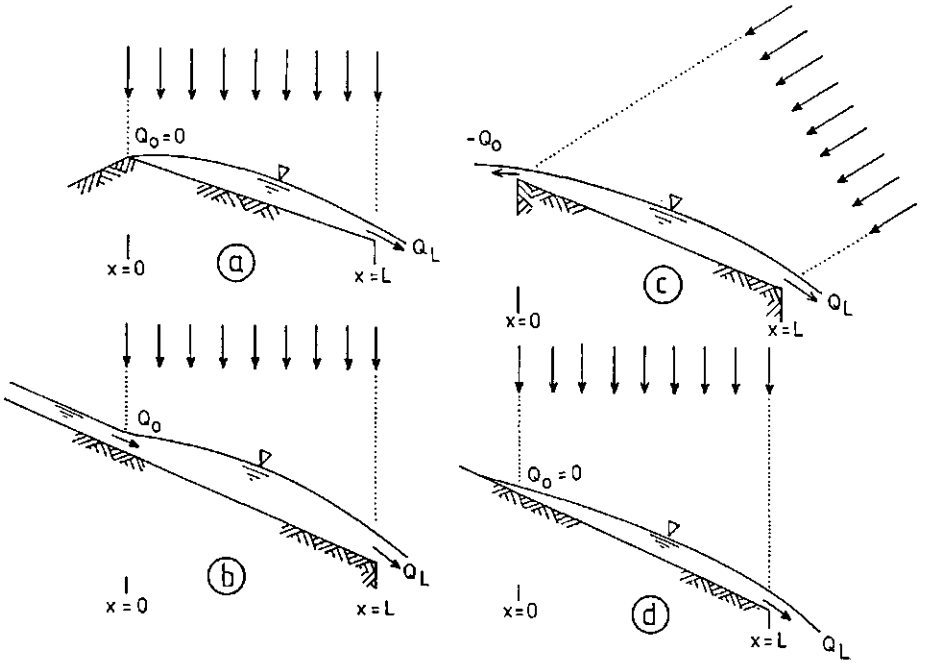

Fig. 1 Upper boundary conditions commonly used for overland flow.

To learn more about the influence of upstream boundary conditions on the hydraulics of overland flow, a laboratory experiment was undertaken. Case d (Fig. 1) was chosen for the laboratory set-up. It tries to represent saturation overland flow (Dunne & Leopold, 1978), where excess rainfall only begins at a certain distance from the top of the slope. This occurs frequently when soils become saturated at the surface because of rising water tables. The increase of water depth observed in this situation could play a role in water erosion (splash and sheet erosion) studies.

For case d, the resistance coefficients for steady uniform turbulent flow are not applicable (flow rate may be zero at x=0, but there is also a non-zero water depth), nor is the initial flow uni-directional, as water will also flow upslope at x=0 (as observed with dye tracing). Moreover, the surface tension forces on small slope gradients and shallow flows shortly after the start of the rainfall can be considerable.

3.2 LABORATORY SET-UP

The laboratory set-up was composed mainly of two units:

(1) a channel with a uniform rectangular cross section 1 m wide. The surface was impermeable (smooth concrete).

(2) a rainfall simulator (described in Lima, 1989b) consisting of circular plates and conveyors extending to the edges of the plates, where the drops are formed. The simulator generates a uniformly distributed and time invariant geometrical rainfall pattern over a length L measured along the plane (from x=0 to x=L; x=0 is defined as the upslope limit of the applied rainfall).

Primary data were collected at steady state for each simulation run (defined as the experiment conducted with fixed length, slope and rainfall intensity). They were: length (L), slope (S), rainfall intensity (P), water temperature, mean depth of flow at flume outlet (h_L), and backwater distance measured upslope of x=0 (D; see Fig. 2). The experiments were repeated for different combinations of lengths (L=3.27 and 4.72 m), slope gradients (ranging from 0.1% to 4%), and rainfall intensities (ranging from 0.0207 to 0.1528 mm/s).

The measuring procedure was the following: (1) start initial rainfall on dry surface; (2) wait until equilibrium (steady state) is reached; (3) measure primary data; (4) increase or decrease discharge and repeat steps (2) to (4). It was possible to install a splash barrier at x=0 (Fig. 2a) to prevent splash droplets from striking the surface upslope of x=0.

3.3 RESULTS

The overland flow sheet observed at steady state during the experimental runs (both with and without the upstream splash barrier) could be divided into the following sections (Fig. 2a and 2b):

(1) Highly disturbed, downslope overland flow with direct impact of raindrops and raindrop splash droplets. Dye injected into the raindrops and the overland water sheet was rapidly dispersed.

(2a) Disturbed, mainly radial flow with small circular wave formation owing to drop impact in section (1).

(2b) Disturbed, mainly radial flow with small circular wave formation owing to drop impact in section (1). Direct impact of splash droplets also existed.

(3) Stagnant water (horizontal water surface). After injection of dye, no water movement was observed (except for gradual dye diffusion).

(4) Adhesive water. Solid-liquid tensions with a contact angle ϵ were present at the bottom of the flume surface.

(5a) Wetted flume bottom (pre-wetted with a moistened cloth).

(5b) Wetted flume bottom (pre-wetted with a moistened cloth) with scattered water bubbles formed by the splash droplets.

(6) Air dry flume bottom.

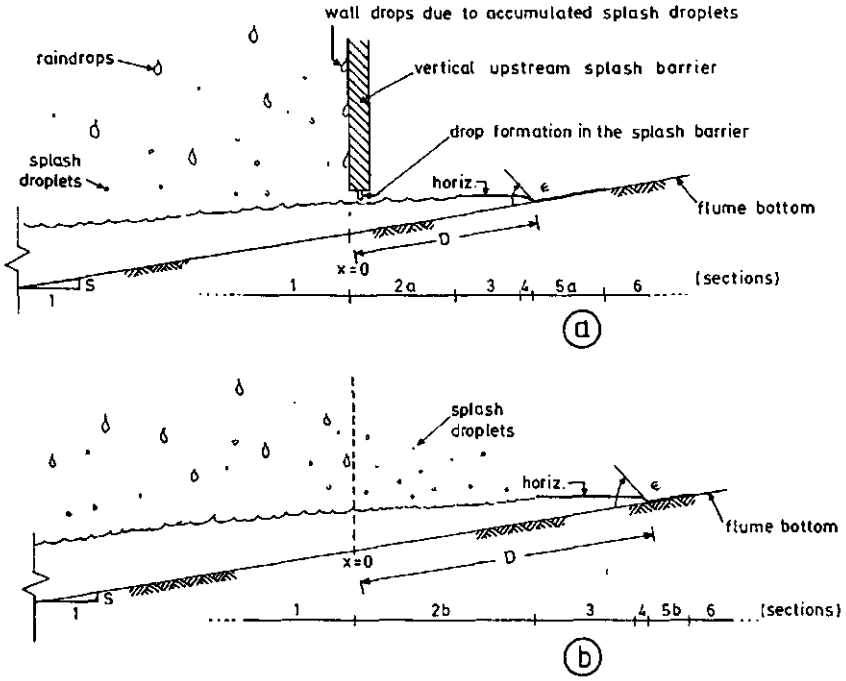

Fig. 2 Observed sections on the overland flow sheet: a) with splash barrier; b) without splash barrier.

Rainfall intensity plotted against the backwater distance, for a fixed slope, was strongly subjected to hysteresis because of surface tension effects on the flume bottom (Fig. 3). The hysteresis effect decreased as the slope gradient increased. For the 0.1 % slope, the backwater effect was pronounced, with D values exceeding 4.0 m.

The removal of the splash barrier increased D (Fig. 2). Apparently, the length L of the rainfall application had no effect on D

for either of the two lengths used. The importance of surface tension and wettability characteristics in the feasibility of scale modelling of the rainfall-surface runoff process on impermeable planes has been investigated by Graveto (1970).

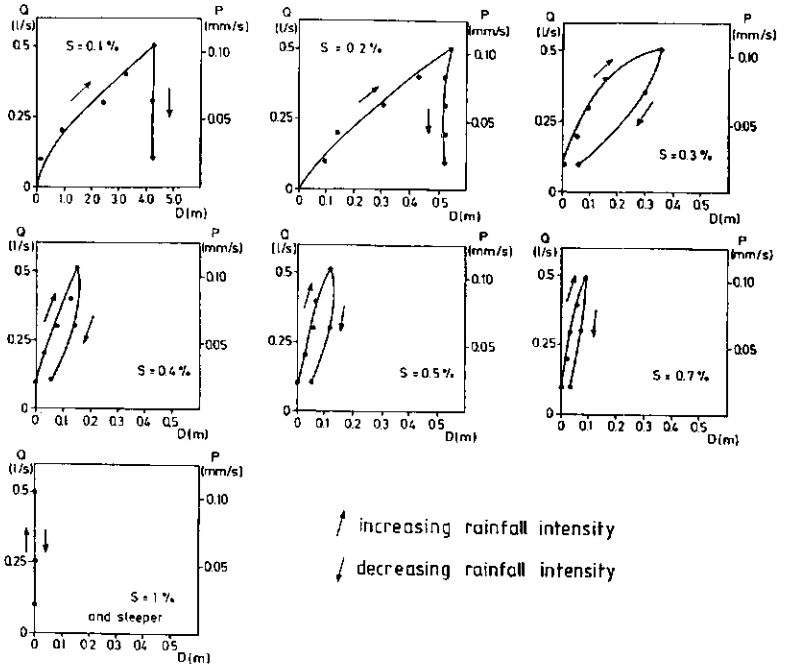

Fig. 3 Hysteresis effect in the rainfall intensity (P) - backwater distance (D) relationship, for different slopes (S).

In Fig. 4a, D was plotted against the slope in linear scales for different rainfall intensities and for L=4.72 m. For a horizontal surface (S=0), D tends to infinity at steady state. In Fig. 4b, ln(D) was plotted against 1/S for the same rainfall intensities. Linear relations were fitted with high regression coefficients. Thus, for a certain rainfall intensity, D was estimated as a function of the slope by:

$$D = C_1 \, e^{C_2/S} \qquad (1)$$

where D is the backwater distance (m), and C_1 (m) and C_2 (-) are parameters. Values of C_1 and C_2 are presented in the Table in Fig. 4.

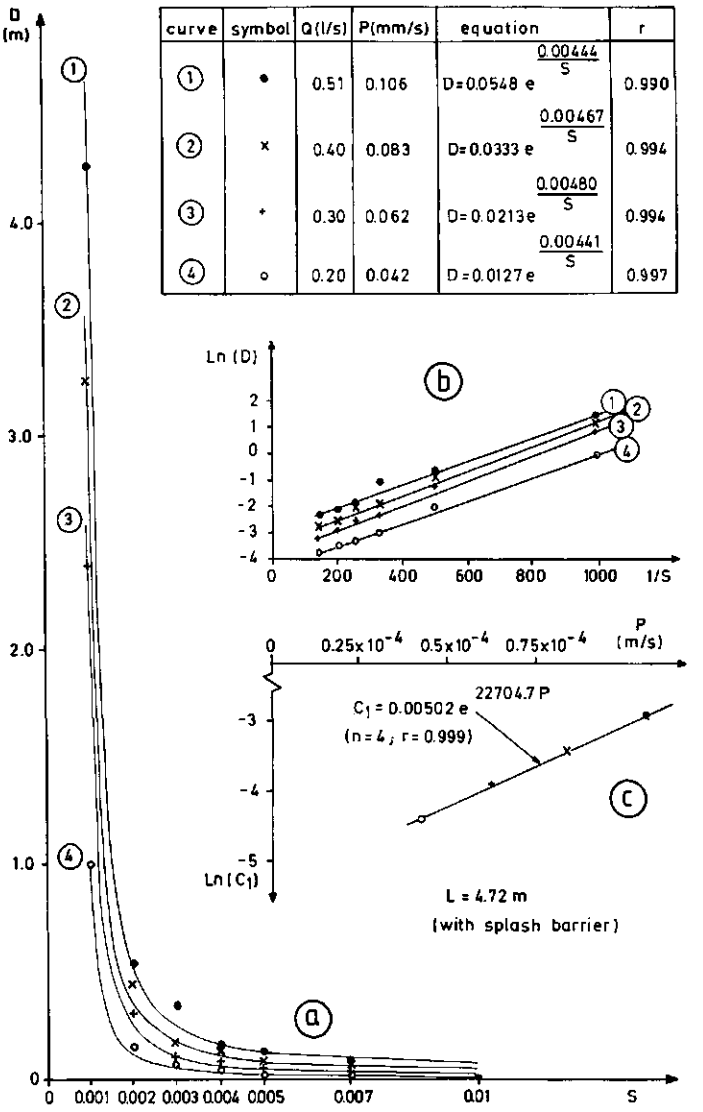

Fig. 4 (a) D-S relationship in linear scales; (b) ln(D) against 1/S; (c) $\ln(C_1)$ against P.

C_2 can be considered independent of slope and rainfall intensity because of the approximately parallel lines in Fig. 4b. Therefore the plot of $\ln(C_1)$ against P results in a straight line, defined by (Fig. 4c):

$$C_1 = C_3 \, e^{C_4 P} \qquad (2)$$

where C_3 (m) and C_4 ($m^{-1}s$) are parameters and P is the rainfall intensity ($m\ s^{-1}$).

Substitution of Eq. (2) into Eq. (1) yields an expression for D as a function of S and P:

$$D = C_3 \, e^{(C_4 P + C_2/S)} \qquad (3)$$

Parameters C_2, C_3, and C_4 were calculated by regression techniques applied to the laboratory data (smooth concrete surface): C_2= 0.00458, C_3= 0.00502 m, and C_4= 22704.7 $m^{-1}s$.

In Fig. 5, the Darcy-Weisbach friction factor (f) was plotted against D for measurements with increasing rainfall intensities (P). The following expression was used to calculate the Darcy-Weisbach friction factor (assuming that the friction slope (S_f) equals the surface slope (S)):

$$f = 8 \, g \, h \, S \, / \, v^2 \qquad (4)$$

where f is the Darcy-Weisbach friction factor (-), v is the flow velocity ($m\ s^{-1}$), g is the acceleration due to gravity ($m\ s^{-2}$), and h is the flow depth (m).

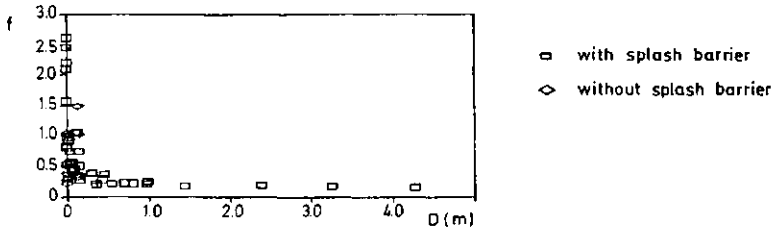

Fig. 5 The relationship between f and D.

A strong reduction of the friction factor (f) was observed for higher values of D, which is in accordance with an increase in the average water depth along the surface.

3.4 CONCLUSIONS

For gently sloping impermeable plane surfaces under vertical rainfall, care should be taken in using $h(0,t)=0$ for $t\geq 0$ as an upper boundary condition for overland flow. The observed non-zero water depth at $x=0$, and the consequent increase of water depth over the surface, radically change the overland flow process over the slope. The form of the f-D relationship and (indirectly) of the f-Re relationship, which are of fundamental importance to the mathematical modelling of overland flow, were affected. The implication of these results for overland flow modelling will be the subject of future work.

Because of the importance of surface tension forces as one of the factors that affect shallow flow processes, additional research could focus on the effects of roughness and surface wettability characteristics.

Acknowledgement

The authors wish to thank Prof. W.H. van der Molen for his helpful suggestions and "Comissão Permanente INVOTAN" for financial support. The first author is very grateful to the University of Coimbra (Portugal) for the permission and partial support of his stay at the Agricultural University Wageningen, where the research was carried out.

REFERENCES

Dunne, T. & L.B. Leopold (1978) "Water in the environment planning". Freeman, San Francisco, 818 p.

Graveto, V.M. do N. (1970) "Scale effects in the physical modeling of surface runoff". Ph.D. thesis, Depart. Civil Eng., Massachusetts Institute of Technology, 328 p.

Kilinc, M. & E.V. Richardson (1973) "Mechanism of soil erosion from overland flow generated by simulated rainfall". Hydrology Papers No. 63, Colorado State University, Fort Collins, Colorado, 54 p.

Lima, J.L.M.P. de (1989a) "The influence of the angle of incidence of the rainfall on the overland flow process". In: Kavvas, M.L. (ed.), New directions for surface water modeling, IAHS publ. 181., 73-82.

Lima, J.L.M.P. de (1989b) "Overland flow under wind-driven rain". Proc. 11th International Congress on Agricultural Engineering, Dublin, Ireland, 4-8 September 1989 (in press).

Robertson, A.F., A.K. Turner, F.R. Crow & W.O. Ree (1966) "Runoff from impervious surfaces under conditions of simulated rainfall". Trans. ASAE, 9(3), 343-351.

Savat, J. (1977) "The hydraulics of sheet flow on a smooth surface and the effect of simulated rainfall". Earth Surface Processes, 2, 125-140.

Singh, V.P. (1978) "Mathematical modelling of watershed runoff". Int. Conf. Water Res. Eng., Bangkok, 703-726.

Shen, H.W. & R.W. Li (1973) "Rainfall effect on sheet flow over smooth surfaces". J. Hydr. Div., ASCE, 99(5), 771-792.

Yoon, Y.N. & H.G. Wenzel (1971) "Mechanics of sheet flow under simulated rainfall". J. Hydr. Div., ASCE, 97: 1367-1386.

Yu, Y.S. & J.S. McNown (1964) "Runoff from impervious surfaces". J. of Hydr. Research, IAHR, 2(1), 2-24.

4 A KINEMATIC OVERLAND FLOW MODEL TO DETERMINE DEPRESSION STORAGE OF TILLED SURFACES

Accepted for publication (31 March, 1989) in Journal of Soil & Tillage Research, Elsevier Science Publishers B.V., Amsterdam.

4. A KINEMATIC OVERLAND FLOW MODEL TO DETERMINE DEPRESSION STORAGE OF TILLED SURFACES

J.L.M.P. de LIMA, L.A.A.J. EPPINK and W.H. van der MOLEN

Agricultural University Wageningen, Department of Land and Water Use, Nieuwe Kanaal 11, 6709 PA Wageningen (The Netherlands)

ABSTRACT

A method of predicting a spatial average value for depression storage of tilled surfaces is proposed. The method is based on the kinematic flow approximation to overland flow on a plane proposed by Rose et al., 1983.

In the laboratory, only the aspects of tillage, rainfall intensity and slope were investigated. The following impermeable models, simulating various tillage techniques, were used: plastic corrugations, concrete ridges, concrete mounds and concrete plane surface as reference. The experiments were repeated for each tillage model with different slopes (varying from 0.5% to 4%), and for each slope with different rainfall intensities (varying from 0.009 to 0.109 mm s^{-1}).

The method was verified by comparing predicted depression storage with depression storage obtained from water-balance considerations based on the experimental data. It is believed that the model can be used to estimate spatial average depression storage if infiltration is known.

4.1 INTRODUCTION

Depression storage as a result of tillage may be of considerable importance in the assessment of water erosion. Infiltration, evaporation, solar radiation reflection, runoff retardation, and other phenomena such as air exchange with the atmosphere have been shown to be closely related with roughness of the soil surface (Linden and Doren, 1986; Zobeck and Onstad, 1987).

The complexity of the process of depressional storage makes it very difficult to find exact solutions based on hydrodynamics, because of the complex boundary conditions. Several researchers have used microrelief measurements to estimate depression storage (Mitchell and Jones, 1976, 1978; Moore and Larson, 1979; Onstad, 1984; Linden and

Doren, 1986; Römkens and Wang, 1986; Lehrsch et al., 1988, etc). Others like Gayle and Skaggs (1978) measured depression storage by sealing the soil surface in small plots and determining the amount of water that could be applied before runoff began.

The work presented here attempts to evaluate a spatial average value for depression storage of tilled surfaces. Conceptual models of the influence of slope steepness on depression storage owing to soil tillage have been elaborated by Eppink (1978). Recent research findings support the view that depression storage decreases with decreasing soil surface roughness and increasing slope steepness (Onstad, 1984).

The complexity of surface depression storage makes simplification from a theoretical and practical point of view imperative, as a means of obtaining a quantitative estimate. In this study, only the aspects of tillage, rainfall intensity and slope are investigated. Its main objective is thus to evaluate the storage capacity of different surfaces, simulating various tillage models, as a function of slope and rainfall intensity. The following impermeable tillage models were used: plastic corrugations, concrete ridges, concrete mounds (in two different arrangements) and concrete plane surface as reference. The various parameters involved are shown in Fig. 1.

Further, the flow resistance of the different tillage models was briefly analysed.

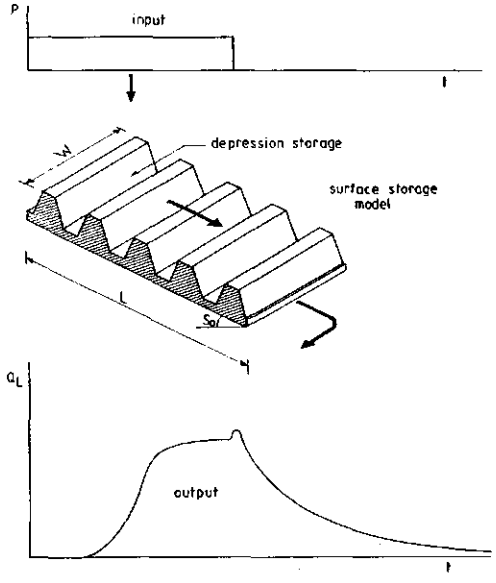

Fig. 1 Sketch of the laboratory experiments with indication of input, output and parameters involved in this study: Q_L is the outflow intensity at x=L, p is the rainfall intensity, t is the time, L is the lenght, W is the width and S_o is the slope gradient of the surface storage model.

4.2 THEORY

Figure 2 illustrates the time sequence of events involved in this particular experiment (relative intensities and cumulative amounts against time). The temporary increase of outflow discharge before the recession will be explained later. Depression storage is the amount of rainfall water held in surface depressions whereas detention storage refers to the amount of water in transit, gradually moving downslope by overland flow. The latter either runs off or is absorbed by "infiltration" after the end of the rainfall. The "infiltration" term represents the sum of all losses owing to evaporation and wetting of the model surface. Moreover, some leakage occurred in the experiment. This explains why some outflow discharge continued to occur after the recession of the detention storage (Fig. 2).

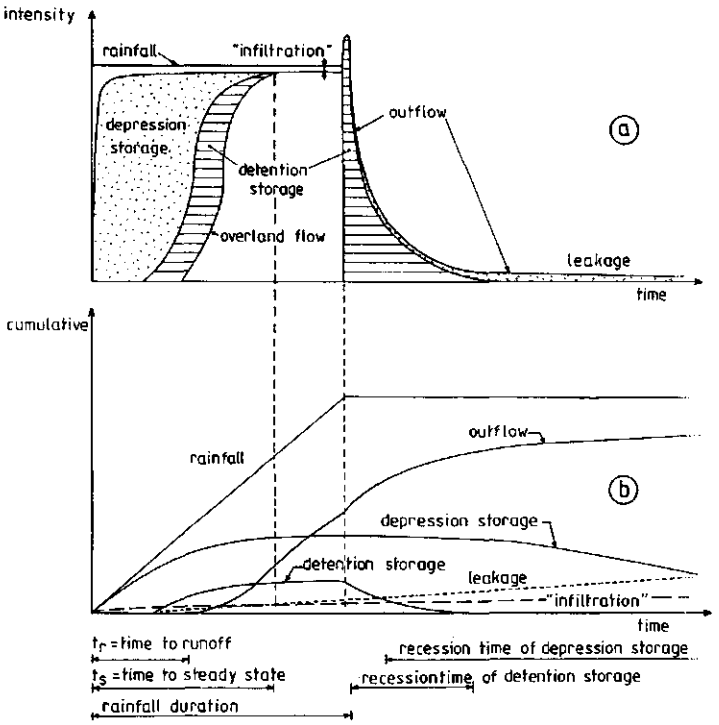

Fig. 2 Illustration of the time sequence of events observed in the experimental runs: (a) intensity versus time; and (b) cumulative quantities versus time.

4.2.1 BASIC EQUATIONS

The basic differential equation for overland flow on a plane under the kinematic wave assumption is:

$$\delta h/\delta t + \delta q/\delta x = R(t) \qquad (1)$$

where h is the depth of flow (m), q is the volumetric water flux per unit plane width ($m^2 s^{-1}$), R(t) is the excess rainfall rate, assumed to be a function of time only ($m\ s^{-1}$), t is the time (s), and x is the distance from top of plane (m).

By assuming that the friction slope equals the bed slope (kinematic wave assumption) and by using existing open-channel flow friction equations we can express the discharge at any point and time as a function of the water depth only, as follows:

$$q = \alpha\, h^{m} \qquad (2)$$

where m is a parameter depending on the flow regime, laminar or turbulent (approximately 5/3 for turbulent flow and 3 for laminar flow), and α is a hydraulic coefficient.

4.2.2 APPROXIMATE ANALYTICAL METHOD

The excess rainfall, R(t), can be defined as:

$$R(t) = p(t) - i(t) - D_S(t) \qquad (3)$$

where p(t) is the rainfall intensity ($m\ s^{-1}$), i(t) is the infiltration rate ($m\ s^{-1}$), and $D_S(t)$ is the rate of depression storage ($m\ s^{-1}$).

Rose et al. (1983) gave an approximate kinematic solution for overland flow on a plane. The approximate relationship between excess rainfall and runoff $q(L) = Q_L L$ was given by:

$$R(t) = Q_L + [m/(m+1)](L/\alpha)^{1/m}(dQ_L^{1/m}/dt) \qquad (4)$$

where Q_L is the outflow intensity at x=L ($m\ s^{-1}$), and can be regarded as the runoff transform of the excess rainfall, and L is the length of the plane (m).

If runoff and rainfall rate are measured and infiltration is predicted, the rate of depression storage can be approximated numerically in time by:

$$\overline{D}_{S_j} = \overline{p}_j - \overline{i}_j - \overline{Q}_{L_j} - [m/(m+1)](L/\alpha)^{1/m}[(Q_{L_j}^{1/m} - Q_{L_{j-1}}^{1/m})/\Delta t] \quad (5)$$

where Δt is the time interval between consecutive times (j-1) and j, and $\overline{X}$ denotes an averaging in Δt of the entity X.

This quasi-steady state approach is exact only at steady state. The average detention storage at steady state per unit area ($\delta h/\delta t=0$ and $h=(Rx/\alpha)^{1/m}$ from equations 1 and 2) is given by (Moore, 1985):

$$\overline{h} = (1/L)\int_0^L h\,dx = [(R/\alpha)^{1/m}/L]\int_0^L x^{1/m}\,dx = [m/(m+1)]\,h_L \quad (6)$$

where h_L is the flow depth at x=L (m).

Thus the shape factor of detention storage for steady state flow condition is m/(m+1). The actual, non-steady shape of the water surface is replaced by a series of steady state profiles for each of which eq. 6 is supposed to hold. Other shape factors have been derived by Moore (1985) and Moore and Kinnell (1987).

4.2.3 APPLICATION TO IMPERMEABLE SURFACES

In the particular solution for impermeable surfaces (i(t)=0), a simplified solution can be obtained considering Δt as the time interval from the beginning of overland flow to steady state condition:

$$\overline{D}_S = \overline{p} \qquad \text{for } 0 < t \leq t_r \quad (7)$$

and

$$\overline{D}_S = \overline{p} - \overline{Q}_L - [m/(m+1)](L/\alpha)^{1/m}\, Q_L(\text{steady state})^{1/m}/(t_s - t_r)$$

$$\text{for } t_r \leq t \leq t_s \quad (8)$$

with

$$\overline{Q}_L = [1/(t_s - t_r)]\int_{t_r}^{t_s} Q_L(t)dt \quad (9)$$

where (t_s-t_r) is the time interval from the start of runoff at x=L (t_r) to steady state situation (t_s).

The average outflow intensity up to steady state, $\bar{Q}_L$, is determined directly from the outflow hydrograph.

The depression storage, taking into consideration the values of $D_S(t)$ before and after time t_r, is calculated from the expression:

$$V_s = [\ \bar{p}\ t_r + \bar{D}_S\ (t_s - t_r)\ ]\ L\ W \qquad (10)$$

where V_s is the spatial average value of depression storage (m^3), and W is the width of the plane (m).

4.2.4 FLOW RESISTANCE FORMULAE

The resistance to overland flow may be expressed by the Darcy-Weisbach friction factor, f, defined as (Abrahams et al., 1986):

$$f = 8\ g\ R_h\ S_e\ /\ v^2 \qquad (11)$$

where g is the acceleration due to gravity ($m\ s^{-2}$), S_e is the energy gradient (-), R_h is the hydraulic radius (m), and v is the mean flow velocity across a section ($m\ s^{-1}$).

The nature of the flow is usually determined by referring to the empirical Reynolds number, Re, which is defined as:

$$Re = 4\ v\ R_h\ /\ \nu \qquad (12)$$

where ν is the kinematic fluid viscosity ($m^2\ s^{-1}$).

Turner et al. (1985) quoted limits for turbulent flow as Re>1500 and laminar as Re<375, with transitional and mixed phases in between. However, these limits are not universally accepted.

4.3 DESCRIPTION OF THE LABORATORY EXPERIMENT

4.3.1 LABORATORY SET-UP

The laboratory experiment was carried out in the Hydraulic Laboratory of the Department of Hydraulics and Catchment Hydrology of the Wageningen Agricultural University (The Netherlands) (Etse and Lima, 1987).

The hydraulic layout of the experiments is shown in Fig. 3.

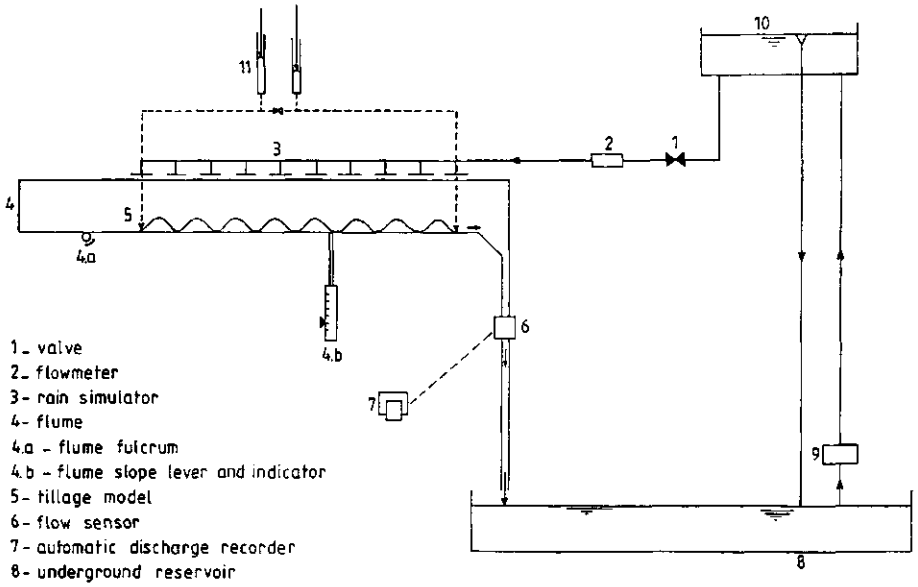

Fig. 3 Hydraulic layout of the experiments.

The laboratory set-up is mainly composed of two units:

- A channel, with an uniform rectangular cross section of 1.02 m width, in which the tillage model is installed. The slope of the channel can be adjusted as required with the aid of a jack.

- A rainfall simulator, consisting of circular plates with conveyors to the edges of the plates where the drops are formed. The rainfall simulator gives a uniform distribution and time invariant geometrical rainfall pattern. Drop shape differed significantly from the equilibrium shape at terminal velocity owing to oscillations after release from the drop formers and small drop fall height (Epema & Riezebos, 1983 and 1984). The equivalent diameter of the drops (defined as the diameter of a spherical drop with the same mass) was rather large at the drop formers (up to 8 mm). However, most simulated drops broke up in falling.

4.3.2 TILLAGE MODELS

The goal of this experiment was an analysis of the influence of the shape of tilled soil on depression storage immediately after soil preparation. The micro-relief of tilled land is subject to continuous changes due to subsidence of the loosened soil and to erosion, which leads to cutting of the ridges and filling of the furrows. As these changes in shape would make repetitions of measurements impossible, 4 well defined forms have been used, representing 3 idealized original stages at preparation and a plane surface as reference. A brief description of each tillage model is as follows (see Fig. 4):

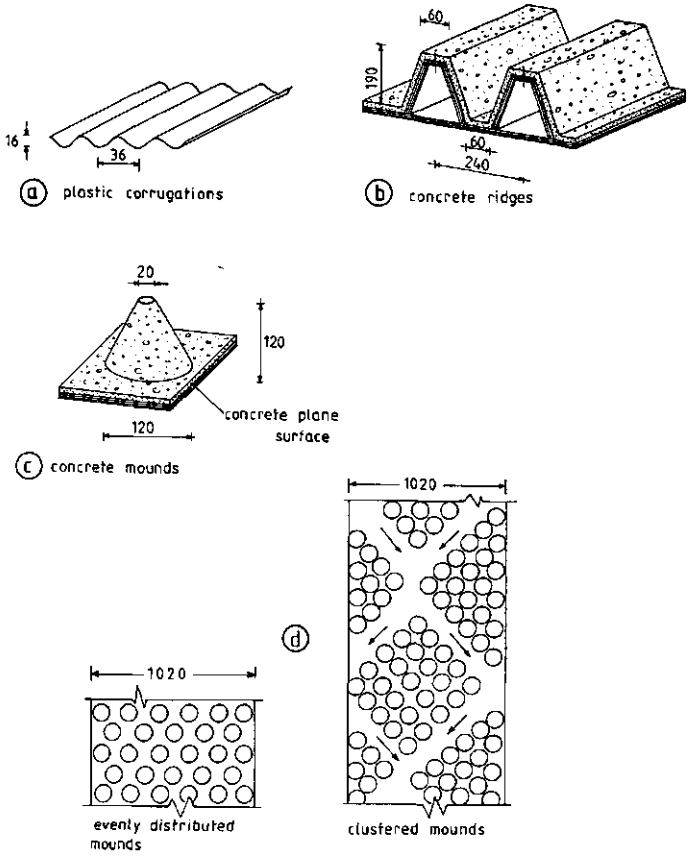

Fig. 4 The tillage models: (a) plastic corrugations; (b) concrete ridges; (c) concrete mounds; and (d) arrangement of mounds (evenly distributed and clustered).

a. Corrugations

Industrial corrugated plastic sheets (commonly used for roofing) were choosen to represent a soil treated with a corrugated roller, e.g. with a Cambridge roller which gives about 8-12 corrugations m^{-1} with a depth of about 50 mm (Krause et al., 1984). The plastic corrugation (27 corrugations m^{-1}) may be considered as a 1:3 scale model.

The total length of the material used in this laboratory experiment was 9.5 m. The corrugations were placed perpendicular to slope direction in the flume. The corrugations then acted as a storage during a rainfall event.

These corrugations are representative of a typical harrowed soil surface for cereal cultivation, such as maize, sorghum, millet. This condition is only possible in mechanized agriculture. With manual implements, a higher degree of geometrical imperfection results.

b. Ridges

In order to prevent soil erosion, contour ridges are practiced for small root crops like potatoes, onions and sugarbeets. Bigger ridges are applied in sugarcane growing. In improved agriculture, where some degree of mechanization has been introduced, yam is often planted on ridges. These ridges are commonly spaced 1-1.2 m apart. The higher and broader the ridge, the better (Onwueme, 1978).

Ridges constructed of concrete using plywood and wire netting, as reinforcement, were placed perpendicular to the slope in the flume, depicting contour furrows. The furrows act as a number of micro-reservoirs in series. The length of the tillage model was 4.8 m.

c. Mounds

Cassava cultivation on mounds is quite common in the semi-arid and sub-humid climates of Africa. They range in height from 0.3 to 0.6 m and are spaced from 0.8 to 1 m (Onwueme, 1978).

Cones, of base diameter 120 mm and apex diameter 20 mm, were made from concrete and placed on a plane concrete surface. These cones are about 1:4 scale models of typical mounds used for cultivation of large root crops.

There exists a wide variety of arrangements in the layout of mounds in cultivation practice, from regular geometric to irregular patterns. In this study two different arrangements of the mounds were used:

i) 6 mounds per unit width alternating with 5 mounds per unit width

of the tillage model, resulting in an even distribution. The mounds (165 in total) were equally spaced from each other. The total length of the tillage model was 4.8 m.

ii) Clustered mounds (214 in total) were placed in such a way as to create a preferential meandering water path as shown in Fig. 4. The length of the tillage model was 4.8 m.

In the laboratory flume, a thin sheet of water may flow downslope with little variation of depth in the cross-slope direction. However, topographic irregularities that occur on natural slopes are sufficient to direct most overland flow water into lateral concentration of flow. Arrangement ii) of the mounds tried to create a preferential meandering water path.

d. Plane surface

To serve as a control for the measurements of the various tillage models described above, a plane concrete surface was also tested.

4.3.3 HYDRAULIC MEASUREMENTS

The rainfall intensity has been measured by a flowmeter. At steady state the rainfall intensity was checked against a volumetric discharge measurement (i.e. a weighing drum and a stopwatch). The range of possible rainfall intensities varied from 0.009 to 0.109 mm s^{-1}.

The outflow hydrograph was registered by a magnetic flow sensor connected to an automatic continuous recorder.

At steady state, the difference in water height between the beginning and end of the tillage models was measured with the help of two point gauges installed within stilling wells.

The experiment was repeated for each tillage model (corrugations, furrows, mounds and plane surface), with different slopes (0.5, 1, 2, 3 and 4%), and each slope with different rainfall intensities (varying from 0.009 to 0.109 mm s^{-1}).

4.4 RESULTS

Primary data collected for each simulation run (defined as the experiment conducted with fixed tillage model, slope and rainfall intensity) were: slope, rainfall intensity, water temperature, mean depth of flow at flume outlet at steady state and overland flow in time also at flume outlet.

For the 4 tillage types, the Darcy-Weisbach friction factor, f, was plotted against Reynolds number, Re, on log-log axis in Fig. 5. Linear fitting was applied by the standard least squares procedure.

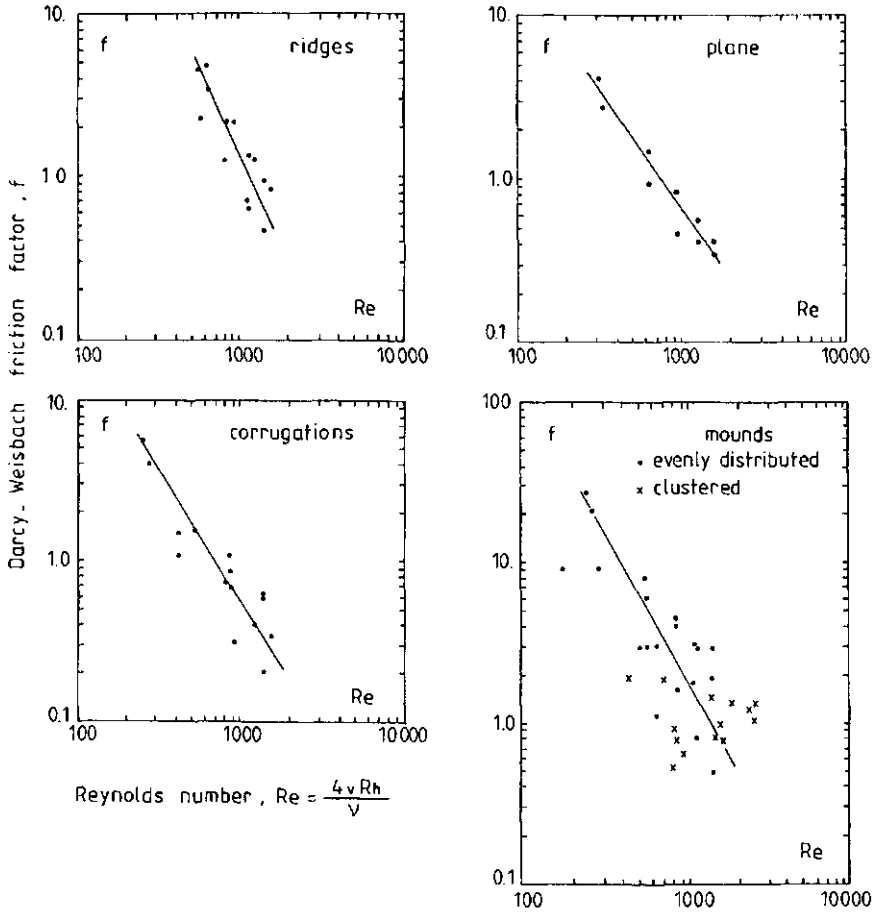

Fig. 5 Darcy-Weisbach friction factor (f) versus Reynolds number (Re), for the different tillage models.

For the different tillage models the rainfall intensity, p, was also plotted against Reynolds number, Re, for steady state conditions, in Fig. 6. Although the values of the flow regime parameter, m, systematically gave values of approximately 5/3 ($1.663 \leq m \leq 1.810$) for all the simulation runs indicating in general turbulent flow, Reynolds number fluctuated greatly. According to the limits quoted by Turner et al. (1985), the flow regime would be mainly transitional.

From Fig. 6 and owing to the small depth of flow, it is observed that Re is highly dependent not only on the rainfall intensity but also on the type of material of the tillage model (rough concrete or smooth plastic surface). Also the available area for overland flow strongly affects the relation p-Re, in Fig. 6 (compare the concrete plane and the concrete mounds).

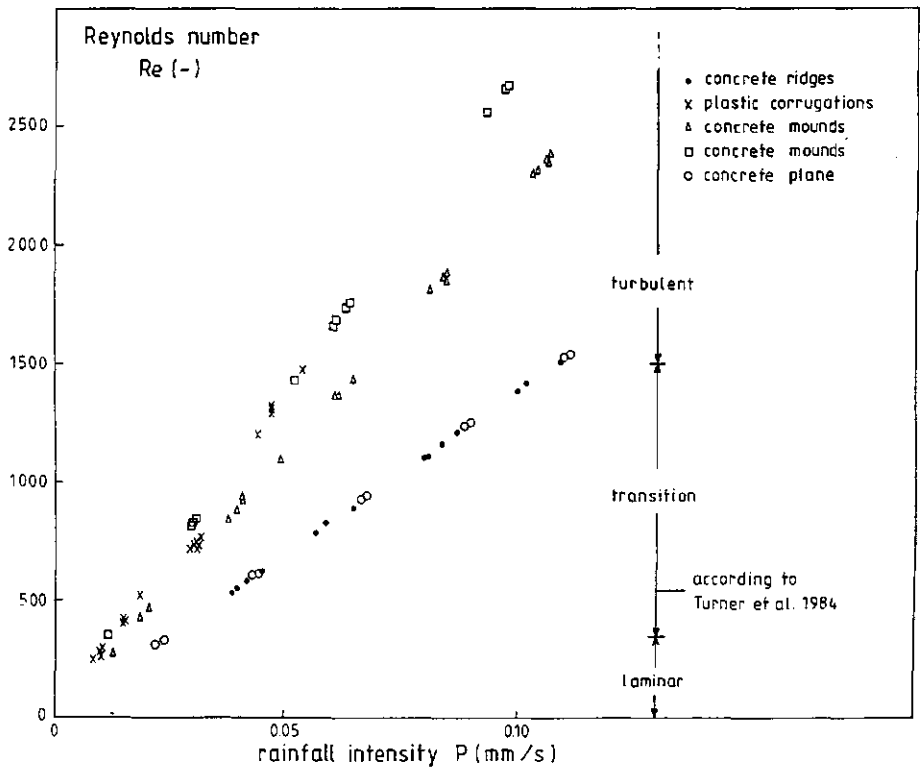

Fig. 6 Reynolds number (Re) versus rainfall intensity (p), for the different tillage models.

As shown in Figures 1 and 2, when rainfall stops outflow discharge increased temporarily before recession. This phenomenon can be explained by the fact that the stopping of raindrop impact causes a change in the friction slope and the energy gradient line, owing to the reduction in the resistance coefficient to a lower value (different dissipation of energy). As a consequence, the outflow has a momentary increase. This peak was not always observed in the outflow hydrograph.

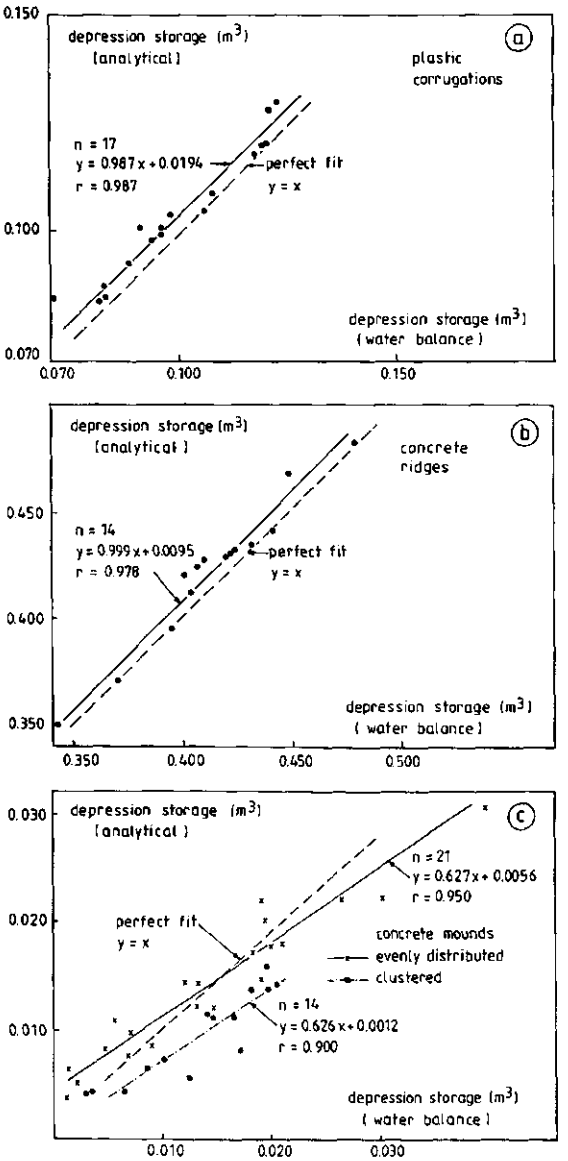

Fig. 7 Depression storage (analytical) versus depression storage from water balance considerations for the different tillage models: (a) plastic corrugations; (b) concrete ridges; (c) concrete mounds (evenly distributed and clustered).

The depression storage, V_s, calculated using eq. 10, was plotted against the values obtained from water balance considerations, for all the tillage models (Fig. 7). The values of m, α, t_r, t_s and Q_L used were obtained from the experimental data. The approximate kinematic theory appears sufficiently accurate for the determination of depression storage of impermeable surfaces.

Clustered mounds gave an underestimation of the depression storage in comparison with the evenly distributed mounds (Fig. 7c). This may be due to a lesser suitability of the kinematic-wave assumptions for the case of the clustered mounds.

In Fig. 8, depression storage determined analytically, V_s, was plotted against slope for the evenly distributed mounds. By linear fitting, lines were drawn connecting points within specified rainfall intensity intervals. As expected the Figure shows that depression storage decreases with increasing slope.

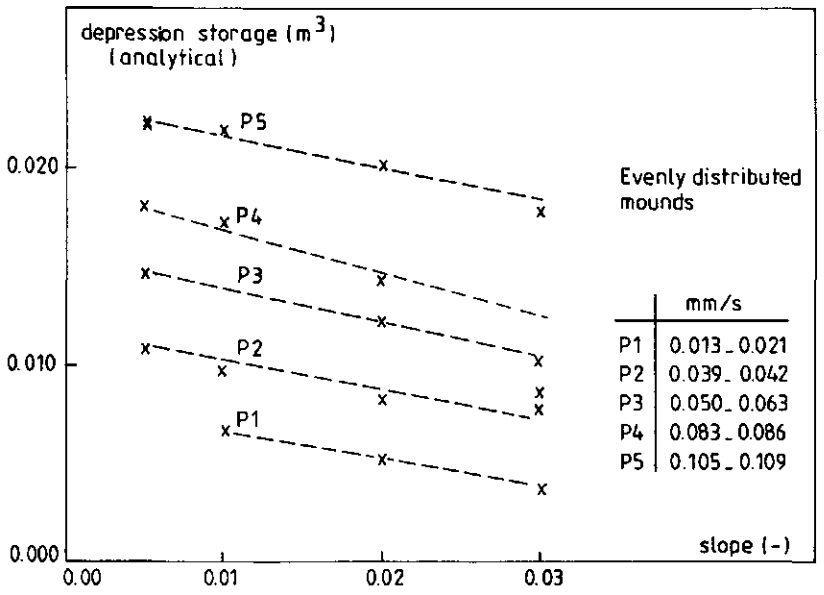

Fig. 8 Depression storage (analytical) versus slope (S_o) for different rainfall intensities (p) and for the evenly distributed mounds.

4.5 CONCLUSION

Surface depression storage is a very complex natural process. A method for determining average spatial values for depression storage from outflow measurements has been developed using simplified assumptions. The depression storage, V_s, of tilled surfaces derived from quasi-steady mathematical analysis of the rainfall-runoff process by means of the kinematic wave equations checked well with the value of depression storage obtained from water-balance considerations.

It is believed that the model can be used for the estimation of a spatial average depression storage if infiltration is predicted. Field data are required to evaluate fully the suitability of this formulation to evaluate depression storage of tilled soil surfaces.

ACKNOWLEDGEMENTS

The authors wish to thank the staff of the Hydraulics Laboratory of the Department of Hydraulics and Catchment Hydrology of the Agricultural University Wageningen for their assistance. This work is the completion of a laboratory experiment carried out by S.K. Etse and the authors from March to June, 1987.

Financial support of "Comissão Permanente INVOTAN" and of the University of Coimbra (Portugal) is acknowledged.

REFERENCES

ABRAHAMS, A.D., PARSONS, A.J. and LUK, S.H., 1986. Resistance to overland flow on desert hillslopes. J. Hydrol., 88: 343-363.

EPEMA, G.F. and RIEZEBOS, H.Th., 1983. Fall velocity of waterdrops at different heights as a factor influencing erosivity of simulated rain. In: J. de Ploey (Ed.), Rainfall simulation, runoff and soil erosion. Catena Supplement 4, Catena Verlag, Cremlingen-Destedt, W. Germany, 2-17.

EPEMA, G.F. and RIEZEBOS, H. Th., 1984. Drop shape and erosivity Part I: experimental set up, theory, and measurements of drop shape. Earth Surfaces Processes and Landforms, 9: 567-572.

EPPINK, L.A.A.J., 1978. Introduction to soil erosion and conservation, Lecture notes. Department of Land & Water Use, Wageningen Agricultural University, 248 pp.

ETSE, S.K. and LIMA, J.L.M.P. de, 1987. Determination and analysis of surface depression storage and overland flow of different tillage models as a function of slope and rainfall intensity. M.Sc. Thesis, Agricultural University Wageningen, 43 pp.

GAYLE, G.A. and SKAGGS, R.W., 1978. Surface storage on bedded cultivated lands. Trans. Am. Soc. Agric. Eng., 21: 101-109.

KRAUSE, R., LORENZ, F. and HOOGMOED, W.B., 1984. Soil tillage in the tropics and subtropics. Schriftenreihe der GTZ No.150, pp. 189-194.

LEHRSCH, G.A., WHISLER, F.D. and RÖMKENS, M.J.M., 1988. Selection of a parameter describing soil surface roughness. Soil Sci. Soc. Am. J., 52: 1439-1445.

LINDEN, D.R. and DOREN Jr., D.M. Van, 1986. Parameters for characterizing tillage-induced soil surface roughness. Soil Sci. Soc. Am. J., 50: 1560-1565.

MITCHELL, J.K. and JONES Jr., B.A., 1976. Micro-relief surface depression storage: analysis of models to describe the depth-storage function. AWRA Water Resources Bull., 12: 1205-1222.

MITCHELL, J.K. and JONES Jr., B.A., 1978. Micro-relief surface depression storage: changes during rainfall events and their application to rainfall runoff models. AWRA Water Resources Bull., 14: 777-802.

MOORE, I.D., 1985. Kinematic overland flow: generalization of Rose's approximate solution. J. Hydrol., 82: 233-245.

MOORE, I.D. and LARSON, C.L., 1979. Estimating micro-relief surface storage from point data. Trans. Am. Soc. Agric. Eng., 22: 1073-1077.

MOORE, I.D. and KINNELL, P.I.A., 1987. Kinematic overland flow: generalization of Rose's approximate solution, part II. J. Hydrol., 92: 351-362.

ONSTAD, C.A., 1984. Depression storage on tilled soil surfaces. Trans. Am. Soc. Agric. Eng., 27: 729-732.

ONWUEME, I.C., 1978. The tropical tuber crops. English Language Book Society and John Wiley & Sons, Chichester, XIV + 234 pp.

RÖMKENS, M.J.M. and WANG, J.Y., 1986. Effect of tillage on surface roughness. Trans. Am. Soc. Agric. Eng., 29: 429-433.

ROSE, C.W., PARLANGE, J.-Y., SANDER, G.C., CAMPBELL, S.Y. and BARRY, D.A., 1983. Kinematic flow approximation to runoff on a plane: an approximate analytic solution. J. Hydrol., 62: 363-369.

TURNER, A.K., McMAHON, T.A. and SRIKANTHAN, R., 1985. Rainfall intensity and overland flow in relation to erosion studies for tropical lands. In: E.T. Craswell, J. V. Remenyi and L.G. Nallana (Eds.) Soil Erosion Management, Proceedings of Workshop held at PCARRD, Los Baños (1984), ACIAR Proceedings Series, No.6: 24-31.

ZOBECK, T.M. and ONSTAD, C.A., 1987. Tillage and rainfall effects on random roughness: a review. Soil Tillage Res., 9: 1-20.

5 OVERLAND FLOW AND INFILTRATION

5.1 INTRODUCTION

Infiltration concerns the movement of water into the soil. The process is affected by the surface entry, the transmission through the soil and the depletion of storage capacity in the soil. It is governed by soil texture and structure and indirectly by the vegetation covering the soil surface. A general approach to solve infiltration problems requires simultaneous solution of the equations describing the process of energy and mass transfer in a complex system embracing all the zones of water movement in the liquid and vapour phases (Maniak, 1982).

The infiltration concepts applied in overland flow models may be considered as a compromise, as they must be comprehensive and practical. Therefore factors of secondary importance, such as temperature and concentration of dissolved substances, must be neglected. Thus, simplified water transport models of one dimension are mostly used.

Literature gives a distinct impression that overland flow and infiltration have been extensively studied as separate components (Woolhiser and Liggett, 1967; Kibler and Woolhiser, 1970 and 1972; Singh, 1975). The conventional approach has been through the rainfall-excess concept (Singh, 1978):

$$\begin{cases} R(x,t) = p(x,t) - i(x,t) & \text{for } p(x,t) > i(x,t) \\ R(x,t) = 0 & \text{for } t \leq 0 \\ R(x,t) > 0 & \text{for } 0 < t < T \\ R(x,t) = 0 & \text{for } t \geq T \end{cases} \qquad (1)$$

where R is the rainfall excess (m/s), p is the rainfall rate (m/s), i is the infiltration rate (m/s), t is the time since the beginning of the rainfall excess (s) and T is the duration of rainfall excess (m).

The concept of rainfall excess is more of an artifice than a reality (Singh, 1978). Although equation (1) describes the principle of mass conservation, and is useful as such, it neglects the dynamics of both infiltration and surface runoff. The processes of overland flow and infiltration occur simultaneously in nature during and after the occurrence of rainfall. What is required in overland flow modelling is a combined study of these two components. Infiltration is generally considered independent of overland flow resulting in weak coupling of the two processes, i.e. infiltration influences overland flow, but not vice versa. Up to the time of ponding, computed infiltration rates with and without accounting for overland flow depth are, of course, identical. Once ponding has occurred, there is a rise in water depth which may affect the infiltration rate. Several studies that combine physically-based models of both overland flow and infiltration components can be found in the literature (Foster et al., 1968; Smith and Woolhiser, 1971a and 1971b; Akan and Yen, 1981; Akan, 1985a, 1985b, 1988; Lima, 1987b; among others).

Infiltration equations are still widely used to estimate the rate of production of Hortonian overland flow. On real surfaces microtopography and soil heterogeneity can modify the mean infiltration rate. In this thesis the rainfall excess concept has been used in Chapters 4 and Sections 2.4 and 7.1. In Chapter 2.4 a Horton type of equation was used for the infiltration process (Morin and Benyamini, 1977):

$$i(t) = f_c + (f_o - f_c)e^{-at} \qquad \text{with} \quad f_c < p \leq f_o \tag{2}$$

where a is a parameter (s^{-1}), f_o is the initial infiltration rate of the soil (m/s), and f_c is the final infiltration rate of the soil (m/s).

This Chapter will be devoted to the development of a model (model KININF) which includes the dynamics of both infiltration and overland flow. Modelling of overland flow is based on the kinematic-wave approximation. Modelling of infiltration is based on soil moisture flow theory (in contrast with the Horton type of infiltration equation mentioned above). Results from a laboratory experiment on a soil flume under simulated rain were used to test the model.

5.2 THE MODEL KININF

5.2.1 Introduction

The model KININF combines a simplified physically based overland flow model, the kinematic-wave equation, with an infiltration model derived from soil moisture flow theory.

Figure 1 gives a schematic representation of the mathematical model and of the notation used, where: X is the space axis along the direction of flow; Y is a horizontal axis perpendicular to X-axis; Z is the vertical axis; H is the axis perpendicular to both X-axis and Y-axis; HOR is a horizontal axis; and θ is the volumetric water content axis. For the grid point j (with a flow depth h_j and a flow velocity v_j) of the X-axis we have in the upper part of the figure an elementary area ($\Delta x.1$) with an area covered by mounds of A, and with an effective area for overland flow of $W=1-A/\Delta x$. In the lower part of the figure the semi-infinite homogeneous soil is subdivided into layers of equal thickness. In each layer the water flux density (F) and the volumetric water content (θ) are also presented. Also in the figure p is the rainfall rate, S is the slope gradient and n is a layer index.

The testing of the mathematical model KININF was done through case studies (documented Dutch soils were used) and by comparison with results obtained on a soil flume under simulated rainfall, for two different soils (a loam from Limburg, The Netherlands, and a clay loam from Alentejo, Portugal).

5.2.2 The infiltration model

Vertical non-steady flow of water in unsaturated soil may be described by the one-dimensional continuity equation and Darcy's law in terms of the matric flux potential concept, respectively:

$$\delta\theta/\delta t = - \delta F/\delta z \qquad (3)$$

$$F = - \delta\Phi(\theta)/\delta z + K(\theta) \qquad (4)$$

where F is the water flux density ($m^3m^{-2}s^{-1}$), θ is the volumetric water content (m^3m^{-3}), $K(\theta)$ is the hydraulic conductivity function ($m\ s^{-1}$), z is the vertical coordinate, positive upwards (m), t is the time (s), and $\Phi(\theta)$ is the matric flux potential (m^2s^{-1}).

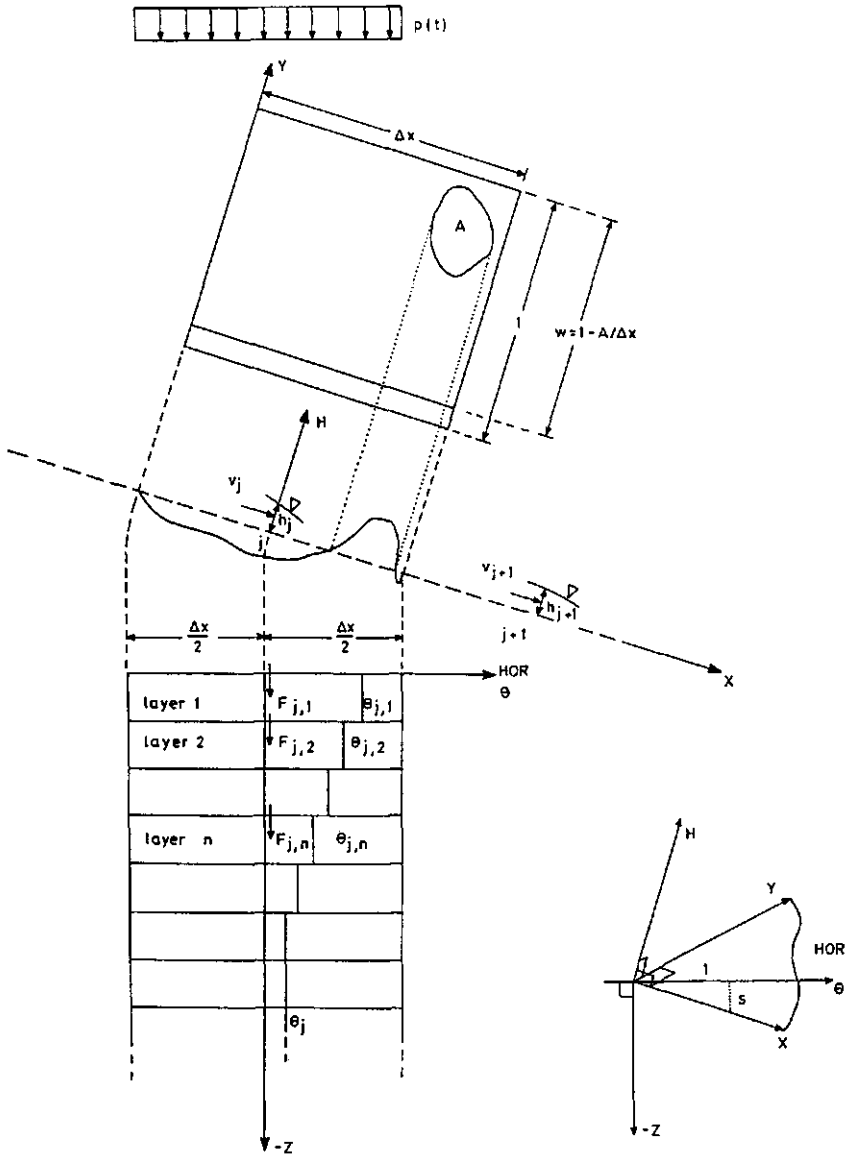

Fig. 1 Schematic representation of the model KININF and of the notation used (see text for explanation of symbols and figure)

The matric flux potential Φ (Kirchhoff transformation) is defined by:

$$\Phi = \int_{h^*_{sat}}^{h^*} K(h^*)dh^* = \int_{\theta_{sat}}^{\theta} D(\theta)\, d\theta \qquad \text{with} \quad D(\theta) = K(\theta)\, \delta h^*/\delta\theta \qquad (5)$$

where $D(\theta)$ is the soil water diffusivity (m^2s^{-1}), $h^*(\theta)$ is the pressure head (m) and the subscript 'sat' refers to saturation.

Infiltration is assumed to be vertical. Any horizontal component in the saturated or unsaturated homogeneous soil under consideration is neglected.

For simplicity, the class of soils characterized by linear retention curves and exponential dependencies of the hydraulic conductivity upon the water content (Raats, 1983) was used:

$$h^*(\theta) = h^*_{sat} + \gamma(\theta - \theta_{sat}) \qquad (6)$$

$$K(\theta) = K_{sat}\, e^{\xi(\theta-\theta_{sat})} \qquad (7)$$

where γ and ξ are empirical constants (-).

The primary relationships (6) and (7) imply the following derived relationships:

$$D(\theta) = D_{sat}\, e^{\xi(\theta-\theta_{sat})} \qquad \text{where} \quad D_{sat} = \gamma\, K_{sat} \qquad (8)$$

$$\Phi(\theta) = D_{sat}\, (e^{\xi(\theta-\theta_{sat})} - 1)/\xi \qquad (9)$$

Equations (3) and (4) were solved numerically using an explicit finite-difference scheme (Lima, 1987):

$$\theta_n^{t+\Delta t} = \theta_n - (F_{n+1} - F_n)\, \Delta t/\Delta z \qquad (10)$$

$$F_n = -(\Phi_n - \Phi_{n-1})/\Delta z + (K_n + K_{n-1})/2 \qquad (11)$$

where the subscript 'n' denotes a space level (layer index) and all non-superscripted variables are evaluated at the time t (see also Fig. 1). $K(\theta)$ and $\Phi(\theta)$ were calculated using equations (7) and (9).

The initial conditions are those for a semi-infinite homogeneous soil, with uniform volumetric water content (θ_o).

5.2.3 The overland flow model

The flow per unit width across a plane surface as a result of rainfall is described by the one dimensional continuity equation:

$$\delta h/\delta t + \delta q/\delta x = R(x,t) \qquad (12)$$

where h is the flow depth at time t and position x (m); x is the space coordinate along the direction of flow (m); q is the volumetric water flux per unit plane width (m^2/s); and R(x,t) is the rainfall excess (m/s).

By assuming that the bed slope equals the friction slope (kinematic wave assumption) and by using existing open-channel flow friction equations the discharge at any point and time can be expressed as a function of water depth only, as follows:

$$q = \alpha h^m \qquad (13)$$

where m is a parameter for the type of flow (-), and α is a hydraulic coefficient (units dependant on the m value).

Equations (12) and (13) were solved numerically using the explicit finite-difference scheme known as the single-step Lax-Wendroff scheme. This scheme is developed by expanding h in a Taylor's series about the point (h, t+Δt). The resulting explicit expression for h is:

$$h_j^{t+\Delta t} = h_j - \frac{\Delta t}{2\,\Delta x}\left[(\alpha h^m)_{j+1} - (\alpha h^m)_{j-1} - 2.\Delta x.R_j \right] +$$

$$+ \frac{\Delta t^2}{4\,\Delta x^2}\left[(\alpha m h^{m-1})_{j+1} + (\alpha m h^{m-1})_{j} \right]\left[(\alpha h^m)_{j+1} - (\alpha h^m)_{j} - \Delta x.R_j \right] -$$

$$- \frac{\Delta t^2}{4\,\Delta x^2}\left[(\alpha m h^{m-1})_{j} + (\alpha m h^{m-1})_{j-1} \right]\left[(\alpha h^m)_{j} - (\alpha h^m)_{j-1} - \Delta x.R_j \right] +$$

$$+ \left(R_j^{t+\Delta t} - R_j \right) \Delta t/2 \qquad (14)$$

where all non-superscripted variables on the right-hand side are evaluated at the time t, and j denotes a space level in the x direction (see also Fig. 1).

This finite difference scheme has been used successfully by Kibler and Woolhiser (1970 and 1972), Lane et al. (1975), Rovey et al. (1977), Freeze (1978), Wu et al. (1978), and Lima (1987b), among others.

In this work the upstream boundary is assumed to be at zero depth ($h(0,t) = v(0,t) = 0$, where v is the overland flow velocity in m/s) and the downstream boundary is a continuing plane (along the direction of flow). In the first phase of modelling zero depth initial conditions were assumed, i.e. an initially "dry" surface ($h(x,0)=0$ for all x; $v(x,0)=0$ for all x) with or without surface depression storage and an upstream boundary condition of no flow.

5.2.4 Depression storage, detention storage and obstacles

In terms of depression storage the model is based on the Hortonian approach: all depression storage must be filled up to allow a thin sheet of overland flow to build up. Depression storage is thus defined as the amount of water held in surface depressions, which may be evaporated or infiltrated.

Detention storage is the storage effect due to overland flow in transit. The water held by detention storage either runs off or infiltrates.

Obstacles like earth and vegetation mounds are taken into account in the overland flow process considering a reduction of the possible available flow path area. The infiltration into the obstacles is supposed to be equal to that of the remaining area.

5.2.5 Stability conditions

The following stability conditions were used respectively for the overland flow (Constantinides, 1981; Stephenson and Meadows, 1988) and the infiltration (Remson et al., 1971; Stroosnijder, 1982) finite difference schemes:

$$\Delta t/\Delta x < 1/(m\alpha h^{m-1}) \quad (15)$$

$$\Delta t < 0.5\ (\Delta z)^2/D(\theta) \quad (16)$$

5.2.6 The combined model of overland flow and infiltration

The mathematical model consists of simultaneous solution of equations 10, 11 and 14. Solution is simultaneous in the sense that solutions move concurrently in time with boundary conditions being interdependant.

The slope is subdivided into compartments, in between grid points, assuming uniform conditions of rainfall, infiltration and soil moisture profile within each compartment. The computational procedure for each time t and for each grid point j starts by solving the finite difference scheme for vertical unsaturated flow (equations 10 and 11) and consequent determination of the infiltration rate (equivalent to the water flux density F at the soil surface) and the rainfall excess rate (equation 1). These calculations are followed by the solution of the explicit Lax Wendroff scheme for overland flow (equation 14).

5.2.7 The computer model

The model consists of a main computer program and three subroutines. The main program performs a major part of the algorithm. The subroutines solve the Lax-Wendroff scheme and the finite differences scheme for unsaturated vertical flow, and print part of the results.

The input data required to run the computer program KININF.FOR are:

surface data:

S = steepest slope of the plane of best fit (-)
L = length of the field (m)
W = width of the field (m)
A = area covered by mounds (%)
α = hydraulic coefficient (-)
m = parameter for the type of flow (-)
D_S = depression storage (m)

rainfall data:

p(1) = rainfall data from time 0 to time t(1) (m/s)
t(1) = end of time interval of p(1) (s)
p(2) = rainfall data from time t(1) to time t(2) (m/s)
t(2) = end of time interval of p(2) (s)
.
.
.
p(j) = rainfall data from time t(j-1) to time t(j) (m/s)
t(j) = end of time interval of p(j) (s)

soil data:

D_{sat} = saturated soil water diffusivity (m^2/s)
ξ = empirical constant (-)
K_{sat} = saturated hydraulic conductivity (m/s)
θ_o = initial volumetric water content (m^3m^{-3})
θ_{sat} = saturated volumetric water content (m^3m^{-3})

other data:

TM = total simulation time (s)
Δt = time increment (s)
Δx = space increment in the x direction (m)
Δz = space increment in the vertical direction (layer index)(m)
File names

Time and space increments (Δt, Δx and Δz) and file names are asked via the monitor. The remainder of the input data required to run the program are read from a data file.

The model KININF creates 4 output data files with:

1) water depth, flow velocity and volume of water stored in depressions per unit area, in time (at chosen intervals) and in space (at grid points). Information of start and stop of the overland flow process is also given.

2) hydrograph of overland flow at x=L.

3) infiltration rate at the soil surface, in time (at chosen intervals), and at any chosen grid points.

4) soil moisture profiles in time (at chosen intervals), and at any chosen grid points.

5.2.8 Test runs

5.2.8.1 Overland flow and infiltration for a medium fine sand

The model KININF was run for a medium fine sand with the following input data:

surface data:		rainfall data:		other data:	
S	= 2%	p(1)	= 0.15 mm/s	TM	= 570 s
L	= 20 m	t(1)	= 180 s	Δt	= 2 s
W	= 1 m	p(2)	= 0.02 mm/s	Δx	= 2 m
A	= 0	t(2)	= 240 s	Δz	= 0.02 m
α	= 2.87	p(3)	= 0.10 mm/s		
m	= 1.68	t(3)	= 360 s		
D_S	= 0.001 m				

The soil data is given in Table 1.

Fig. 2 shows, in graphic form, some possible outputs of the model KININF, namely advance of the wetting front at x=L/2, overland flow hydrograph at x=L and infiltration rate in time at x=L/2, and water depth and flow velocities in time and space. In Fig. 2 Q is the overland flow discharge.

5.2.8.2 Comparison of overland flow hydrographs for different soils

In Fig. 3 a comparison is made of hydrographs of overland flow for 6 different soils (see characteristics in Table 1), assuming equal friction factors, rainfall pattern and geometric surface characteristics. Also, the same space and time increments have been used:

surface data:		rainfall data:		other data:	
S	= 2%	p(1)	= 0.15 mm/s	TM	= 570 s
L	= 20 m	t(1)	= 180 s	Δt	= 2 s
W	= 1 m	p(2)	= 0.02 mm/s	Δx	= 2 m
A	= 0	t(2)	= 240 s	Δz	= 0.02 m
α	= 2.87	p(3)	= 0.10 mm/s		
m	= 1.68	t(3)	= 360 s		
D_S	= 0				

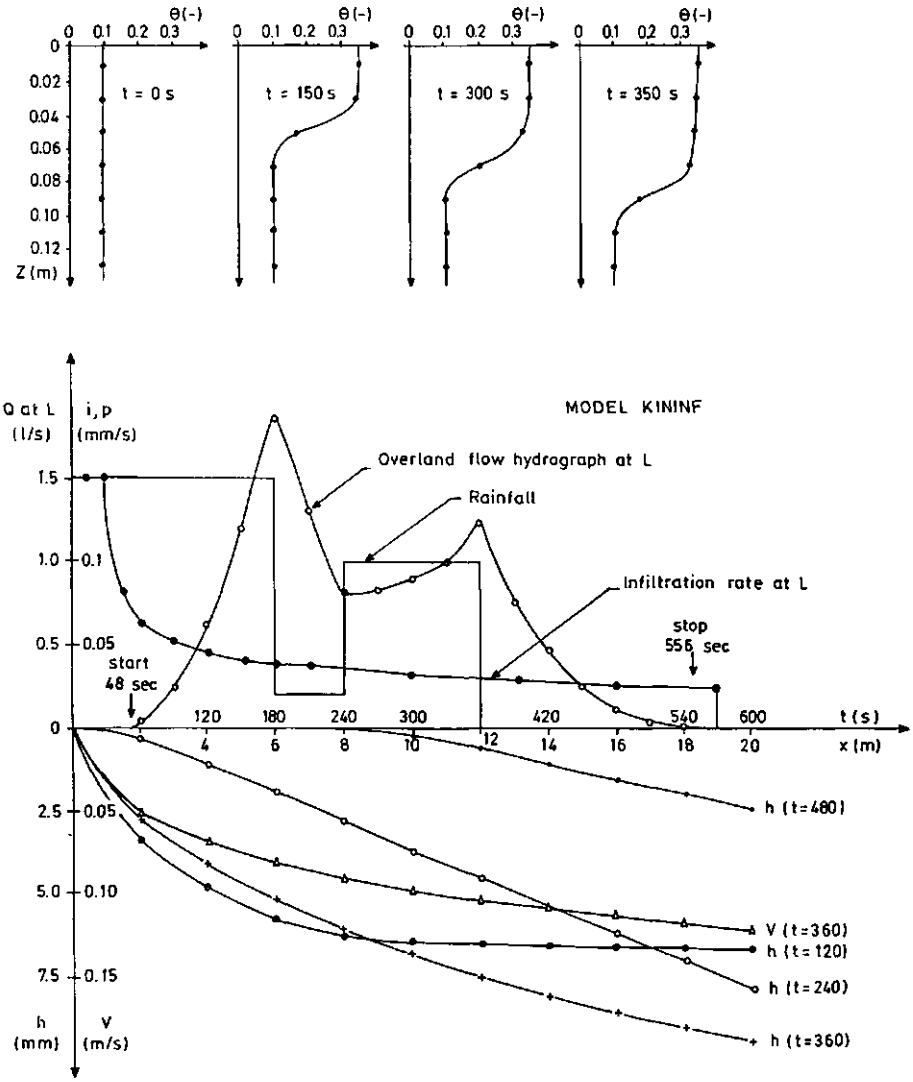

Fig. 2 Outputs of model KININF for a medium fine sand.

Table 1 Measured physical data of some Dutch soils (After Rijtema, 1969 and Stroosnijder, 1976)

SOIL TYPE	K_{sat}(m/s) x10^{-6}	D_{sat}(m^2/s) x10^{-6}	ξ(-)	θ_{sat}(m^3/m^3)
medium coarse sand	34.72	88.3	53.0	0.365
medium fine sand	12.70	100.0	60.8	0.350
fine sand	5.89	18.3	27.6	0.364
loess loam	1.67	8.3	25.9	0.455
loam	0.59	4.0	22.8	0.503
light clay	0.15	4.2	20.3	0.453

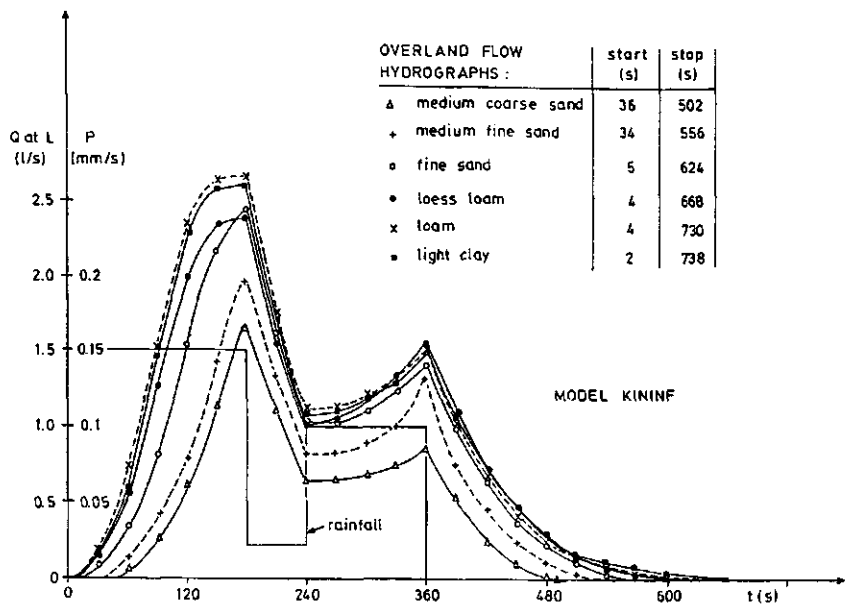

Fig. 3 Comparison of hydrographs of overland flow for 6 different soils (see Table 1 for soil physical data).

5.3 LABORATORY EXPERIMENTS ON SOIL FLUME UNDER SIMULATED RAIN

5.3.1 Introduction

To determine the performance of the model KININF in predicting overland flow, infiltration and soil moisture movements, laboratory experiments have been carried out, by using a soil flume and a rainfall simulator.

The experiments referred to in this Section are part of research carried out in the Department of Hydrology, Soil Physics and Hydraulics of the Agricultural University Wageningen to study water erosion processes like crust formation, erosion of soils with rock fragments, overland flow and sediment discharges.

The rainfall simulator used in the experimental work belongs to the Department of Irrigation and Civil Engineering of the Agricultural University Wageningen.

5.3.2 Laboratory set-up

The laboratory set-up (Fig. 4) was mainly composed of two units: a soil flume and a rainfall simulator.

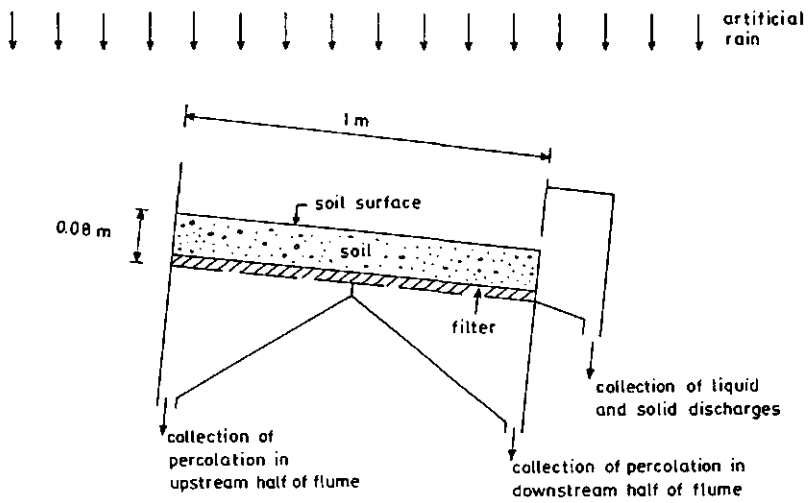

Fig. 4 Sketch of the laboratory set-up

The laboratory soil flume is 1 m long, 0.5 m wide, and 0.08 m deep. The sides are made of Perspex up to a height of 0.12 m above the soil surface. The flume has no buffer zone for splash. The bottom of the flume consists of a metallic perforated plate to collect percolation water; a synthetic filter was placed over this perforated plate. Percolation discharge can be collected separately for the upper and downstream halfs of the soil flume. Subdivision of the flume area into five independent strips of 0.1 m wide is possible (designated here as plots 1 to 5). Accordingly, in the downstream end of the flume, one or a group of five discharge collectors can be installed.

The programmable rainfall simulator used is similar to the one described by Neibling et al. (1981) and Foster et al. (1982). The simulator uses oscillating nozzles (continuous spraying with lateral oscillation across slope) of the type Spraying Systems Veejet 80100, sprinkling downwards and producing intermittent rainfall. Four aluminium troughs, each with three nozzles, are installed across slope to cover an area of 6x2.5 m^2. Nozzle height is set at about 2.4 m and nozzle spacing at 1.10 m apart in each trough. The spacing between troughs is 1.52 m. Different rainfall intensities are obtained by controlling the frequency with which the nozzle sweeps across an opening above the surface under study. The duration of off-periods between spray applications and the frequency with which each nozzle sprays significantly affects infiltration rates, uniformity of flow depth, and smoothness of the rising limb of the overland flow hydrograph (Sloneker and Moldenhauer, 1974; Foster et al., 1982).

The rainfall simulator is claimed to generate an uniformely distributed rainfall pattern. The uniformity of the rain flux was studied by Foster et al. (1982) and Maanen and Vincentie (1986). Foster et al. (1982) found for the same type of rainfall simulator a coefficient of uniformity (Christiansen, 1942) of approximately 86% for the rainfall intensity within an area bounded by four corner nozzles. This percentage was found independent of the rainfall intensity over the range 25 to 125 mm/hr. For the rainfall simulator used in the present study Maanen and Vincentie (1986) obtained uniformity coefficients of around 85% in an area covered by 12 nozzles (6x2.5 m^2), over a rainfall intensity range of about 16 to 112 mm/hr.

The impact velocity of the drops generated by this type of nozzles are nearly equal to impact velocities of natural raindrops when the nozzles are about 2.4 m above the surface (Neibling et al., 1981). However, it has been reported by Foster et al. (1982) that the drops are slightly smaller than natural raindrops and, consequently, the impact energy of the drops is about 75% of natural rainfall, the median drop size being 2.25 mm, with drop terminal velocity of 6.8 m/s. The experiments have been carried out in stagnant air with room temperature of approximately 18 degrees. Rain water temperature was approximately 13 degrees.

Two soils were studied: a loam from Limburg (The Netherlands) and a clay loam from Alentejo (Portugal). Soil properties are presented in Table 2, where ρ_s is the average particle density (kg/m^3) and ρ is the average soil bulk density (kg/m^3).

Other input data for the model KININF are:

(a) for the soil from Limburg:

surface data:		rainfall data:		other data:	
S	= 10%	p(1)	= 0.03741 mm/s	TM	= 1020 s
L	= 1 m	t(1)	= 900 s	Δt	= 0.25 s
W	= 0.1 m	p(2)	= 0 mm/s	Δx	= 0.1 m
A	= 0	t(2)	= 0 s	Δz	= 0.0025 m
α	= 100	p(3)	= 0 mm/s		
m	= 1.67	t(3)	= 0 s		
D_S	= 0				

(b) for the soil from Alentejo:

surface data:		rainfall data:		other data:	
S	= 10%	p(1)	= 0.03741 mm/s	TM	= 1020 s
L	= 1 m	t(1)	= 900 s	Δt	= 0.10 s
W	= 0.1 m	p(2)	= 0 mm/s	Δx	= 0.1 m
A	= 0	t(2)	= 0 s	Δz	= 0.002 m
α	= 40	p(3)	= 0 mm/s		
m	= 1.67	t(3)	= 0 s		
D_S	= 0				

Table 2 Measured and estimated physical data of the loam from Limburg and the clay loam from Alentejo.

SOIL TYPE :	Loam (Limburg)	Clay loam (Alentejo)
Measured (After Lima, 1989)		
θ_o (m^3/m^3)	0.0107	0.006
θ_{sat} (m^3/m^3)	0.506	0.411
ρ_s (kg/m^3)	2640	2730
ρ (kg/m^3)	1150	1370
Estimated (After Rijtema, 1969 and Stroosnijder, 1976)		
K_{sat} (m/s) $x10^{-6}$	1.67	0.1134
D_{sat} (m^2/s) $x10^{-6}$	13.3	5.0
ξ (-)	25.9	66.8

The experiments have been performed for initially dry soil conditions, i.e., using soil which was air-dried during several weeks. The soils have been sieved through a 5.6 mm mesh screen, and placed loosely in the flume. Constant rainfall rates have been used.

The solid and liquid discharges from the experimental runs have been collected in pre-weighted containers at variable time intervals (depending on discharge variations). Sediment discharges have been determined by oven-drying and weighing of the samples.

Overland flow velocity measurements were done using dye tracing (Abrahams et al., 1986).

For some of the runs, the advance of the soil moisture front in time was recorded by observing at several locations the advance of the wet front through the Perspex wall, over the length of the flume. Boundary problems were negligible in comparison with spatial variation of the advance of the wetting front.

Further details on the laboratory set-up and procedures are presented by Lima (1989) and Giménez (1989).

5.3.3 Results

For both soils the physical properties θ_o, θ_{sat}, ρ_s and ρ were determined experimentally, and K_{sat}, D_{sat} and ξ were estimated (Table 2: Rijtema, 1969 and Stroosnijder, 1976)). The parameters α and m were estimated from overland flow velocity measurements. No calibration procedure was applied to the parameters.

Experimental and simulated (predicted with model KININF) overland flow hydrographs show good agreement (Figures 5 and 6). With respect to the overland flow hydrographs, the model efficiency coefficient is 94.2% and 93.1% for the soils from Limburg and Alentejo, respectively. The model efficiency coefficient is defined as:

$$RE = (C-B)/C \tag{17}$$

with

$$B = \Sigma(Q_{obs,t} - Q_{pred,t})^2 \tag{18}$$

$$C = \Sigma[Q_{obs,t} - \Sigma(Q_{obs,t}/n)]^2 \tag{19}$$

where RE is the model efficiency coefficient (RE=1 indicates a perfect fit, while negative values indicate poorer estimates than by using the mean runoff), B is the sum of squares of residuals, C is the sum of squares of deviations of observed flow values from their mean, and n is the number of observed values.

The observed advance of the soil moisture fronts over the length of the flume are given in Figures 7 and 8. Figures 9 and 10 compare measured soil wetting fronts (average over the flume length) with KININF's estimate of the soil moisture profiles at different times. For the soil from Limburg the model efficiency is, in this case, of 72.2%; for the soil from Alentejo this analysis is not possible due to the small number of observed data.

Differences between observed and simulated values may be caused by many factors. Although care was taken in placing the soil in the flume, uniform density has not been achieved. Also the measurements of the physical properties of the soil have not been made exactly for the same conditions. Further, the estimated soil parameters may deviate from the real values.

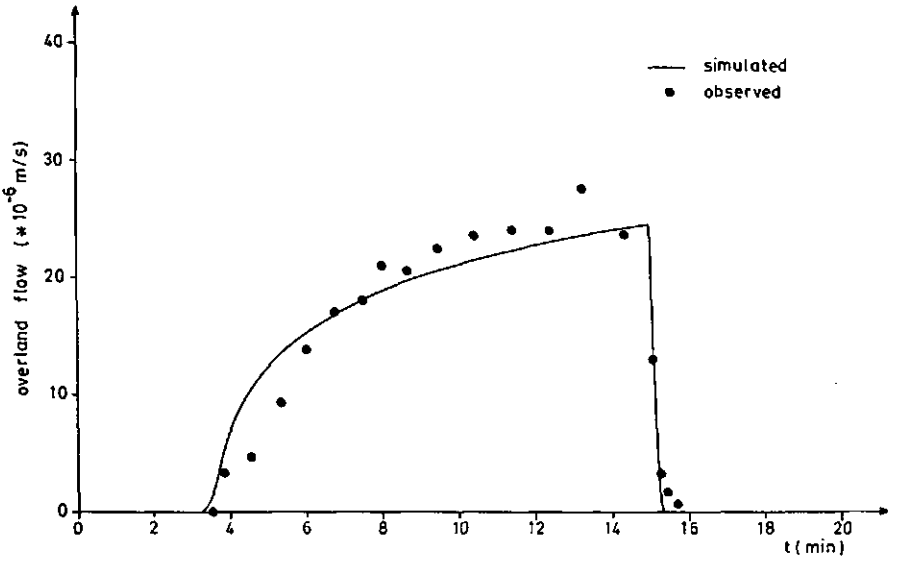

Fig. 5 Measured and simulated overland flow hydrographs (model KININF) for the loam from Limburg (The Netherlands)

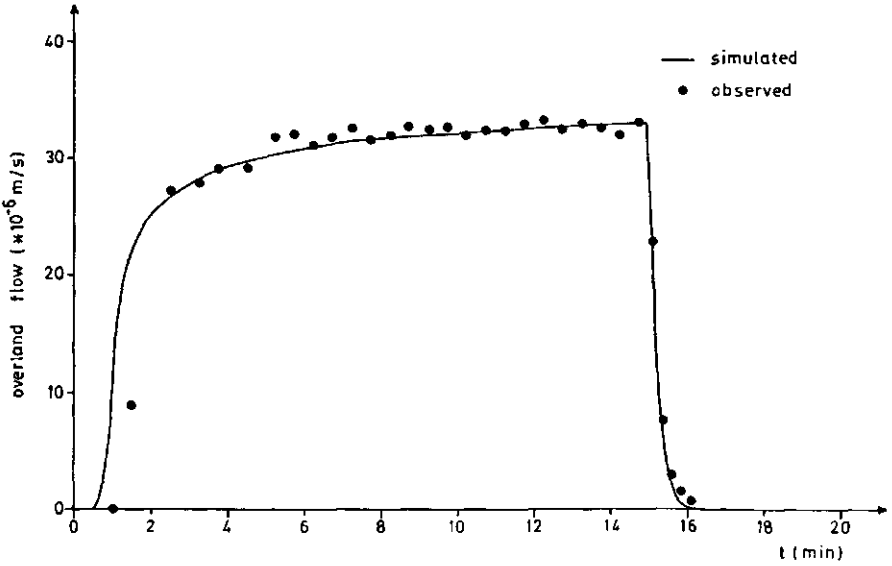

Fig. 6 Measured and simulated overland flow hydrographs (model KININF) for the clay loam from Alentejo (Portugal)

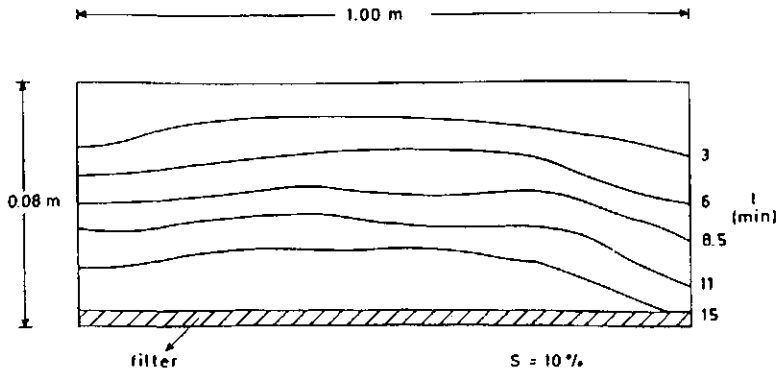

Fig. 7 Observed saturation profiles over the flume length for the loam from Limburg (The Netherlands)

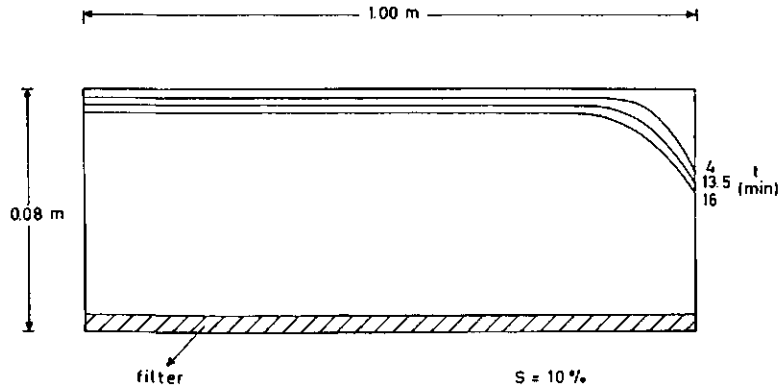

Fig. 8 Observed saturation profiles over the flume length for the clay loam from Alentejo (Portugal)

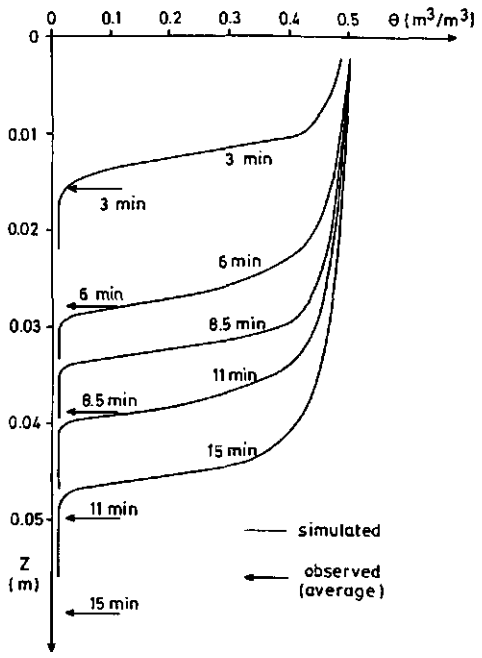

Fig. 9 Comparison of measured soil moisture profile fronts and corresponding results from the model KININF for the loam from Limburg (The Netherlands)

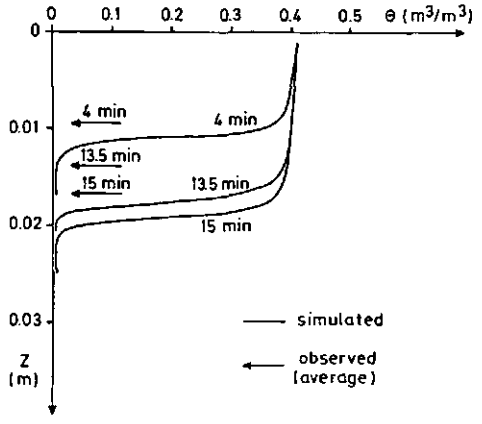

Fig. 10 Comparison of measured soil moisture profile fronts and corresponding results from the model KININF for the clay loam from Alentejo (Portugal)

5.4 CONCLUSION

An infiltration model has been combined with the kinematic-wave equations for overland flow, with interacting boundary conditions at the soil surface, resulting in a mathematical model of overland flow under rainfall on an infiltrating surface. The model KININF is based on a much simpler concept of unsaturated flow through porous media than, for example, the model by Smith and Woolhiser (1971) which is based on the Richardson equation.

The model can be used to describe overland flow in small plots or microcatchments when appropriate physical parameters are known. It provides a simple way of visualizing overland flow in different infiltrating surfaces.

Sensitivity analysis has been done through case studies (Lima, 1987). The performance of the model has been tested with data from a laboratory soil flume under simulated rainfall. The results show good agreement between the model and the experiments. Further refinement of the proposed model is possible and desirable. This may include coupling of the model with a sediment transport model, and testing of the model against field data.

Acknowledgement

The author acknowledges the suggestions of Prof. Dr. W.H. van der Molen (Department of Land and Water Use), Dr. J.V. Witter (Department of Physical Geography and Soil Science of the University of Amsterdam) and Ir. H.J. van Ieperen (Department of Hydraulics and Catchment Hydrology). The laboratory experiments on the soil flume (Section 5.4) were executed in collaboration with M.I.M.L.P.P. de Lima and D. Giménez as part of the programme of the M.Sc. Course on Soil Science and Water Management of the Agricultural University Wageningen. The author also wishes to thank the Department. of Irrigation and Civil Engineering for the use of the rainfall simulator.

REFERENCES

Abrahams, A.D., A.J. Parsons and S.-H. Luk, 1986. Field measurement of the velocity of overland flow using dye tracing. Earth Surface Processes and Landforms, 11: 653-657.

Akan, A.O., 1985a. Predicting overland flow and infiltration. In: W.R. Waldrop (Ed.) Hydraulics and hydrology in the small computer age. Proc. of the Specialty Conference, ASCE, Lake Buena Vista, Florida, Vol. 1, 79-83.

Akan, A.O., 1985b. Similarity solution of overland flow on pervious surface. J. of Hydraulic Engineering, ASCE, 111: 1057-1067.

Akan, A.O., 1988. Overland flow on pervious, convergent surface. Nordic Hydrology J., 19: 153-164.

Akan, A.O., and B.C. Yen, 1981. Mathematical model of shallow water flow over porous media. J. of the Hydraulics Division, ASCE, 107: 479-494.

Christiansen, J.E., 1942. Irrigation by sprinkling. Univ. of California Agric. Exp. Station Bull. 670.

Constantinides, C.A., 1981. Numerical tecniques for a two-dimensional kinematic overland flow model. Water SA, 7(4): 234-248.

Foster, G.B., L.F. Huggins and L.D. Meyer, 1968. Simulation of overland flow on short field plots. Water Resources Research, 4(6): 1179-1188.

Foster, G.B., W.H. Neibling and R.A. Nattermann, 1982. A programmable rainfall simulator. American Society of Agricultural Engineers, paper no. 82-2570.

Giménez, D., 1989. Effect of rainfall patterns and intensities on the surface of a silt loam soil: laboratory experiments. M.Sc. Thesis, Agricultural University Wageningen, The Netherlands, 73 p.

Kibler, D.F. and D.A. Woolhiser, 1970. The kinematic cascade as a hydrologic model. Hydrology Paper no. 39, Colorado State University, Fort Collins, Colorado, 27 p.

Kibler, D.F. and D.A. Woolhiser, 1972. Mathematical properties of the kinematic cascade. Journal of Hydrology, 13: 131-147.

Lima, J.L.M.P. de, 1987a. Methods and models in surface and subsurface hydrology - a review and some applications. M.Sc. Thesis, Agricultural University Wageningen, The Netherlands, 71 p.

Lima, J.L.M.P. de, 1987b. Overland flow on an infiltrating surface: the model KININF. Depart. of Land & Water Use, Agricultural Univ. Wageningen, Wageningen, The Netherlands, Internal Report No. 36, 13 p.

Lima, M.I.M.L.P.P. de, 1989. Water erosion in relation to stony soils, overland flow and sediment discharges: a laboratory experiment. M.Sc. Thesis, Agricultural University Wageningen, Wageningen, The Netherlands, 96 p.

Maanen, J. van and R. Vincentie, 1986. De ijking van een programmeerbare regensimulator. Department of Irrigation and Civil Engineering, Agricultural University Wageningen, Wageningen, The Netherlands.

Maniak, U., 1982. Rainfall-runoff processes. Proc. Symp. Hydrolog. Research Basins, Sonderh. Landeshydrologie, Bern, 433-453.

Morin, J. and Y. Benyamini, 1977. Rainfall infiltration into bare soils. Water Resources Research, 13(5): 813-817.

Neibling, W.H., G.R. Foster, R.A. Nattermann, J.D. Nowlin and P.V. Holbert, 1981. Laboratory and field testing of a programmable plot-sized rainfall simulator. In: Erosion and sediment transport measurement, Proc. of the Florence Symposium, IAHS, publ. no. 133, 405-414.

Raats, P.A.C., 1983. Implication of some analytical solutions for drainage of soil water. Agricultural Water Management, 6: 161-175.

Remson, I., G.M. Hornberger and F.J. Molz, 1971. Numerical methods in subsurface hydrology. Wiley-Interscience, New York.

Rijtema, P.E., 1969. Soil moisture forecasting, ICW, Wageningen, The Netherlands.

Singh, V.P., 1975. A laboratory investigation of surface runoff. J. of Hydrology, 27: 33-50.

Singh, V.P., 1976. Comparison of two mathematical models of surface runoff. International Association of Hydrological Sciences Bulletin, 21(2): 285-299.

Singh, V.P., 1978. Mathematical modelling of watershed runoff. Proc. of International Conference on Water Resources Engineering (Vol. II), Bangkok, Thailand, 10-13 January 1978, 703-726.

Sloneker, L.L. and W.C. Moldenhauer, 1974. Effect of varying on-off time of rainfall simulator nozzles on surface sealing and intake rate. Soil Science Society of American Proceeding, 38(1): 157-159.

Smith, R.E. and Woolhiser, D.A., 1971a. Mathematical simulation of infiltrating watersheds. Colorado State University Hydrology paper No. 47, Fort Collins, Colorado.

Smith, R.E. and Woolhiser, D.A., 1971b. Overland flow on an infiltrating surface. Water Resour. Res., 7(4): 899-913.

Stephenson, D. and M.E. Meadows, 1986. Kinematic hydrology and modelling. Developments in Water Science, 26, Elsevier Science Publishers, Amsterdam, 250 p.

Stroosnijder, L., 1976. Infiltratie en herverdeling van water in grond, Ph.D. Thesis, Agricultural University Wageningen, PUDOC, Wageningen, The Netherlands.

Stroosnijder, L., 1982. Computer solutions of the mathematical models describing unsaturated soil water flow. Department of Soil Science and Plant Nutrition, Agricultural University Wageningen, Wageningen, 26 p.

Woolhiser, D.A. and J.A. Liggett, 1967. Unsteady, one-dimensional flow over a plane - the rising hydrograph. Water Resour. Res., 3(3): 753-771.

Wu, Y.-H., V. Yevjevich and D.A. Woolhiser, 1978. Effects of surface roughness and its spatial distribution on runoff hydrographs. Colorado State University Hydrology paper No. 96, Fort Collins, Colorado, 44 p.

6 MORPHOLOGICAL FACTORS AFFECTING OVERLAND FLOW ON SLOPES

Published in: Bouma, J. and Bregt, A.K. (Eds.), Land Qualities in Space and Time, Proceedings of a Symposium organized by the International Society of Soil Science (ISSS), 22-26 August 1988, PUDOC, Wageningen, 321-324.

The experimental station of Vale Formoso (Alentejo, Portugal), referred to in this Section, is described in Appendix C.

MORPHOLOGICAL FACTORS AFFECTING OVERLAND FLOW ON SLOPES

J.L.M.P. de Lima

Department of Land & Water Use and Department of Hydraulics & Catchment Hydrology, Agricultural University Wageningen, The Netherlands

Summary

Many morphological factors affect overland flow namely: slope gradient, slope length, shape of the slope and slope exposure to prevailing winds. This paper contains a discussion of the effect of morphological characteristics of slopes on the overland flow process. The analysis of the different effects is presented through case studies.

Although the effect of the morphological factors on the overland flow process may be strongly reduced by soil properties, soil roughness, vegetation cover and effective rainfall patterns, it is believed that its effect can not be neglected.

Keywords: overland-flow, slopes, hillslopes, morphology, water-erosion.

Introduction

Overland flow is affected by many factors such as soil characteristics, climate, vegetation, topography, geology, land use, man made constructions such as roads, etc. The size of a drainage basin and the areal distribution of all those factors also have a strong influence. Overland flow is the primary flow in urban runoff, in runoff from rock outcrops and in surface runoff from some small drainage basins.

Many morphological factors affect overland flow on slopes namely: slope gradient, slope length, shape of the slope and slope exposure to prevailing winds. The degree to which morphological aspects influence overland flow is closely related to other factors such as soil characteristics, climate, vegetation, etc. For example in semi-arid areas, where Horton overland flow is a fairly common phenomenon, topography seems to have a slight influence on the overland flow production (Dunne & Leopold, 1978). Most humid regions may experience saturation overland flow (Dunne & Leopold, 1978), and topography is of importance in determining where overland flow will occur. The removal of vegetation from a forest area can lower the infiltration capacity enough to generate large amounts of overland flow where previously runoff was a slow subsurface percolation.

This paper contains a discussion of the effect of morphological characteristics of short slopes on overland flow. Use is made of both numerical and analytical techniques, and laboratory and field experiments.

Results

Slope gradient

Slope gradient is one of the major factors affecting overland flow. The interdependence of slope gradient and water erosion hazard has been studied by various authors and shows that the intensity of the erosion process increases with growing tangential shear stress and velocity of the overland flow sheet both of which are closely related to the slope (Holy, 1980).

Slope gradient influences the amount of infiltration and consequently of overland flow. The greater the slope gradient, the greater is the portion of the rain that runs off as overland flow. As more water runs off, the velocity is increased both as a consequence of the steepness of the slope and the greater depth of overland flow. However for a vertical rainfall the amount of rain per unit area decreases with slope steepness, this effect being considerable for very steep slopes. For inclined rainfall the effect may be even more significant.
Fig. 1 shows hydrographs of overland flow obtained in a laboratory experiment in an impermeable concrete model with mounds simulating the cultivation of large root crops - like yam - in Africa. The rainfall intensity was approximately the same in the different cases. Slope affects the shape of the outflow hydrographs.

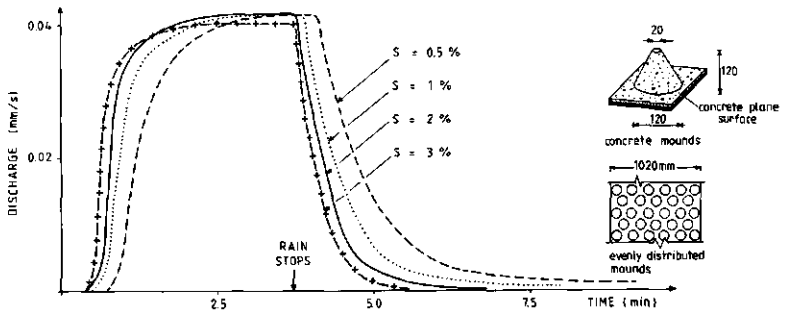

Fig. 1. Effect of slope gradient on overland flow hydrographs.

Slope length

For the same conditions, slope length will affect discharges and water depths and consequently overland flow hydrographs. This is particularly important with respect to water erosion problems.
Fig. 2 illustrates the effect of slope length on simulated overland flow hydrographs in a sandy loam. Use was made of the model KININF, that combines the kinematic wave equations for overland flow with an infiltrating model derived from soil moisture theory (Lima, 1987).

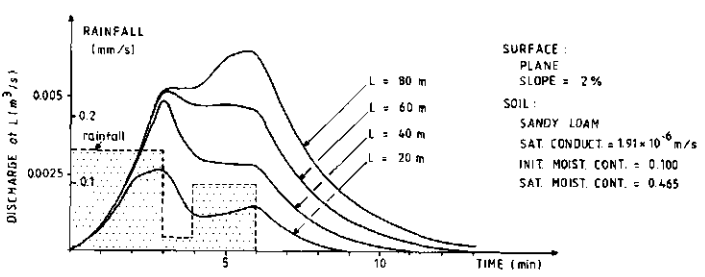

Fig. 2. Effect of slope length on overland flow hydrographs.

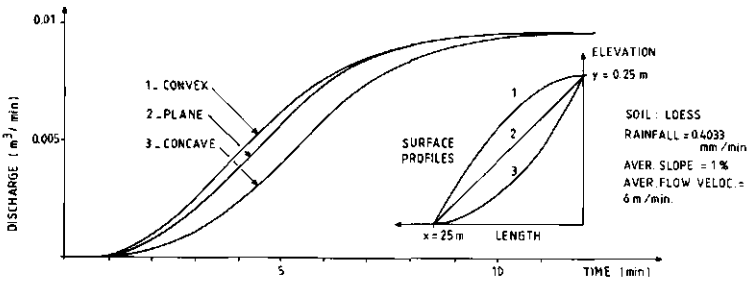

Fig. 3. Effect of slope shape on the rising limb of hydrographs.

Slope shape

Many are the shapes used to represent real slopes in overland flow studies: planes, cascade of planes, convex and concave surfaces, segments of cones etc. The overland flow process is strongly affected by the shape of the slopes. This is not only because of the overland flow process itself but also because of the effective rainfall rate at the surface.

Fig. 3 gives the overland flow hydrographs for strips of concave, convex and plane surfaces using the analytical kinematic model of Lima & Molen, 1988. The shape of the slope is determinant in the assessment of the shape of the rising limb of the overland flow hydrographs.

In convex slopes both steepness, drainage area, and depth of overland flow increase towards the foot of the slope. Comparisons made of erosion intensity on different slopes (Holy, 1980) have shown that the highest intensities are reached on convex slopes, and the lowest on concave slopes for the same length and elevation. These results are in accordance with the form of the rising limb of the hydrographs (Fig. 3).

Slope exposure

In an experimental station located in Alentejo (semi-arid region of Portugal), 15 standard field plots of 20x8.33 m^2 with slopes ranging from 10 to 20% were studied with respect to rain water erosion. It was found that fields with slopes of around 20% showed less erosion than slopes of 10% for the same amount of runoff, which is attributed, to the orientation of the fields with respect to the dominant direction of the winds.

Lima (1988) showed the influence of wind intensity and prevailing wind direction with respect to the position of the slope on both the effective rainfall intensity and the mechanics of the overland flow process on slopes. They affect overland flow in the following ways: angle and velocity of impact of raindrops, splash shape, tangential shear stress in the water-air boundary, and effective rainfall pattern at ground level.

Consider two impermeable slopes approximated by two impermeable planes of different orientations with respect to the inclined rainfall. Assuming equal slope characteristics and an angle of incidence of the rain of 45°, the overland flow hydrographs at the bottom of the two slopes are compared for two different rainfall patterns measured with horizontal raingauges (Fig. 4). The hydrographs for the two slopes have remarkable differences, as expected.

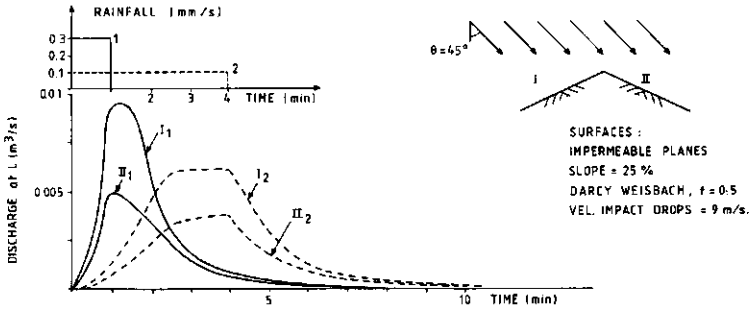

Fig. 4. Effect of slope exposure on overland flow hydrographs.

Conclusion

The major morphological factors affecting overland flow are: slope gradient, slope length, shape of the slope and slope exposure. Although the effect of the morphological factors on the overland flow process may be strongly reduced by soil properties, soil roughness, vegetation cover and effective rainfall patterns, it is believed that it cannot be neglected. Slope gradient and length are presumed to be factors that more strongly affect overland flow process. The shape of the slope is determinant in the assessment of the time to peak and of the shape of the rising limb of the overland flow hydrographs. The slope exposure is also of great importance in case of slopes exposed to strong winds from some prevalent direction.

Acknowledgements

The author wish to thank Prof. W.H. van der Molen, Dr. R.W.R. Koopmans, and Ir. P.M.M. Warmerdam for their helpful suggestions.

References

Dunne, T. & L.B. Leopold, 1978. Water in environment planning. Freeman, San Francisco, 818 p.

Holy, M., 1980. Erosion and environment. Environment Sciences and Applications, vol. 9, Pergamon Press, Oxford, 225 p.

Jansson, M.B., 1982. Land erosion by water in different climates. UNGI report No. 57, Uppsala University, Department of Physical Geography, Sweden, 151 p.

Lima, J.L.M.P. de, 1987. Overland flow in an infiltrating surface: the model KININF. Department of Land & Water Use, Internal Report No. 36, Agricultural University Wageningen, The Netherlands, 13 p.

Lima, J.L.M.P. de & W.H. van der Molen, 1988. An analytical kinematic model for the rising limb of overland flow on infiltrating parabolic shaped surfaces. J. Hydr. (in press).

Lima, J.L.M.P. de, 1988. The effect of the angle of incidence of rainfall on the overland flow process (in preparation).

7 OVERLAND FLOW UNDER WIND-DRIVEN RAIN

For purpose of clarity some equations presented in Section 7.1 are derived in Appendix A.

Recognition of the key assumptions is essential for understanding the type and limitations of a model and its role in practical applications. In Appendix B the assumptions behind model WROF (described in Sections 7.1 and 7.2) are presented together with a listing of model inputs and outputs.

Also the experimental station of Vale Formoso (Alentejo, Portugal), referred to in Section 7.1, is described in Appendix C.

7.1 THE INFLUENCE OF THE ANGLE OF INCIDENCE OF THE RAINFALL ON THE *OVERLAND FLOW PROCESS*

Published in: International Association for Hydrological Sciences (IAHS), Publ. no. 181 (Proc. IAHS Third Scientific Assembly, 10-19 May 1989, Baltimore, USA), 73-82.

New Directions for Surface Water Modeling (Proceedings of the Baltimore Symposium, May 1989)
IAHS Publ. no. 181, 1989.

The influence of the angle of incidence of the rainfall on the overland flow process

J.L.M.P. de LIMA
Department of Land & Water Use, and Department of Hydraulics & Catchment Hydrology, Agricultural University Wageningen, Nieuwe Kanaal 11, 6709 PA Wageningen, The Netherlands

ABSTRACT This paper analyses the influence of the angle of incidence of rainfall in the overland flow process. A method, based on the kinematic wave theory, is presented in which overland flow, under rainfall from any dominant direction, is simplified by taking a one-dimensional flow process by means of spatial rotation of the surface (assumed to be a plane). Further the acceleration of gravity is modified at every instant to take into account the effect of the impinging raindrops. A computer program was developed to solve numerically the kinematic-wave equations for overland flow under inclined rainfall and also considering the effect of the wind shear stress and of the splash. Wind tunnel experiments in the laboratory were conducted in order to test the model.

INTRODUCTION

Agricultural use of the soil is mostly limited to the upper few decimeters. Through natural but also social and political decisions, through haste and carelessness, soils are being needlessly eroded by both wind and water. Loss of surface soil through wind and water erosion means decreased soil fertility as well as reduced storage in reservoirs and reduced capacity of rivers to carry flood flows because of sedimentation.

Wind erosion as well as rainwater erosion have drawn the attention of various researchers. Several factors that affect wind erosion are also influencing rainwater erosion, namely soil erodability, surface roughness, climate, relief, vegetation, tillage practices, etc.. However, wind velocity and wind-velocity profiles over different types of soil surfaces were studied only with respect to wind erosion. Wind effects are not generally considered in overland flow and rainfall erosion studies.

Wind may cause rain to fall at considerable inclination. Resultant angles of 40 to 60° (measured from the vertical) have been found in storms with wind speeds of up to 10 m/s (Sharon, 1980). Moreover, the effective depth of rainfall that is actually incident on sloping ground differs greatly from measurements in conventional raingauges (Struzer, 1975). Also the hydraulics of the overland flow process is affected.

In an experimental station located in Alentejo (semi-arid region of Portugal), 15 standard field plots of 20x8.33 m^2 with slopes ranging from 10 to 20% were studied with respect to rain water erosion. It was found that fields with slopes of around 20% showed less erosion than slopes of 10% and 11% for the same amount of runoff, which is attributed to the orientation of the fields with respect to the dominant direction of the winds (Ferreira *et al.*, 1985).

DESCRIPTION OF THE MODEL

The angle of incidence of the rainfall

The rain can be represented by a vector **r** making an angle θ (0(vert.) $\leqslant \theta$(rad) $\leqslant \pi/2$(hor.)) with the vertical and having an azimuth ω($0 \leqslant \omega$(rad) $\leqslant 2\pi$). The determination of ω can be made with any recording wind vane. The angle θ is assumed constant within each time interval, in space and over the drop spectrum and may be measured directly by means of photography, by simple visual observation, or can be estimated by:

$$\theta = \arctan (\overline{V} / V_T) \qquad (1)$$

where $\overline{V}$ (m s^{-1}) is the average horizontal wind speed near the soil surface (during rain storm) and V_T (m s^{-1}) is the terminal vertical speed of raindrops.

The terminal vertical velocity of the raindrops may be estimated as a function of their size (Epema & Riezebos, 1983). Wind may limit the upper size of raindrops.

Actual impact velocity is often greater than the terminal velocity of the raindrops because of wind effects which may impart an added velocity component (thus increasing the kinetic energy of the raindrops). The speed of impact will be

$$V^* = \sqrt{(V_T^2 + \overline{V}^2)} \qquad (2)$$

where V^* (m s^{-1}) is the impact speed of the raindrops.

The rain gauges measure the intensity of rainfall which is the projection of the rainfall vector **r**(t) on a vertical line and

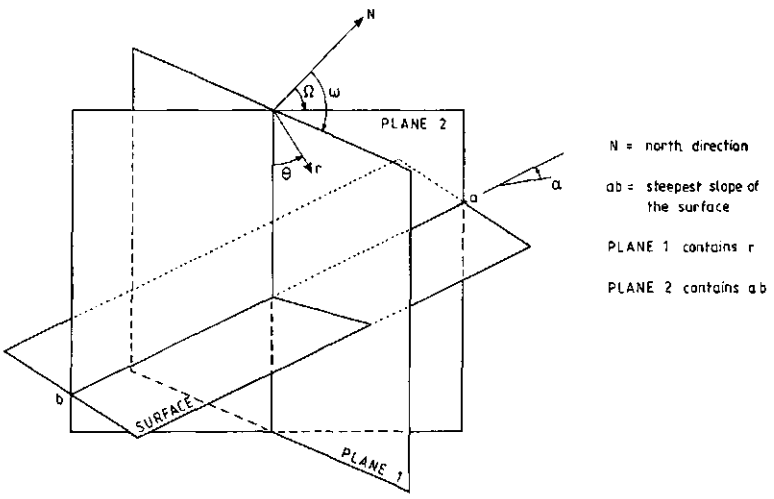

Fig. 1 Sketch showing the different angles.

integrated over a horizontal surface (neglecting the possible influence of the wind pattern around the rain gauge):

$$P_{gau} = r(t) \cos \vartheta \qquad (3)$$

The rain intensity has to be adjusted to the overland flow surface, according to the relation between the steepest line of the ground surface and the rain vector (Fig. 1):

$$P_{er} = P_{gau} C_{gau} = P_{gau} [\cos \alpha + \tan \vartheta \sin \alpha (\cos \omega \cos \Omega + \sin \omega \sin \Omega)] \qquad (4)$$

where α (0(hor.) $< \alpha$ (rad) $< \pi/2$(vert.)) is the angle of the surface with the horizontal, Ω ($0 < \Omega$(rad) $< 2\pi$) is the azimuth of the slope (uphill direction), and C_{gau} a raingauge efficiency coefficient.

The rotation directions in three dimensions (Fig. 1) were chosen in such a way that in the two dimensional case (Fig. 3) the positive angle is measured in the clockwise direction.

In Fig. 2, C_{gau} (eq. 4) was plotted in three dimensions against ϑ and $(\omega - \Omega)$ for a fixed slope gradient of $\pi/16$, illustrating the importance of the correction for inclined rainfall on sloping surfaces.

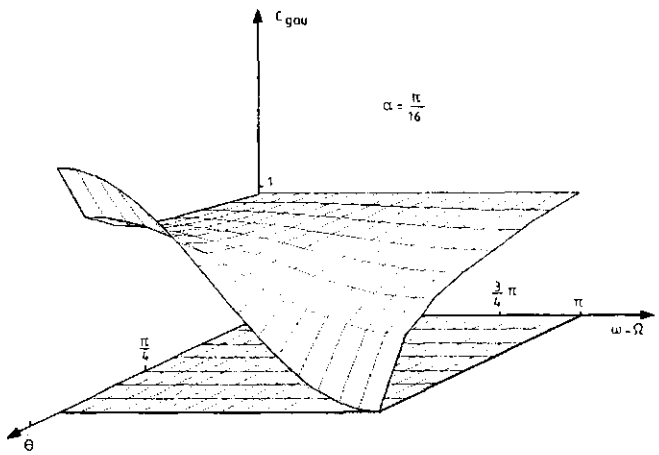

Fig. 2 C_{gau} against ϑ and $(\omega - \Omega)$ for fixed α.

Considering the effect of inclined rainfall

Owing to its simplicity, the kinematic wave approach has been frequently used to solve unsteady flow problems. The equation of continuity for shallow water flow may be written as:

$$\partial h/\partial t + \partial q/\partial x = p(t) - i(t) \qquad (5)$$

where h is the flow depth (m) at time t, and position x, q is the volumetric water flux per unit plane width ($m^2\ s^{-1}$), p(t) is the rainfall rate ($m\ s^{-1}$), and i(t) is the infiltration rate ($m\ s^{-1}$).

A method, based on the kinematic wave theory, is presented in which overland flow, under rainfall from any dominant direction, is simplified by taking a one-dimensional flow process by means of spatial rotation of the surface (assumed to be a plane). Further the acceleration of gravity is modified at every instant to take into account the effect of the impinging raindrops (Kilinc & Richardson, 1973). According to the sketch of Fig. 3, the new angle α' of the plane and the new ficticious acceleration of gravity g' ($m\ s^{-2}$) will be:

$$\alpha' = \alpha - \phi \tag{6}$$

$$g' = g\ F \cos \phi / F_1 \tag{7}$$

moreover

$$\phi = \arcsin (F_2 \sin\theta' / F) \tag{8}$$

$$\theta' = \arctan (\tan \theta \cos(\omega - \Omega)) \tag{9}$$

$$F = \sqrt{(F_1^2 + F_2^2 + 2 F_1 F_2 \cos \theta')} \tag{10}$$

$$F_1 = g \int_x^{x+\Delta x} h(\bar{x},t)\ d\bar{x} \tag{11}$$

where ϕ is the angle of rotation of the surface (rad), θ' ($-\pi/2 \leqslant \theta'$(rad) $\leqslant \pi/2$) is the angle of incidence of the rain with the vertical , $\mathbf{F_1}$ is the force expressing gravity in the elementary section (N), $\mathbf{F_2}$ is the force coming from raindrops impinging on the elementary section (N), $\mathbf{F}$ is the sum of forces $\mathbf{F_1}$ and $\mathbf{F_2}$, and Δx is the space increment of the numerical scheme. To obtain an estimate of the force F_2, the impulse-momentum principle was used:

$$F_2 = \Delta x\ \rho\ P_{er}\ V^2\ a \tag{12}$$

where ρ is the density of the water ($Kg\ m^{-3}$), and a is the fraction of F_2 transmitted to the flowing water sheet (N). The remaining fraction would go to the soil , detaching and splashing soil particles in bare soil, for example.

By assuming that the bed slope equals the friction slope (kinematic wave assumption) and by using Darcy-Weisbach equation, we can express the discharge at any point in space and time as a function of the water depth only, as follows:

$$q = \beta h^m \qquad \text{with} \quad \beta = \sqrt{(8\ g' \tan\alpha' / f)} \tag{13}$$

where m (approximately 3/2) is a parameter for the type of flow, β is a hydraulic coefficient, and f is the Darcy-Weisbach friction factor.

The parameter m, is relatively stable (Singh, 1975) and is kept constant throughout the simulation. On the other hand β will be given a physical or quasi-physical interpretation, reflecting the effects of surface slope, rainfall, wind and hydraulic roughness on the depth of flow, and will change continuously according to eq. (13).

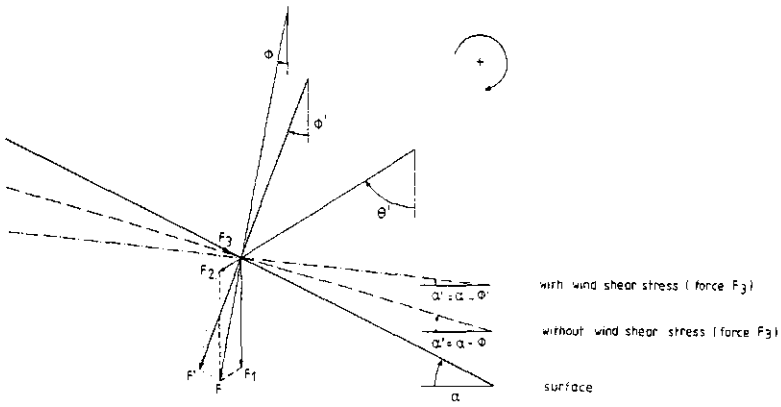

Fig. 3 Determination of α'.

Considering the effect of the wind in the water-air boundary

Wind velocity is never constant but highly turbulent. Under neutral conditions, when temperature is constant with height, the mean wind speed increases linearly with the logarithm of the height (Sellers, 1965):

$$V_w = C \ln(z/z_0) \tag{14}$$

where V_w (m s^{-1}) is the wind speed at the height z, z_0 is the roughness length (m), and C is a constant (m s^{-1}).

Laboratory as well as outdoor experiments of turbulent flows show that (Vennard et al., 1982)

$$C = u^*/k = (1/k) \sqrt{(\tau/\rho_{air})} \tag{15}$$

where k is the Von Karman constant (approximately 0.4), τ is the frictional shear stress (Pa), ρ_{air} is the density of the air (Kg m^{-3}), and u^* is the friction velocity (m s^{-1}).

The tangential wind shear force, F_3, can then be expressed in terms of τ by:

$$F_3 = \Delta x \, W \, \tau \cos(\omega-\Omega) \tag{16}$$

with

$$\tau = \rho_{air} [V_w k / \ln(z/z_0)]^2 \tag{17}$$

where W is the fraction per meter of surface width covered by the water sheet.

u^* and z_0 can be obtained from the wind profile (using logarithm scale in the vertical axis). Otherwise, knowing the velocity V at the height z and using equations (16) and (17), F_3 can be estimated, taking the roughness length of the overland flow sheet as approximately 0.2 mm (Holtslag, 1987). In slopes with many mounds (vegetation, earth, rocks, etc) F_3 may become negligible because of higher roughness lengths of the mounds and smaller area covered by the water sheet. In unstable conditions, when the temperature increases or decreases strongly with height, the procedure proposed by Holtslag (1987), might be applied instead of equation (17).

Taking into consideration the effect of the wind (force F_3) the following changes have to be made in equations (8) and (10):

$$\phi' = \arcsin\left[(F_2 \sin\theta' + F_3 \cos\alpha)/F\right] \tag{18}$$

$$F' = \sqrt{\left[F_1^2 + F_2^2 + F_3^2 + 2(F_2 F_3 \cos\theta' \sin\alpha + F_2 F_3 \sin\theta' \cos\alpha + F_1 F_2 \cos\theta' + F_1 F_3 \sin\alpha)\right]} \tag{19}$$

where ϕ' is the angle of rotation of the surface (rad), considering F_3, and F' is the sum of forces F_1, F_2 and F_3.

The wind velocity used in the calculation of θ (eq. 1), may be obtained by averaging the wind profile from z_0 to the height z (standard measuring height of the wind speed at the meteorological station - normally 10 m)

$$\bar{V} = u^* z \left[\ln(z/z_0) - 1\right]/\left[(z - z_0) k\right] \tag{20}$$

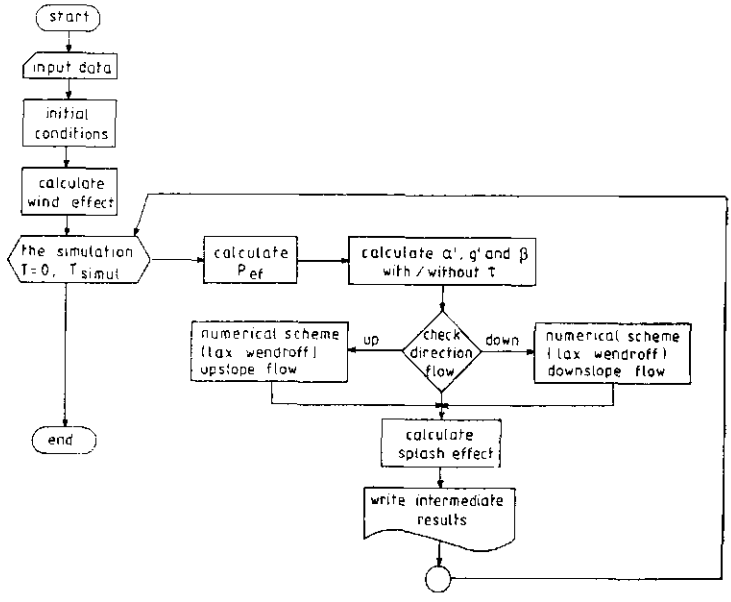

Fig. 4 Master flowchart of the model.

Considering the effect of the splash

The simple model developed by Zaslavsky & Sinai (1981) was used. Additionally, the effect of oblique rain was considered altering the magnitude of the asymmetry of the splash of an angle α, in the direction of the wind.

The computer program

A computer program WROF (Wind, Rain and Overland Flow) was developed to solve the kinematic-wave equations for overland flow under inclined rainfall from any direction and also considering the effect of the wind shear stress and of the splash. The numerical scheme used was the explicit single step Lax-Wendroff method. It allows flow of water both up and down the slope according to rainfall conditions, plane surface position, wind characteristics, splash characteristics and hydraulic overland flow characteristics (Fig. 4).

The elevation at grid points in any shape of field can be fed into the program. However, care must be taken in the application of the program in the case of non-homogeneous topography. The plane of best fit will be assumed as the average overland flow (sheet flow) basis. The area covered by mounds was estimated by comparing at every instant the topographic elevations of the field at grid points with those of the plane of best fit raised with the depth of overland flow. Since WROF is a numerical model it is possible to have variable parameters, in time and space, without any serious computational difficulty.

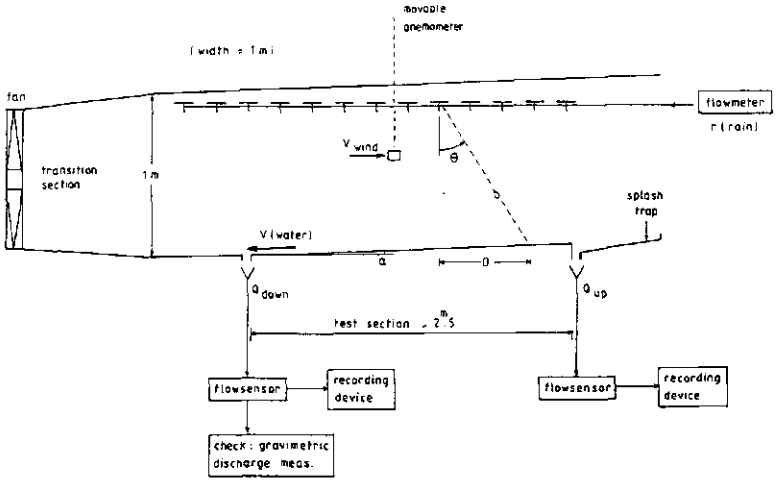

Fig. 5 Schematic representation of the experimental set-up and variables measured.

VERIFICATION OF THE MODEL: WIND TUNNEL EXPERIMENT

Evaluating efficiently in the field the phenomena in study is very difficult due to the factor of time and space, and lack of control over the variables envolved. Wind tunnel experiments in the laboratory were undertaken (Lima, 1989) in order to provide a preliminary insight into the problem and to test the model.

The wind tunnel is a low-speed, open-circuit one and is made of wood and plastic sheets (Fig. 5). A rainfall simulator was installed inside the wind tunnel. The wind profile obtained is an effect of the tunnel construction and of the rainfall simulator and does not agree with natural wind velocity profiles. The model WROF was adapted for that situation. Wind speed is adjusted roughly by means of the velocity of rotation of the fan and checked with a portable anemometer. The angle of incidence of the rain was estimated by injection of dye in the drop formers, and measuring the distance at which the coloured drops hit the water sheet.

Fig. 6 shows the effect of different wind velocities in the overland flow hydrographs. Less discharge at L (Q_{down}) for higher wind velocities is due to an increase of discharge at the origin of the impermeable plane(Q_{up}).

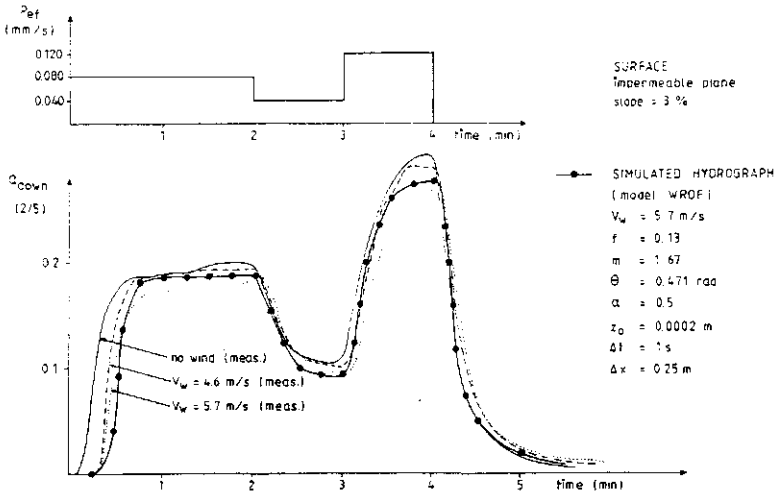

Fig. 6 Influence of the wind in the hydrographs of overland flow.

Simulation with the model WROF gave good results (Fig. 6) both in the estimation of the initiation of the overland flow process at L, and with respect to the shape of the hydrographs. In these experiments the effect of the wind shear stress was very pronounced due to the small impact velocity of the raindrops and because of the smoothness of the surface. The model was run with hydraulic data (i.e. f and m) obtained from vertical rainfall experiments.

EXAMPLE OF APPLICATION

Consider two impermeable slopes approximated by two impermeable planes of different orientations with respect to the inclined rainfall. Assuming equal slope characteristics and an angle of incidence of the rain of 45°, the overland flow hydrographs at the bottom of the two slopes are compared for two different rainfall patterns measured with horizontal rain-gauges (Fig. 7). The hydrographs for the two slopes have remarkable differences, as expected (Lima, 1988).

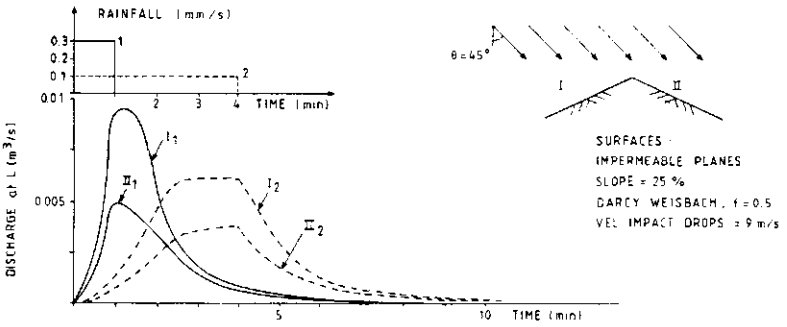

Fig. 7 Overland flow hydrographs at the bottom of two slopes.

CONCLUSION

Wind intensity and direction influence both the effective rainfall pattern and the mechanics of the overland flow process on slopes. They affect overland flow in the following ways: shape, size, angle and velocity of impact of raindrops, splash shape, and tangential shear stress in the water-air boundary.

The effects of the wind shear stress and splash are small in comparison with the effect of the inclined impinging raindrops for high intensity rainfalls. However the effect of wind shear stress may be significant when a thin water sheet covers the entire soil surface and for low intensity rainfalls.

The physically based mathematical model introduced and verified in this study is not the most sophisticated one possible. The simplified model may prove to be accurate enough for practical purposes in the assessment of the factors affecting overland flow under inclined rainfall. This may lead to a better understanding of the water erosion problem and how it can be coped with.

Further improvement could be the coupling of this model with a sediment transport model.

ACKNOWLEDGEMENT

The author wishes to thank Prof. W.H. van der Molen, Dr. R.W.R. Koopmans, and Dr. A.F.G. Jacobs for their helpful suggestions and "Comissão Permanente INVOTAN" for financial support. The author is very grateful to the University of Coimbra (Portugal) for the

permission and partial support of his stay at the Agricultural University Wageningen.

REFERENCES

Epema, G.F. & Riezebos H.Th. (1983) Fall velocity of waterdrops at different heights as a factor influencing erosivity of simulated rain. In: Rainfall Simulation, Runoff and Soil Erosion (ed. by J. de Ploey), Catena Supplement 4, Braunschweig, 2-17.

Ferreira, I.M.M., A.J.R. Ferreira and D.A. Sims (1985) USLE adapted for use in Portugal. Land and Water (FAO), 22, April, 21-24.

Holtslag, A.A.M. (1987) Surfaces fluxes and boundary layer scaling: Models and applications. Ph.D. Thesis. Agricultural University Wageningen.

Kilinc, M. & Richardson E.V. (1973) Mechanics of soil erosion from overland flow generated by simulated rainfall. Report no. 63, Colorado State Univ., Fort Collins, Colorado.

Lima, J.L.M.P. de (1988) Morphological factors affecting overland flow on slopes. Proc. Symp. on Land Qualities in Space and Time, August, Wageningen.

Lima, J.L.M.P. de (1989) Overland flow under simulated wind-driven rain (in preparation).

Sellers, W.D. (1965) Physical climatology. University of Chicago Press.

Sharon, D. (1980) The distribution of hydrologically effective rainfall incident on sloping ground. J. Hydrol., 46, 165-188.

Singh, V.P. (1975) A laboratory investigation of surface runoff. J. Hydrol., 25, 187-200.

Struzer, L.R. (1972) Problem of determining precipitation falling on mountain slopes. Sov. Hydrol. Selected Pap., 2, 129-142.

Vennard, J.K. & Street R.L. (1982) Elementary fluid mechanics, SI version, John Wiley & Sons.

Zaslavsky, D. & Sinai, G. (1981) Surface hydrology: II-distribution of raindrops. J. Hydraul. Div. ASCE, 107, HY1, 17-36.

7.2 OVERLAND FLOW UNDER SIMULATED WIND-DRIVEN RAIN

Published in: V.A. Dodd and P.M. Grace (Eds.), Agricultural Engineering, Vol 1 - Land and Water Use, Proceedings of the Eleventh International Congress on Agricultural Engineering, Dublin, Ireland, 4-8 September 1989, A.A. Balkema, Rotterdam, 493-500.

Land and Water Use, Dodd & Grace (eds), © 1989 Balkema, Rotterdam. ISBN 90 6191 980 0

Overland flow under simulated wind-driven rain

J.L.M.P. de Lima
Department of Land and Water Use, and Department of Hydraulics and Catchment Hydrology, Agricultural University Wageningen, Wageningen, Netherlands

ABSTRACT: The effects of inclined rainfall and the wind induced shear-stress on overland flow have been investigated in an experimental study. These processes have been simulated in a wind tunnel having variable slope. Upslope blowing wind was found to delay the occurrence of overland flow and increase the depth of water over an impermeable plane. Even upstream discharge has been observed. The implications of these results to overland flow modelling are discussed.

RESUME: Cet article traite l'effet de la pluie inclinée et de l'effort de cisaillement du vent sur l'écoulement superficiel. Des expériences ont été effectuées au moyen d'une soufflerie aérodynamique à pente variable. L'effet du vent soufflant vers l'amont se manifeste par un retard de l'écoulement superficiel et par une plus grande épaisseur de la couche d'eau sur une surface imperméable. Une décharge à l'amont a aussi été observée. Les conséquences de ces résultats pour la modélisation de l'écoulement superficiel sont discutées.

ZUSAMMENFASSUNG: Einflüsse von schrägfallendem Regen und vom Wind verursachten Schubspannung auf den Oberflächenabfluss wurden in einer experimentelle Studie untersucht. Diese physikalische Vorgänge wurden in einem Windkanal mit variablen Gefälle simuliert. Der bergauf wehende Wind hat nicht nur den Beginn des Abflusses verzögert und die Wassertiefe über die undurchlässige Oberfläche vergrössert, er sorgte sogar für Abfluss gegen Gefälle. Die Folgen obengenannter Resultate auf die Modellierung von Oberflächenabflussvorgänge werden in diesem Aufsatz erörtert.

NOTATION

The following symbols are used in this paper:

a = discharge variation due to wind (l/s)
b = discharge variation due to wind (l/s)
c = discharge variation due to wind (l/s)
d = discharge variation due to wind (l/s)
D = distance at which drops hit the water sheet (m)
e = discharge variation due to wind (l/s)
f = Darcy-Weisbach friction factor
k = von Karman's constant (≈0.4)
L = lenght of working section of the overland flow surface (m)
m = exponent of flow depth (kinematic flow approximation) (approximately 5/3 for turbulent flow)
n = number of observations
Qdown= discharge at x=L (l/s)
Qup= discharge at x=0 (l/s)
r = regression coefficient
R = effective rainfall rate (m/s)
S = slope gradient
t = time (s)
t_r = time from beginning of rain to start of outflow at x=L (s)
Vw = wind speed at the height z (m/s)
Vwater = overland flow velocity (m/s)
x = distance from top of plane (m)
WROF = numerical model (Wind, Rain, and Overland Flow)
z = measuring height of Vw (in this experiments half distance between water sheet and drop formers) (m)
zo= roughness length (m)
α = angle of the surface with the horizontal (degrees)
θ = angle of incidence of the rainfall with the vertical (degrees)
ρ air = density of the air (Kg/m3)
τ = wind frictional shear stress (Pa)

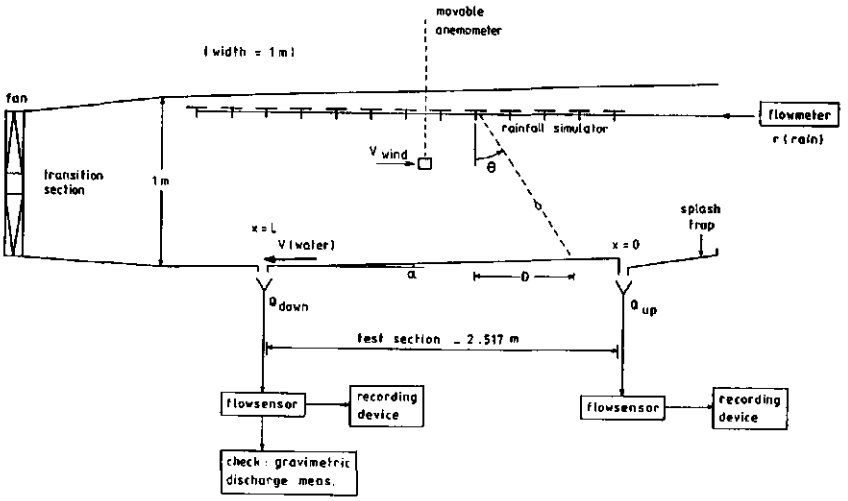

Fig. 1 Schematic representation of the experimental set-up and variables measured.

1 INTRODUCTION

Wind action on the surface of bodies of water produces such phenomena as wind waves, wind driven and wave currents, seiches, wind tides, etc (Baines & Knapp, 1965, Wu, 1975, Kranenburg, 1987, etc). Also wind may cause rain to fall at considerable inclination (Umback & Lembke, 1966, Struzer, 1972, Sharon, 1980). Falling through a logarithmic wind profile (expected profile under rainstorm conditions, Rosenberg et al., 1983), raindrops arrive at the surface retaining most of the horizontal momentum they possessed at 10 m height (Caldwell & Elliott, 1972). All these factors affect the overland flow process, which is further complicated by the effects of impinging raindrops (Shen & Li, 1973). Although many rainfall events are accompanied by strong winds (Lyles et al., 1974, Lyles, 1977), only limited knowledge is available on the influence of wind on overland flow.

This paper deals with the effects of inclined rainfall and wind induced shear-stress on the overland flow process. Wind affects overland flow in the following ways: effective rainfall pattern, shape, size, angle and velocity of impact of raindrops, splash shape, and tangential shear stress in the water-air boundary (Lima, 1989).

Evaluating these phenomena, in the field, is very difficult due to the factors of time and space, and lack of control over the variables involved. In order to provide a preliminary insight into the problem and to test the numerical kinematic model WROF (Lima, 1989) a laboratory experiment was undertaken.

Wind blowing over the overland flow sheet can be divided into two components: (1) longitudinal wind blowing along the steepest line of the surface, and (2) the cross wind blowing perpendicularly to the same line. The longitudinal wind causes a change of the driving force of the overland flow. Moreover, these effects become even more pronounced as an upslope and a downslope wind induce opposite effects. The cross wind causes a change of flow path as the overland flow sheet is pushed sideways. In this experiment wind direction was always upslope and parallel to the surface.

The results of the experimental runs are analysed. In these experiments the effect of the wind shear stress was very pronounced due to the small impact velocity of the raindrops and because of the smoothness of the surface. The implications of these results to overland flow modelling are discussed.

2 EXPERIMENTAL SET-UP

The laboratory experiment was carried out in the Hydraulic Laboratory of the Department of Hydraulics & Catchment Hydrology of the Wageningen Agricultural University. The laboratory set-up was

mainly composed of three units:

(a) channel, with an uniform rectangular cross section 1 m wide, in which a wind tunnel was installed. The surface was a smooth impermeable plane (painted plywood). The slope of the channel was adjustable;

(b) rainfall simulator consisting of circular plates with conveyors to the edges of the plates where the drops are formed. The rainfall simulator gives a uniformly distributed and time invariant geometrical rainfall pattern. Drop shape differed significantly from the equilibrium shape at terminal velocity due to oscillations after release from the drop formers and small fall height (Epema & Riezebos, 1984). The equivalent diameter of the drops (defined as the diameter of a spherical drop with the same mass) was rather large at the drop formers (up to 8 mm). However, drop breakup existed, increasing with wind speed;

(c) low-speed, open-circuit wind tunnel made of wood and plastic sheets, having a working section 1 m wide, 1 m high and 2.517 m long. The rainfall simulator was installed inside the wind tunnel.

Fig. 1 shows a schematic representation of the laboratory set-up and the variables measured.

The rainfall intensity was measured by a flowmeter. The outflow hydrographs (of Qup at x=0, and of Qdown at x=L) were registered by a magnetic flow sensor connected to an automatic continuous recorder. At steady state Qdown was checked against a gravimetric discharge measurement (i.e. a weighing drum and a stopwatch). For no-wind conditions, velocity measurements of overland flow (Vwater) were made using dye tracing.

The wind profile obtained was an effect of the tunnel construction and of the presence of the rainfall simulator inside it, and does not agree with natural wind velocity profiles. A decrease of the wind profile at higher level was due to friction with the rainfall simulator. Wind speed was adjusted roughly by means of the velocity of rotation of the fan and checked with a movable anemometer. The anemometer permits measurements at a distance of 25 mm of any border. Note that the wind direction in this experiments was always upslope and parallel to the surface.

The fan (axial fan) had a 1.64 kW electric motor at 1200 r.p.m., which was connected to a variable transformer. This fan type is commonly used for the ventilation of stables and cereal storage buildings. The air sucked to the wind tunnel was dry air from the centrally heated hydraulic laboratory room.

The angle of incidence of the rain was estimated by injection of dye in the drop formers, and measuring the distance at which the coloured drops hit the water sheet.

The angle of incidence of the simulated rain was found to be independent of the rainfall intensity. However this angle was slighly changed by the slope gradient because the slope affected the position of the rainfall simulator (kept horizontal inside the wind tunnel) (Fig. 1 and 2).

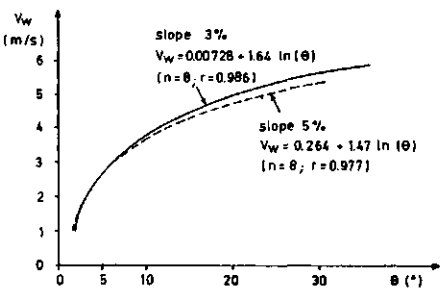

Fig. 2 Wind speed versus angle of incidence of rainfall, for slopes of 3 and 5 %.

Raindrops falling through the wind profile do not adjust their speeds immediately to the wind. The trajectory of the drops was approximately linear due to nearly constant acceleration components in the vertical and wind directions, an initial zero velocity at the drop formers, and a small fall height. The velocity component of the drops in the wind direction at impact point was much smaller than the average wind velocity (Vw): for the slope of 5%, around 0.4 Vw for θ = 30 degrees, and 0.15 Vw for θ = 5 degrees. Thus, stresses developed which deccelerate the air. However, the resulting decrease of wind speed was very slight and was neglected.

Experiments (54 runs) were repeated for each slope (3 and 5%) with different average wind speed (ranging from 0 to 6 m/s), and each wind speed with different rainfall intensities (ranging from 0.04 to 0.18 mm/s). In some runs it was the rainfall intensity that was kept constant for varying wind speeds.

3 RESULTS

Less discharge at x=L (Qdown) for higher wind velocities is due to an increase of discharge at the origin, x=0, of the impermeable plane (Qup)(Fig. 1). In these experiments the effect of the wind shear

stress was very pronounced due to the small impact velocity of the raindrops and because of the smoothness of the surface.

The frictional wind shear stress τ, assuming that the mean wind speed increases linearly with the logarithm of the height (Rosenberg et al., 1983), can be expressed by:

$$\tau = \rho_{air} [Vw\ k / \ln(z/zo)]^2 \quad (1)$$

where z was taken as half the distance between water sheet and drop formers, because of the decrease in wind speed near the rainfall simulator. (See the notation list for symbols and units.)

The value of the hydrodynamical roughness length (zo) was for these experiments 0.0002 m, and was found through calibration of various runs with the model WROF (see section 3.3). In these experiments the water sheet covered the entire surface (a smooth impermeable plane). Higher values of zo should be expected for rougher surfaces.

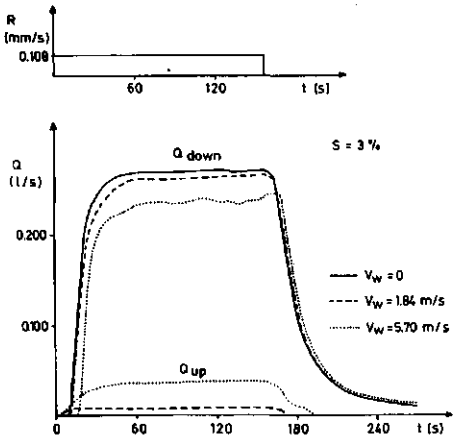

Fig. 3 Influence of wind on observed hydrographs of overland flow (both for Qdown and Qup).

3.1 Experiments with constant wind speed

In Fig. 3, the effect of the wind speed is assessed for approximately equal rainfall patterns. Wind speed delayed the start of overland flow at x=L (t_r), and increased the amount of water pushed slope upwards (Qup). Fig. 4 presents the effect of slope for approximately the same wind and rectangular rainfall patterns. At a steeper slope we obtain more discharge at x=L (Qdown). For the same rainfall intensity the time of initiation of overland flow at x=L decreases for increasing slope steepness. This can be seen in Fig. 5 comparing the solid lines (S = 3%) with the dashed lines (S = 5 %) for approximately the same effective rainfall rate, R. Also the form of τ-t_r (assumed linear due to high regression coefficients: 0.977 to 0.999) is affected. The steeper the slope the smaller is the effect of τ on t_r (Fig. 5).

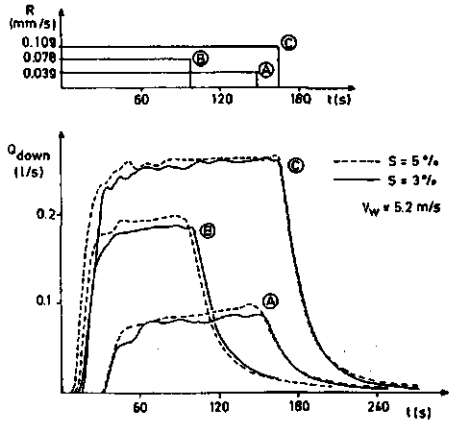

Fig. 4 Effect of slope on observed hydrographs of overland flow (Qdown), for three rainfall rates (R).

3.2 Experiments with variable wind speed

Experiments with variable wind speed consisted mainly in starting and stopping wind at fixed intervals and observing the discharge behaviour at the extremes of the surface (Qdown and Qup). Fig. 6 shows the general behaviour of Qdown in time and for a certain fixed rainfall when a wind speed of 5.9 m/s is suddenly started and stopped after one minute. The decrease of discharge due to sudden start of wind was found to be approximately equal to the increase of discharge due to the sudden cessation of the same wind (b=-d in Figures 6 and 8, and also b-a+c). However b became larger than -d for higher rainfall intensities (Fig. 8). Fig. 11 shows a complete sequence of discharge variations due to a sudden stop and start of a series of different wind speeds.

Discharge variations considered as a function of the effective rainfall rate (R), can be correlated with the wind speed, i.e. with the wind frictional shear stress

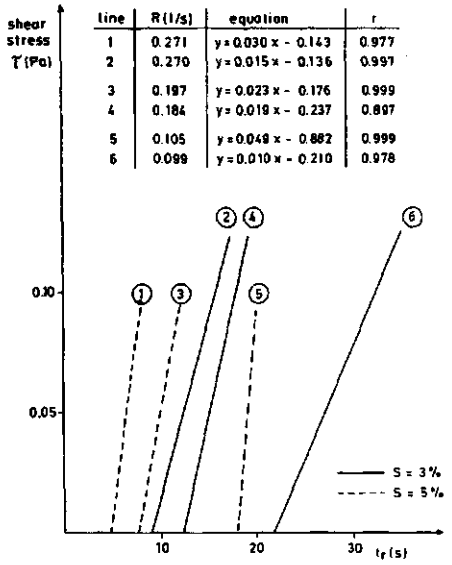

line	R (l/s)	equation	r
1	0.271	y = 0.030 x - 0.143	0.977
2	0.270	y = 0.015 x - 0.136	0.991
3	0.197	y = 0.023 x - 0.176	0.999
4	0.184	y = 0.019 x - 0.237	0.897
5	0.105	y = 0.049 x - 0.882	0.999
6	0.099	y = 0.010 x - 0.210	0.978

Fig. 5 Shear stress as a function of time to start overland flow (t_r), for various rainfall rates (R) and slopes of 3 and 5 %.

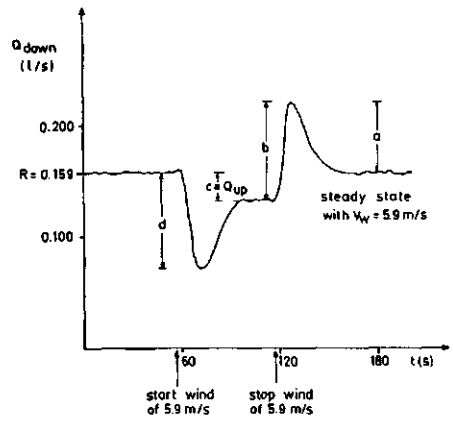

Fig. 6 Discharge variations in time, at x=L, for a sudden start and stop of a wind of 5.9 m/s.

(τ). When plotting (b/R) and (-d/R) against shear stress τ a linear relation is found (Fig. 9), but (Qup/R) against τ yields a curve to which an exponential relation has been fitted (In Fig. 10, simple exponential curve was fitted to the data). Fig. 7 gives discharge variations, i.e., a, b, c and d (see Fig. 6) as a function of wind speed for the 5% slope gradient. Remarkably the shape of a tends to a constant value for higher wind velocities (within the same measured range of Vw).

The different effects which induce the temporary increase of downstream discharge with respect to steady state conditions were (ranking by importance):

(i) sudden stop of wind;
(ii) sudden stop of wind and rain;
(iii) sudden stop of rain.

These effects are shown for two rainfall rates in Fig. 12.

The increase of discharge due to a sudden stop of rain and wind (case ii) is lower than the increase due to only the sudden stop of the same wind (case i), mainly because in the latter case a new higher steady state discharge under rainfall will be reached. Case (iii) created the smallest increase of the three cases.

When rainfall stops (case iii) outflow discharge (Qdown) increases temporarily before recession. This phenomenon can be

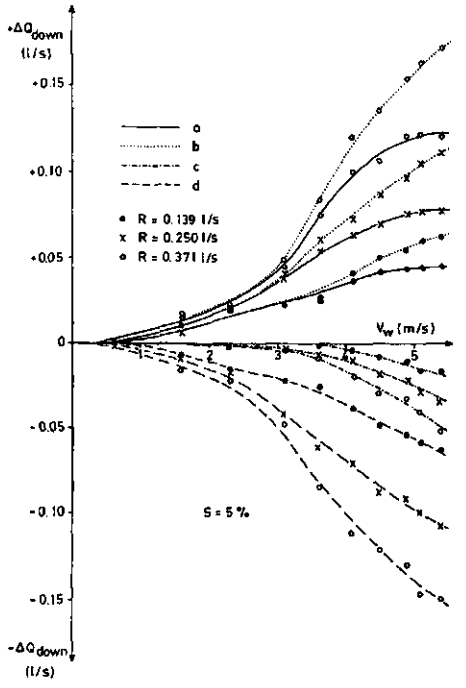

Fig. 7 Discharge variations as a function of wind speed (Vw), for various rainfall rates (R). For a, b, c and d see Fig. 6.

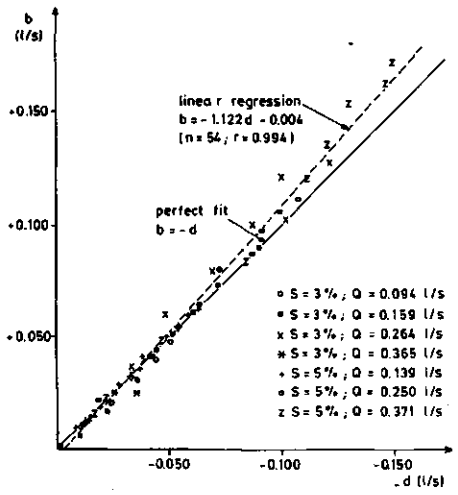

Fig. 8 Plot of b versus -d (see also Fig. 6)

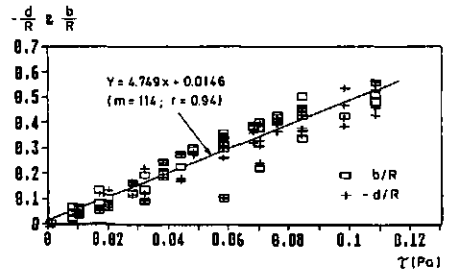

Fig. 9 Plot of b/R and -d/R versus τ.

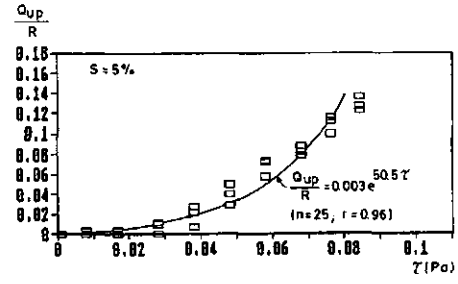

Fig. 10 Plot of Qup/R versus τ for the 5% slope.

explained by the fact that the stopping of raindrop impact causes a change in the friction slope and the energy gradient line, due to reduction of the resistance coefficient to a lower value (different dissipation of energy). As a consequence, the outflow has a temporary increase. This peak was not always observed in the outflow hydrograph.

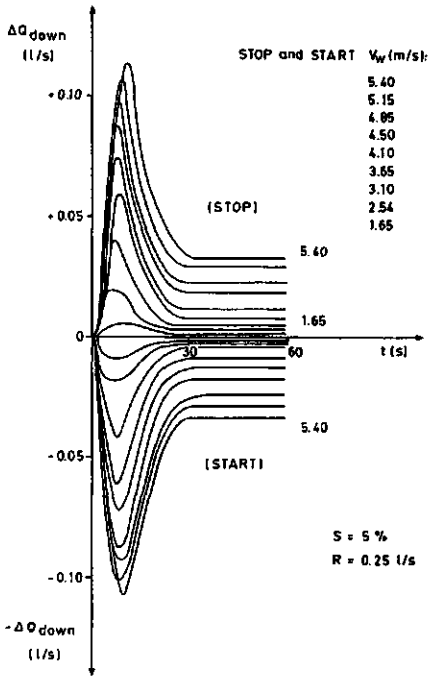

Fig. 11 Observed discharge variations as a function of time, for sudden start and stop of various wind speeds (Vw).

3.3 Testing of the model WROF (Lima, 1989)

Simulation with the numerical kinematic model WROF (Wind, Rain, and Overland Flow) gave good results both in the estimation of the initiation of the overland flow process at x=L, and the shape of the hydrographs, although the stronger the wind speed the more fluctuations were observed (Fig. 13).

The model was run with hydraulic data (i.e. f and m) obtained from vertical rain experiments. Sensitivity analysis showed that the roughness length (zo) is an important parameter in the assessement of wind effects on sheet flow.

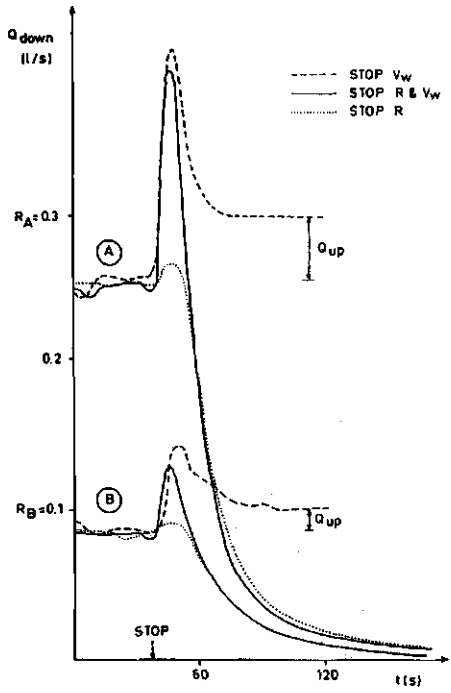

Fig. 12 Effects inducing temporary increase of discharge, at x-L (Qdown), for two rainfall rates (R).

4 CONCLUSIONS

The role of wind on overland flow was discussed. Wind intensity and direction influence both the effective rainfall pattern and the mechanics of the overland flow process.

Wind blowing upslope was found to delay the start of overland flow and increase water depth along the surface, leading to the existence of a finite water depth at x=0 accompanied by upslope discharge (Qup). The decrease of overland flow at x-L due to the start of a certain wind speed was highly correlated with the subsequent increase of flow due to stopping the same wind.

The effect of the wind shear stress and splash were small in comparison with the effect of the inclined impinging raindrops for high intensity rainfalls. However the effect of wind shear stress may be significant when a thin water sheet covers the entire surface and for low kinetic energy of the rain (low intensity rainfalls or, as in these experiments, small drop fall height).

The results of the laboratory experiments describe the importance of wind in the overland flow process under rainfall. Neglecting wind effects in rainfall simulation studies might be a cause of errors. Transferability of these results to the field is not obvious. More research is needed on effects of wind-rain forces on overland flow and soil surface, and on the magnitude and frequency of winds associated with rains in areas susceptible to water erosion.

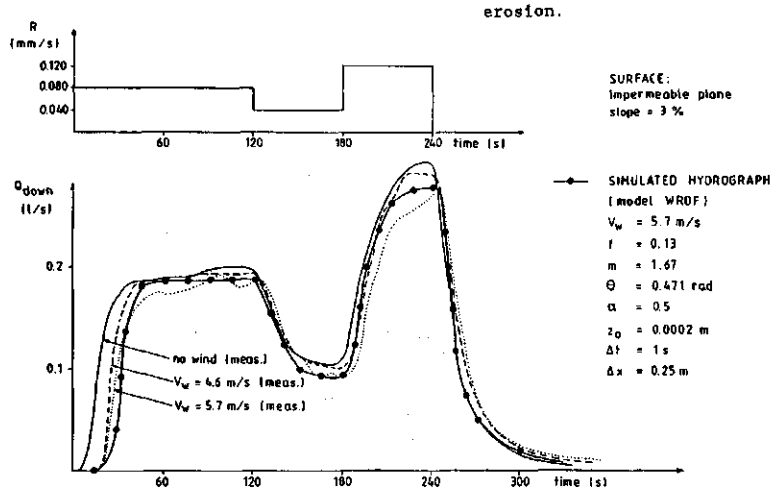

Fig. 13 Simulation with the model WROF (Lima, 1989).

ACKNOWLEDGEMENT

The author wishes to thank Prof. W.H. van der Molen, Dr. R.W.R. Koopmans and Dr. A.F.G. Jacobs for their helpful suggestions, the assistance of Mrs. G. Kranjac-Berisavljevic in the laboratory work, and the staff of the hydraulics laboratory for the installation of the equipment. The author is indebted to "Comissão Permanente INVOTAN" for financial support and is also very grateful to the University of Coimbra (Portugal) for the permission and partial support of his stay at the Wageningen Agricultural University.

REFERENCES

Baines, W.D. & D.J. Knapp 1965. Wind driven water currents. J. of Hydraulics Division, ASCE, 95: 205-221.

Caldwell, D.R. & W.P. Elliott 1972. The effect of rainfall on the wind in the surface layer. Boundary-Layer Meteorology, 3: 146-151.

Epema, G.F. & H. TH. Riezebos 1984. Drop shape and erosivity Part I: experimental set up, theory, and measurements of drop shape. Earth Surfaces Processes and Landforms, 9: 567-572.

Kranenburg, C. 1987. Turbulent surface boundary-layer induced by an off-shore wind. J. of Hydraulic Research, 25: 53-65.

Lima, J.L.M.P. de 1989. The influence of the angle of incidence of the rainfall on the overland flow process. Proc. IAHS Third Scientific Assembly, Baltimor, USA, May 10-19 (accepted).

Lyles, L. 1977. Soil detachment and aggregate disintegration by wind-driven rain. SCSA Special Publ. no. 21: 152-159.

Lyles, L., J.D. Dickerson & N.F. Schmeidler 1974. Soil detachment from clods by rainfall: effects of wind, mulch cover, and initial soil moisture. Transactions of the ASAE, 17: 697-700.

Rosenberg, N.J., B.L. Blad & S.B. Verma 1983. Microclimate: the biological environment. John Wiley & Sons, New York.

Sharon, D. 1980. The distribution of hydrologically effective rainfall incident on sloping ground. J. Hydrol., 46: 165-188.

Shen, H.W. & R.M. Li 1973. Rainfall effect on sheet flow over smooth surfaces. Journal of the Hydraulics Division, ASCE, 99: 771-791.

Struzer, L.R. 1972. Problem of determining precipitation falling on mountain slopes. Sov. Hydrol. Selected Papers, 2: 129-142.

Umback, C.R. & W.D. Lembke 1966. Effect of wind on falling water drops. Transactions of the ASAE, 9: 805-808

Wu, J. 1975. Wind effects on stream flows. J. of Hydraulic Research 13: 405-423.

7.3 THE EFFECT OF OBLIQUE RAIN ON INCLINED SURFACES: A NOMOGRAPH FOR THE RAIN-GAUGE CORRECTION FACTOR

Accepted for publication in Journal of Hydrology, Elsevier Science Publishers B.V., Amsterdam.

7.3 THE EFFECT OF OBLIQUE RAIN ON INCLINED SURFACES: A NOMOGRAPH FOR THE RAIN-GAUGE CORRECTION FACTOR

J.L.M.P. de LIMA

Department of Hydrology, Soil Physics and Hydraulics, Agricultural University Wageningen, Nieuwe Kanaal 11, 6709 PA Wageningen, The Netherlands

ABSTRACT

Inclined rainfall leads to errors in the assessment of effective precipitation in areas with rugged relief. This affects many hydrologic studies like hydrologic forecasts, water erosion, determination of conditions for flash flood formation, determination of cropping conditions, etc..

In this paper a nomograph is presented for the rain-gauge correction factor (C_{gau}). C_{gau} is a factor by which rainfall measured in a standard horizontal rain-gauge (P_{gau}) has to be corrected to obtain the rainfall flux actually received on the inclined surface under study ($P_{act}= C_{gau} P_{gau}$). The correction factor is assumed to be a function of wind (with constant wind velocity), type of rainfall, and inclination and orientation of the sloping surface with respect to the oblique rain.

7.3.1 INTRODUCTION

When computing the rate of soil erosion by rainfall, or when determining the amount of water available to crops, for example, it is important to assess by how much the amounts of precipitation received on sloping ground differ from the amounts measured by a standard horizontal rain-gauge, and by how much they differ from one valley slope to another.

The actual rainfall (P_{act}), i.e. the rainfall flux intercepted on sloping ground, depends on the angle of incidence of the rain, the inclination of the surface, and the relative orientation of the sloping surface to the rain vector (Struzer, 1972; Sharon, 1980; Wakimizu et al., 1988). Thus, for a given inclination of rainfall, the proportion of rain actually intercepted by a sloping surface will differ from the rainfall collected in a horizontal rain-gauge (P_{gau}). The rain-gauge correction factor (C_{gau}) is a multiplier by which rainfall measured in a standard horizontal rain-gauge (P_{gau}) has to be corrected to obtain

the rainfall flux actually received on the inclined surface under study ($P_{act} = C_{gau} P_{gau}$).

Knowledge of the predominant direction and inclination of rainfall would be of assistance in planning the use of hillslopes as water catchment areas. The predominant direction of wind-driven rain is often different from that of the general prevailing winds.

As an illustration let us consider the four cases of Fig. 1. In case (a) the rainfall is vertical, the surface is horizontal and, consequently, $C_{gau}=1$. If the trajectories of the raindrops are rectilinear and parallel in the entire space above the three surfaces of cases (b), (c) and (d), standard horizontal rain-gauges installed on those surfaces will show the same precipitation. In case (b) the rain-gauge and the horizontal surface will receive the same amount of rainfall, thus C_{gau} is also 1. However, the rainfall flux intercepted on slope (d) ($C_{gau}>1$) is higher than on slope (b) ($C_{gau}=1$) and (c) ($C_{gau}<1$).

Mounting a rain-gauge at ground level parallel to the slope would give a direct sample of the rain received per unit area of slope. In this case application of the nomograph suggested herein is no longer necessary.

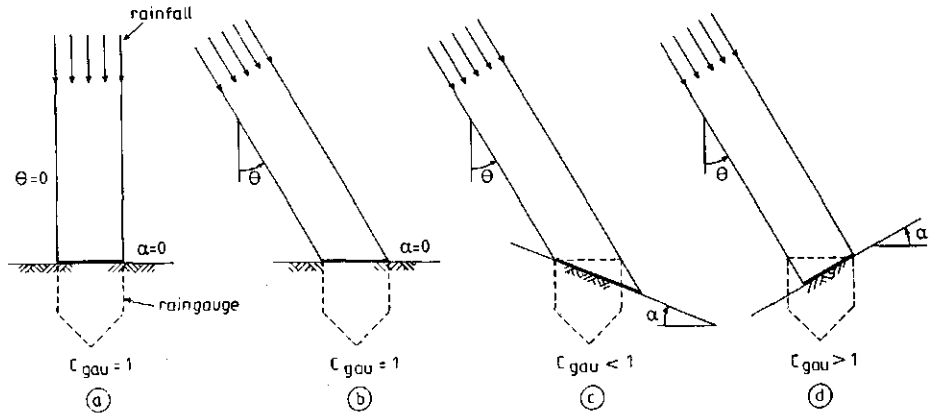

Fig. 1 The rain-gauge correction factor (C_{gau}) for different relative positions of the rainfall and receiving ground surface (in two dimensions).

7.3.2 THE NOMOGRAPH

To facilitate the determination of the rain-gauge correction factor a nomograph is presented (Fig. 2) where C_{gau} is assumed to be a function of wind, type of rainfall, and inclination and orientation of the receiving surface with respect to the oblique rain. The nomograph is based on trigonometrical equations and on a logarithmic wind-profile (see Appendix).

In the upper-left quadrant of the nomograph we read the angle of incidence of the rainfall (θ, on the vertical axis, in both degrees and radians) from the wind speed (V_w, on the horizontal axis, positive to the left) and type of rainfall. The types of rainfall used in the nomograph are: drizzle, normal, and shower with terminal vertical raindrop speeds (V_T) in the range of 1-2, 2-6, and 6-10 m/s, respectively. The wind speed (V_w) used in the calculation of the nomograph is the wind measured at 10 m height (standard measuring height at meteorological stations). In the calculation of the wind profile, the value of the roughness length (z_o) used was 0.0002 m (fetch of water as in sheet flow, Holtslag, 1987). Although other values of z_o may alter the wind profile near the surface, the angle of incidence is not significantly affected, since raindrops falling through a logarithmic wind profile arrive at the surface retaining most of their horizontal speed (Caldwell & Elliott, 1972). Therefore, a height of 10 m for measuring wind speed is considered representative for determining θ.

In the upper-right quadrant the orientation of the receiving ground surface with respect to the rain vector is taken into account through the difference between the azimuth of the rain vector (ω) and the azimuth of the slope (Ω) (uphill direction), both angles measured clockwise. Again we have the angle of incidence of the rainfall (θ) in the vertical axis. For values of the angle (ω-Ω) larger than π, the value 2π -(ω-Ω) should be used. Notice that the pairs of (ω-Ω) values are symmetric with respect to $\pi/2$.

In the lower-right quadrant of the nomograph we find the slope gradient (S, in %) of the receiving ground surface, or the angle with the horizontal (α, in radians) for surfaces steeper than S=30% . The rain-gauge correction factor (C_{gau}) is read on the vertical axis (positive downwards). In this quadrant attention should be paid to the value of the angle (ω-Ω). For values of (ω-Ω) greater than $\pi/2$ (i.e., for wind blowing downslope) the dashed lines should be used, and for values of (ω-Ω) smaller than $\pi/2$ (i.e., for wind blowing upslope) the continuous and dotted lines.

In case of vertical rain (V_w=0 and θ=0), C_{gau} can be read directly on the vertical axis (C_{gau} axis, positive downwards) at the intersection of the dashed lines (ω-Ω > $\pi/2$) with the continuous lines (ω-Ω < $\pi/2$), for the respective value of α or S.

Results obtained using the nomograph are correct insofar as the resultant azimuth and inclination of drops (function of the wind speed) can be specified within narrow limits. This implies that a constant wind speed is assumed, which may be unrealistic in a convec-

tive storm when drop size and wind velocities vary all the time. Other aspects that may cause error in the utilization of the nomograph are the effects of topography on local variations in rainfall (Sharon, 1980), and the fact that no allowance is made for local turbulence created by the rain-gauge, or for its exposure.

7.3.3 EXAMPLES OF APPLICATION

Consider a measured wind speed of V_w=10 m/s (measured at 10 m height) during a rainfall event of normal characteristics, i.e. with an assumed average terminal raindrop speed of V_T=4 m/s. The azimuth of the slope (uphill direction) and of the rain are, respectively, Ω=0 rad and $\omega=\pi/8$ rad. The slope gradient is S=20% . Questions: (1) What is the average angle of incidence of the rain?; (2) What is the precipitation received in relation to horizontal rain-gauge?; (3) Same as (2) but wind blowing in the opposite direction, i.e. in the downslope direction?. Following the arrows in Fig. 2, the answers are: $\theta \simeq 3\pi/8$ rad, and $C_{gau} \simeq 1.4$ and $C_{gau} \simeq 0.6$ entering $\omega-\Omega=\pi/8$ and $\omega-\Omega = 7\pi/8$, respectively.

In case of no wind (V_w), rain will be vertical (θ=0), and C_{gau} independent of the type of rain and of the orientation of the receiving ground surface. C_{gau} can be read directly on the vertical axis (C_{gau} axis, positive downwards) only as a function of the inclination of the receiving surface. For example, if V_w=0 and $\alpha=\pi/4$ (S=100%) we find $C_{gau} \simeq 0.7$.

7.3.4 CONCLUSION

Inclined rainfall leads to errors in the assessment of the actual precipitation in areas with rugged relief. This affects many hydrologic studies like hydrologic forecasts, water erosion, determination of conditions for flash flood formation, determination of cropping conditions, etc.. The nomograph presented enables a quick quantitative estimation of the correction factor (C_{gau}) of horizontal rain-gauges, for both vertical and inclined rainfall falling on sloping surfaces. However, care should be taken in the use of the nomograph and in the interpretation of the results. In the construction of the nomograph drop size and wind velocities were assumed constant in time, and no allowance is made for the local turbulence created by the rain-gauge, or for its exposure. Also the effects of topography on local variations in rainfall may cause an error in the utilization of the nomograph.

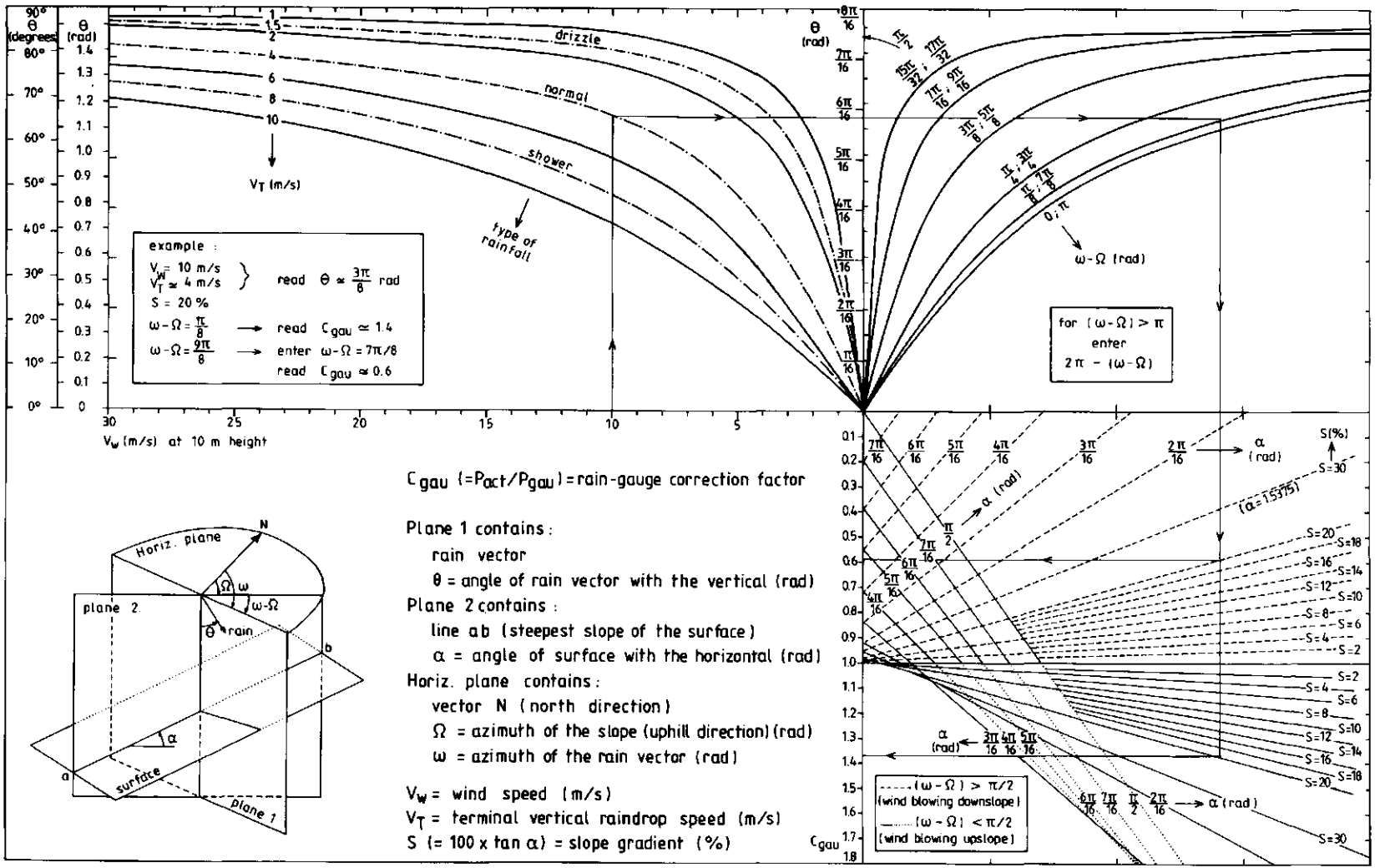

C_{gau} (=P_{act}/P_{gau}) = rain-gauge correction factor

Plane 1 contains :
- rain vector
- θ = angle of rain vector with the vertical (rad)

Plane 2 contains :
- line ab (steepest slope of the surface)
- α = angle of surface with the horizontal (rad)

Horiz. plane contains :
- vector N (north direction)
- Ω = azimuth of the slope (uphill direction) (rad)
- ω = azimuth of the rain vector (rad)

V_w = wind speed (m/s)
V_T = terminal vertical raindrop speed (m/s)
S (= 100 x tan α) = slope gradient (%)

Fig. 2 Nomograph for the rain-gauge correction factor (C_{gau}) as a function of wind, type of rainfall, and surface inclination and orientation with respect to the oblique rain (See text for examples of application).

APPENDIX - Equations used to construct the nomograph

The rain can be represented by a vector making an angle θ [0 (vertical downwards) $\leq \theta$ (rad) $\leq \pi/2$ (horizontal)] with the vertical and having an azimuth ω [$0 \leq \omega$ (rad) $\leq 2\pi$, with ω measured in clockwise direction]. The angle θ can be estimated by:

$$\theta = \arctan (\bar{V}/V_T) \qquad (1)$$

where $\bar{V}$ (m/s) is the average horizontal wind speed near the soil surface (during rain storm) and V_T (m/s) is the terminal vertical speed of raindrops.

The rain measured with a horizontal rain-gauge is adjusted to the rain actually received on inclined ground surface, using the correction factor (Lima, 1989):

$$C_{gau} = \cos\alpha + \tan\theta \sin\alpha \cos(\omega - \Omega) \qquad (2)$$

where α [0 (horizontal) $\leq \alpha$ (rad) $\leq \pi/2$ (vertical)] is the angle of the surface with the horizontal, Ω [$0 \leq \Omega$ (rad) $\leq 2\pi$] is the azimuth of the slope (uphill direction, measured in the clockwise direction), and C_{gau} is the rain-gauge correction factor.

Under neutral conditions, when temperature is constant with height, the mean wind speed increases linearly with the logarithm of the height (Rosenberg et al., 1983). The average wind velocity, $\bar{V}$, used in the calculation of θ, is obtained by averaging the wind profile from z_o (roughness length) to the height z (measuring height of the wind speed at the meteorological station, V_w):

$$\bar{V} = z \left[\ln(z/z_o) - 1 \right]/[(z - z_o)\, k] \, (\tau/\rho_{air})^{1/2} \qquad (3)$$

with

$$\tau = \rho_{air} \left[V_w\, k/ \ln(z/z_o) \right]^2 \qquad (4)$$

leading to

$$\bar{V} = z \quad V_w \, [1 - 1/\ln(z/z_o)] \, / \, (z - z_o) \qquad (5)$$

where k is the Von Karman constant (approximately 0.4), τ is the frictional shear stress (Pa), and ρ_{air} is the density of the air (1.209 Kg m^{-3} at 100 kPa).

ACKNOWLEDGEMENT

The author wishes to thank Prof. W.H. van der Molen, Ir. H.F. Ledeboer and Eng. M.I.M.L.P. de Lima for their helpful suggestions. The author is indebted to "Comissão Permanente INVOTAN" for financial support and is also very grateful to the University of Coimbra (Portugal) for the permission and partial support of his stay at the Agricultural University Wageningen.

REFERENCES

Caldwell, D.R. & W.P. Elliott, 1972. The effect of rainfall on the wind in the surface layer. Boundary-Layer Meteorology, 3: 146-151.

Holtslag, A.A.M., 1987. Surfaces fluxes and boundary layer scaling: Models and applications. Ph.D. Thesis. Agricultural University Wageningen, Wageningen, The Netherlands.

Lima, J.L.M.P. de, 1989. The influence of the angle of incidence of the rainfall on the overland flow process. In: New Directions for Water Modeling (Proc. IAHS Third Scientific Assembly, Baltimore, 10-19 May 1989), IAHS Publ. no. 181, 73-82.

Rosenberg, N.J., B.L. Blad & S.B. Verma, 1983. Microclimate: the biological environment. John Wiley & Sons, New York.

Sharon, D., 1980. The distribution of hydrologically effective rainfall incident on sloping ground. J. Hydrol., 46: 165-188.

Struzer, L.R., 1972. Problem of determining precipitation falling on mountain slopes. Sov. Hydrol. Selected Papers, 2: 129-142.

Wakimizu, K., S. Hayashi & Y. Motoda, 1988. Estimating the precipitation on a mountain slope with a vector rain-gauge. Transactions of the Japanese Society of Irrigation, Drainage and Reclamation Engineering, 137: 65-70.

7.4 RAINFALL SPLASH ANISOTROPY: SLOPE, WIND AND OVERLAND FLOW VELOCITY EFFECTS

Published in: Journal of Soil Technology, Catena Verlag, Cremlingen-Destedt, West Germany, 2(1989), 71-78.

SOIL TECHNOLOGY vol. 2, p. 71–78 Cremlingen 1989

RAINDROP SPLASH ANISOTROPY: SLOPE, WIND AND OVERLAND FLOW VELOCITY EFFECTS

J.L.M.P. **De Lima**, Wageningen

Summary

This study emphasises the importance of raindrop splash anisotropy as a factor affecting splash erosion. Slope, wind and overland flow velocity were found to be the factors contributing to the anisotropy of the splash. With the help of photography the asymmetry of the corona shape of the raindrop splash was recorded for the different factors. Only one equivalent drop diameter (3.5 mm) was studied.

Résumé

Cette étude met an évidence l'importance de l'anisotropie de l'éclaboussement des gouttes de pluie comme facteur responsable de l'érosion d'éclaboussure. Il a été démontré que les facteurs qui déterminent cette anisotropie sont la pente de la surface, le vent et la vitesse de l'écoulement superficiel. L'asymétrie de la forme coronaire de l'éclaboussure des gouttes à été enregistrée à l'aide de photographies pour les trois facteurs indiqués. Seulement les gouttes de diamètre equivalent à 3.5 mm ont été considérées.

ISSN 0933–3630

D–3302 Cremlingen-Destedt, W. Germany
0933–3630/89/5011851/US$ 2.00 + 0.25

1 Introduction

Detachment of soil particles by raindrop impact is the first and fundamental phase of sediment production (MORGAN 1981).

The surface water depth is the major variable affecting splash shape. At zero depth droplets leaving the impact point have strong horizontal components (photo 1). If the surface is covered with water, the familiar splash corona is created (photo 2). Radial and circumferential irregularities then develop on the corona, initiating the break away of splash droplets from the corona edge (confirmation of the works of MUTCHLER 1967, MUTCHLER & LARSON 1971, MUTCHLER & YOUNG 1975, GHADIRI & PAYNE 1980, SAVAT & POESEN 1981, POESEN & SAVAT 1981, MOSS & GREEN 1983, FERREIRA 1984, TORRI et al. 1987, etc.).

However, splash anisotropy should be identified as an important factor in the determination of the direction and extent of soil erosion. Asymmetry of individual splashes can be caused by a combination of the following factors:

(i) slope,

(ii) wind, and

(iii) overland flow velocity.

Photo 1: *Impact of a 3.5 mm diameter drop on a rough dry surface (sand roughness). Scale is in mm.*

Photo 2: *Impact of a 3.5 mm diameter drop on a stagnant water layer with a depth of approximately 3 mm. Scale is in mm.*

Using a photographic set-up the asymmetry of the corona shape was assessed for the different factors in a qualitative way. Only one equivalent drop diameter (3.5 mm) was studied (see photo 1).

2 Experimental set-up

In splash studies, photographic equipment is generally necessary (ELLISON 1947a, b, MUTCHLER 1967, MUTCHLER & YOUNG 1975, MOSS & GREEN 1983, GHADIRI & PAYNE 1980, EPEMA & RIEZEBOS 1984, etc.). The laboratory set-up consisted of a dark

room in which a falling drop interrupts an infra-red beam connected to a time delay device which triggers a flash light. The time delay device can be adjusted in order to trigger the flash at the instant when the drop or splash are in the required position.

Two major set-ups were used: set-up (a) for oblique and vertical drops falling into a stagnant water layer with a depth of approximately 3 mm (fig.1); and set-up (b) for drops falling vertically into a sloping surface (of Perspex) covered with a flowing water layer with a depth of approximately 3 mm (fig.2). The drop former (tubing-tip drop former) was installed at 3.5 m height and generated drops with 3.5 mm equivalent diameter. Tap water was used for both drop former and overland flow. The latter issued from a constant head tank. The slope of the overland flow Perspex surface was adjustable. The drop formation time interval was long enough to let the generated waves in the shallow water dissipate. Water temperature was around 20°C.

The angle of incidence of the drops was estimated by measuring the distance D, i.e. the horizontal distance from initial vertical fall position to point of impact (fig.1).

The shape of simulated raindrops and the relation between size and drop velocity have been discussed elsewhere (EPEMA & RIEZEBOS 1983, 1984).

3 Results and Discussion

Slope, wind (affecting both drop and splash droplet trajectories) and overland flow velocity were found to be the factors contributing to the anisotropy of the splash:

3.1 The effect of slope

REEVE (1982) explained the asymmetry of splash on sloping surfaces as well as the reason why more splash droplets are ejected downhill, by generalizing the droplet ejection velocity vectors to all azimuthal angles on a slope.

Photo 3 shows the splash asymmetry of a vertical drop falling on a sloping, flowing water layer.

3.2 The effect of the wind: oblique drop trajectories

Several physically based models for the dispersion of splash droplets ejected from a water drop impact have been constructed (ZASLAVSKY & SINAI 1981, REEVE 1982, etc.). In these models splash droplets disperse in stagnant air after impact of vertically falling raindrops. In nature, however, rain more often falls inclined under the effect of the wind and it is desirable to have a model to allow for such conditions.

The dependence of net soil transport under oblique rain has been experimentally observed by MOEYERSONS (1983) and by POESEN (1986) in the field. In the model described by WRIGHT (1987) the effect of the oblique rain is to alter the values of the parallel and normal components of the incident drop velocity, and consequently to alter the direction and magnitude of the anisotropy of the splash. This means that, neglecting the effect of wind on the corona and droplets, the splash obtained from (a) a raindrop falling at an angle Θ with the vertical (fig.1) on a stagnant water layer is assumed to have exactly the same splash shape as (b) a drop falling vertically on a sloping surface making the same angle $\alpha = \Theta$ with the horizontal (fig.2) and with a water layer of the

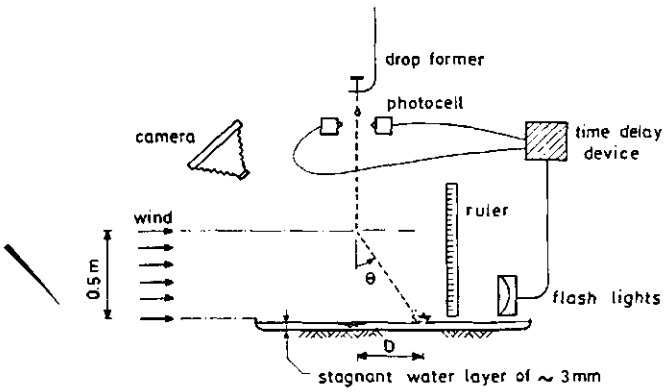

Fig. 1: *Laboratory set-up (a): oblique and vertical drops falling into a stagnant water layer with a depth of approximately 3 mm.*

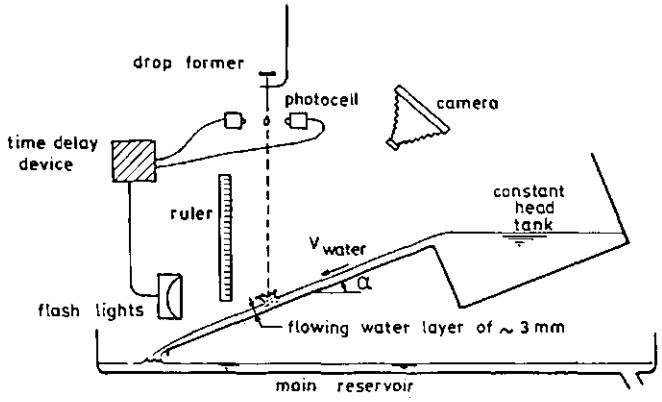

Fig. 2: *Laboratory set-up (b): vertical drop falling into a sloping surface (of Perspex) covered with a flowing water layer with a depth of approximately 3 mm.*

same thickness. To prove this assumption in the laboratory is rather difficult. With zero depth surface water it is possible to compare the two cases, but due to the strong horizontal component of the ejected droplets it is not easy to visualize the difference, if any. Trying to use a surface layer creates a lot of technical problems:

a) how to create a stagnant water layer on a sloping surface,

b) how to deviate falling drops at near terminal velocity without disturbing too much the water layer and the drop itself.

In order to have some insight into the problem two cases were compared:

i) Oblique drops falling on a stagnant water layer of approximately 3 mm depth (set-up (a)). In photo 4 the value of Θ was 17 degrees.

ii) Vertical drops falling on a sloping surface covered with a flowing water layer of approximately 3 mm thickness (set-up (b)). In photo 3 the value of α was 22 degrees and the flow velocity was 1 m/s (rather high in comparison with overland flow velocities in the field).

When comparing photo 3 and 4, the observed distortions of the corona are similar, though not equal. This is not surprising because in case (a) we have drop shape deformation and an added horizontal component of the drop velocity due to wind, and in case (b) we have a flowing water layer. Also, the angles Θ and α were different in the two cases.

3.3 The effect of wind: splash droplet trajectories

Besides inclining drop trajectories, wind also alters the trajectory of the ejected droplets. Previous attempts to calculate the ranges and trajectories of droplets have neglected the effect of air resistance (ZASLAVSKY & SINAI 1981, REEVE 1982).

GHADIRI & PAYNE (1978) showed that the smallest splash droplets travel the least distance from a drop impact and that droplet range generally increases with droplet size. GHADIRI & PAYNE (1978), however, also measured ejection velocities and found that the smallest droplets were ejected with the greatest velocities and that the ejection velocities decreased with increasing droplet diameter. If air resistance is neglected the fast small droplets would travel the greatest distance. When compared to the experiments mentioned above, it is clear that this is in error.

WRIGHT (1987), in his model, took into consideration the drag force due to the effect of the air. He also made a comment that the effect of the wind could be taken into account simply by altering the direction and magnitude of the drag force.

In the present experiments wind had an important role in deviating splash droplet trajectories towards the direction of the wind.

3.4 The effect of overland flow velocity

The velocity of a thin water layer moving over a sloping surface, as in overland flow, seems to have a remarkable influence on the splash shape and symmetry. TUONG & PAINTER (1974) considered the case of a drop falling vertically in a shallow (46 mm deep), moving

Photo 3: *Splash shape of a vertical drop (3.5 mm diameter) falling into a sloping (α=22°), flowing water layer (flow velocity of 1 m/s) with a depth of approximately 3 mm. Scale is in mm.*

Photo 4: *Splash shape of oblique drops (Θ=17°) falling into a stangant water layer with a depth of approximately 3 mm. Scale is in mm.*

(flow velocities tested: 0.18 and 0.35 m/s), nearly horizontal, channel flow. They noticed that there is deformation, although the upward splash and the cavity were formed in the same way as when the receiving water is stationary.

The velocity of the water affects splash in the following ways (see photo 3 and 5):

i) additional distortion of the corona,

ii) displacement of the entire corona in time and along the direction of the flow,

iii) added displacement of droplets in the downhill direction due to i) and ii).

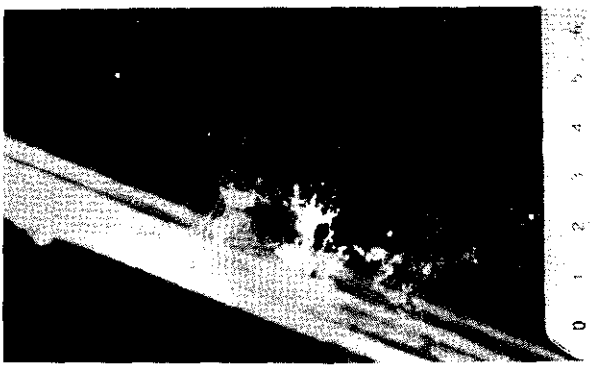

Photo 5: *Splash shapes of a vertical drop (3.5 mm diameter) falling into a sloping (α=22°), flowing water layer (flow velocity of 1 m/s) with a depth of approximately 3 mm: two different stages of the corona break away. Scale is in mm.*

In photo 5 (splash corona break away at two different stages) the combined effect of slope (distortion) and overland flow velocity (additional distortion and displacement) can be visualized.

4 Conclusion

This study emphasises the importance of raindrop splash anisotropy as a factor affecting splash erosion.

Most authors agree on the importance of slope effect on splash asymmetry. The experimental results, however, show that a model for splash cannot completely ignore wind and overland flow velocity effects.

A more general study should be undertaken with improved photographic equipment (for example using high speed cine-photography), in order to analyse and quantify slope, wind and overland flow velocity effects on splash anisotropy. An understanding of this mechanism should facilitate the development of methods for assessment of splash erosion.

Acknowledgements

The author is indebted to Mr. H.V. Veen for his effort in the development of the photographic experimental set-up, and to Prof. W.H. van der Molen and Dr. R.W.R. Koopmans for their helpful suggestions. The author wishes also to thank "Comissão Permanente INVOTAN" for financial support. The author is very grateful to the University of Coimbra (Portugal) for the permission and partial support of his stay at the Agricultural University Wageningen.

References

ELLISON, W.D. (1947a): Soil erosion studies — part II: Detachment hazard by raindrop splash. Agricultural Engineering **28**, 197–201.

ELLISON, W.D. (1947b): Soil erosion studies — part V: Soil transportation in the splash process. Agricultural Engineering **28**, 349–352.

EPEMA, G.F. & RIEZEBOS, H. Th. (1983): Fall velocity of waterdrops at different heights as

a factor influencing erosivity of simulated rain. In: Rainfall simulation runoff and soil erosion. J. de Ploey (ed.), CATENA SUPPLEMENT **4**, 1–17.

EPEMA, G.F. & RIEZEBOS, H. Th. (1984): Drop shape and erosivity Part I: experimental set up, theory, and measurements of drop shape. Earth Surface Processes and Landforms **9**, 567–572.

FERREIRA, A.A.C.G. (1984): Influence of a shallow water layer over the soil in the erosion by raindrop impact. Ph.D. Thesis, Univ. California, Davis.

GHADIRI, H. & PAYNE, D. (1980): A study of soil splash using cine-photography. In: Assessment of erosion. M. de Boodt & D. Gabriels (eds.), John Wiley & Sons, Chichester, 185–192.

MOEYERSONS, J. (1983): Measurements of splash-saltation fluxes under oblique rain. In: Rainfall simulation runoff and soil erosion. J. de Ploey (ed.), CATENA SUPPLEMENT **4**, 19–31.

MORGAN, R.P.C. (1981): Field measurement of splash erosion.In: Erosion and sediment transport measurement. (Proc. of the Florence Symposium), *IAHS, Publ.* **133**, 373–382.

MOSS, A.J. & GREEN, P. (1983): Movement of solids in air and water by raindrop impact: effects of drop-size and water-depth variations. Aust. J. Soil Res. **21(3)**, 257–269.

MUTCHLER, C.K. (1967): Parameters for describing raindrop splash. J. of Soil and Water Conservation **22(3)**, 91–94.

MUTCHLER, C.K. & LARSON, C.L. (1971): Splash amounts from waterdrop impact on a smooth surface. Water Resources Research **7**, 195–200.

MUTCHLER, C.K. & YOUNG, R.A. (1975): Soil detachment by raindrops. In: Present & prospective technology for predicting sediment yields and sources, ARS 1-S-40, USDA, 113-117.

POESEN, J. (1986): Field measurements of splash erosion to validate a splash transport model. Z. Geomorph., Suppl.-Bd. **58**, 81–91.

POESEN, J. & SAVAT, J. (1981): Detachment and transportation of loose sediments by raindrop splash, Part II. CATENA **8**, 19–41.

REEVE, I.J. (1982): A splash transport model and its application to geomorphic measurement. Z. Geomorph. **26**, 55–71.

SAVAT, J. & POESEN, J. (1981): Detachment and transportation of loose sediments by raindrop splash, Part I. CATENA **8**, 1–17.

TORRI, D., SFALANGA, M. & DEL SETTE, M. (1987): Splash detachment: Runoff depth and soil cohesion. CATENA **14**, 149–155.

TUONG, T.P. & PAINTER, D.J. (1974): the interaction between a raindrop and a shallow body of water. Proc. Fifth Austalasian Conference on Hydraulics and Fluid Mechanics, Univ. of Canterbury, Christchurch, New Zealand, 96–102.

WRIGHT, A.C. (1987): A physically-based model of the dispersion of splash droplets ejected from a water drop impact. Earth Surface Processes and Landforms **11**, 351–367.

ZASLAVSKY, D. & SINAI, G. (1981): Surface hydrology: II. Distribution of raindrops. A.S.C.E. proceedings, Journal of the Hydraulics Division **107**, 17–36.

Address of author:
J.L.M.P. de Lima
Department of Land & Water Use, and
Department of Hydraulics & Catchment Hydrology
Agricultural University Wageningen
Nieuwe Kanaal 11
6709 PA Wageningen
The Netherlands

SUMMARY AND CONCLUSIONS

In this thesis several aspects related to the overland flow process under rainfall are discussed:

Chapter 1 presents general concepts perceived to be background information. Overland flow is defined and related to other disciplines such as (agro)hydrology, water erosion, water quality, surface irrigation and drainage, and waste water treatment.

The objective of Chapter 2 is to give a short introduction of the possibilities for the mathematical modelling of the overland flow process. Special attention is given to the kinematic wave theory since it was the basis for the models developed in this thesis.

The overland flow process is strongly affected by the shape of the slopes. Therefore for a realistic simulation of overland flow it is necessary to attempt simulation on surfaces that are not restricted to a plane of fixed slope. Using the kinematic wave theory and Zarmi's hypothesis, an analytical solution for overland flow over an infiltrating surfaces, with longitudinal section of parabolic shape (concave or convex surfaces, that may be represented by a quadratic equation), is presented in Section 2.4. The velocity of the water flow is assumed to be independent of time. The analytical solution developed is easier to utilize than numerical simulation and can be used to calibrate numerical methods devised for more complicated cases. An illustration is presented.

The laboratory experiment described in Chapter 3 was done to evaluate the influence of upstream boundary conditions on overland flow under rainfall. The experiment was done on an impermeable plane surface with rainfall simulator. For overland flow under vertical rainfall, on gentle slopes, the results show the importance of considering upstream boundary conditions other than the most frequently used $h(0,t)=0$ for $t \geq 0$, where $h(x,t)$ is the flow depth as a function of position x and time t.

With oblique rainfall under wind blowing upslope there is also a non-zero water depth at $x=0$, depending strongly on slope, rainfall intensity and wind speed (Sections 7.1 and 7.2). In this case the condition $h(0,t)=0$ for $t \geq 0$ is no longer applicable.

Surface tension, particularly for shallow flows shortly after the start of the rainfall, requires more experimental attention. The hysteresis effect observed is caused by these surface tension forces. Additional research could focus on the effects of roughness and surface wettability characteristics.

A method of predicting a spatial average for the amount of depression storage on tilled surfaces is proposed in Chapter 4. The method is based on the kinematic flow approximation to overland flow on a plane proposed by Rose et al. (1983). In the laboratory work only the aspects of tillage, rainfall intensity and slope were investigated. The following impermeable models, simulating various tillage techniques, were used: plastic corrugations, concrete ridges, concrete mounds and a concrete plane surface as reference.

The method was verified by comparing predicted depression storage with depression storage obtained from water-balance considerations based on the experimental data. It is believed that the model can be used for the estimation of a spatial average for depression storage on tilled surfaces if infiltration is predicted. Field data are required to evaluate the suitability of this formulation for practical purposes.

The model KININF, described in Chapter 5, combines a simplified physically based overland flow model, the kinematic-wave equations, with an infiltration model derived from soil moisture flow theory. This mathematical model can be used to describe overland flow in small plots or microcatchments. It provides a simple way of visualizing overland flow on different infiltrating surfaces. Further refinement of the proposed model is possible and desirable. This may include the coupling of the model with a sediment transport model.

Although the effect of the morphological factors on the overland flow process may be strongly reduced by soil properties, soil roughness, vegetation cover and effective rainfall patterns, it is believed that it cannot be neglected. Chapter 6 contains a discussion of the effects of morphological characteristics of slopes on the overland flow process. The analysis of the different effects is presented through case studies.

The major morphological factors affecting overland flow are: slope gradient, slope length, shape of the slope and slope exposure to prevailing rain-bringing winds. Slope gradient and length are presumed to be factors that most strongly affect overland flow processes. The shape of the slope influences the time to peak and the shape of the rising limb of the overland flow hydrographs. The slope exposure is also of great importance in case of slopes exposed to strong winds from some prevalent direction.

Wind effects are seldom considered in overland flow and rainfall erosion studies. In Sections 7.1 and 7.2, the effects of inclined rainfall and the wind induced shear-stress on overland flow have been investigated in an experimental study. These processes have been

simulated in a wind tunnel having variable slope. Wind blowing upslope was found to delay the occurrence of overland flow and to increase the depth of water over an impermeable plane. In some experiments, even upstream discharge has been observed.

Wind intensity and direction influence both the effective rainfall pattern and the mechanics of the overland flow process on slopes. They affect overland flow in the following ways: shape, size, angle of incidence and velocity of impact of raindrops, splash shape, and tangential shear stress at the water-air boundary. For high intensity rainfalls the effect of the wind shear stress and splash shape were small in comparison to the effect of the inclined impinging raindrops. However, the effect of wind shear stress may be significant when a thin water sheet covers the entire surface and for low kinetic energy of the rain (low intensity rainfalls or, as in these experiments, small drop fall height).

The physically based mathematical model WROF (Wind, Rain and Overland Flow) introduced and verified in Sections 7.1 and 7.2 is a simplified model, but it may prove to be accurate enough for practical purposes in the assessment of the factors affecting overland flow under inclined rainfall.

More research is needed on the effects of wind-rain forces on overland flow, and on the velocity and frequency of winds associated with rains in areas susceptible to water erosion. Further improvement could be the coupling of this model with a sediment transport model.

Inclined rainfall leads to errors in the assessment of effective precipitation in areas with rugged relief. It affects many hydrologic studies like hydrologic forecasts, water erosion, determination of conditions for flash flood formation, determination of cropping conditions, etc.. In Section 7.3 a nomograph is presented for the rain-gauge correction factor (C_{gau}). C_{gau} is a factor by which rainfall measured in a standard horizontal rain-gauge (P_{gau}) has to be corrected to obtain the rainfall flux actually received on the inclined surface under study ($P_{act} = C_{gau} P_{gau}$). The correction factor is assumed to be a function of wind, type of rainfall, and inclination and orientation of the sloping surface with respect to the oblique rain. The effect of topography on local variations in rainfall may cause an error in the utilization of the nomograph.

Section 7.4 emphasises the importance of raindrop splash anisotropy as a factor affecting splash erosion. Slope, wind and overland flow velocity were found to be the factors contributing to the anisotropy of the splash. With the help of time-lapse photography the asymmetry of the corona shape of the raindrop splash was recorded. Only one equivalent drop diameter (3.5 mm) was studied.

Most authors agree on the importance of slope effect on splash asymmetry. The experimental results, however, show that a model for splash cannot completely ignore wind and overland flow velocity effects. A more general study should be undertaken with improved

photographic equipment (for example using high speed cine-photography), in order to analyse and quantify slope, wind and overland flow velocity effects on splash anisotropy.

The author hopes that this thesis will be useful as a stepping stone towards a more complete understanding of the overland flow process as it occurs in the field.

SUMÁRIO E CONCLUSÕES

Esta tese aborda vários aspectos relacionados com o escoamento superficial sob a acção da chuva.

O Capítulo 1 pretende servir de introdução aos capítulos subsequentes apresentando conceitos e definições e focando a importância do escoamento superficial em relação a áreas como agro-hidrologia, erosão hídrica, qualidade da água, rega e drenagem de superfície, e tratamento de águas residuais.

O Capítulo 2 aborda a modelação matemática do escoamento superficial. Atenção especial é dada ao método da onda cinemática, método usado nos modelos apresentados nesta tese. O escoamento superficial é fortemente influenciado pela forma das superfícies, pelo que a sua modelação matemática não se deve restringir a superfícies planas. No Subcapítulo 2.4 apresenta-se uma solução analítica para o escoamento superficial em superfícies infiltrantes de forma longitudinal parabólica (superfícies côncavas ou convexas cuja forma é dada por uma equação quadrática), obtida usando o método da onda cinemática e a hipótese de Zarmi; a velocidade do escoamento é suposta independente do tempo. Esta solução, de mais simples utilização que outras soluções numéricas, poderá servir para calibrar métodos numéricos formulados para resolver casos mais complexos. Um exemplo de aplicação é também apresentado.

No trabalho laboratorial descrito no Capítulo 3, executado com o objectivo de estudar a influência das condições de fronteira de montante no escoamento superficial sob a acção da chuva, utilizou-se uma superfície de escoamento plana e impermeável e um simulador de chuva. Para o escoamento superficial sob a acção da chuva em superfícies pouco inclinadas, os resultados obtidos provaram a importância de considerar outras condições de fronteira de montante para além da condição geralmente utilizada: $h(0,t)=0$ para $t\geq 0$, onde $h(x,t)$ é a altura de escoamento em função da posição x e do tempo t. Verificou-se, também, que esta condição não é válida para o caso de escoamento superficial sob a acção de chuva inclinada devido à acção do vento soprando de jusante, tendo sido observada a existência de uma altura de

lâmina líquida no ponto x=0. Este fenómeno depende fortemente da inclinação da superfície, intensidade da chuva e velocidade do vento (Subcapítulos 7.1 e 7.2). A importância de tensões superficiais no início do escoamento superficial, especialmente para pequenas alturas de lâmina líquida, requer mais investigação experimental como, por exemplo, o estudo do efeito da rugosidade e características da superfície.

O Capítulo 4 apresenta um método de cálculo para estimar o valor médio da retenção superficial em superfícies lavradas. O método é baseado no modelo cinemático para o escoamento superficial numa superfície plana proposto por Rose et al. (1983).

No trabalho laboratorial estudaram-se somente os aspectos relacionados com as características da retenção superficial em superfícies lavradas, a inclinação da superfície e a intensidade da precipitação. Os modelos impermeáveis utilizados, simulando diferentes armações do terreno, foram: plástico ondulado, montículos cónicos e camalhões de betão, e também uma superfície plana de betão como referência.

O método foi verificado comparando os valores simulados para a retenção superficial com os valores obtidos através de balanços hídricos. Pensa-se que o método poderá ser utilizado para calcular a retenção superficial em superfícies lavradas se a infiltração for estimada. No entanto, dados de experiências de campo são necessários para verificar esta hipótese.

O modelo KININF é descrito no Capítulo 5. Este modelo combina um modelo simplificado de escoamento superficial (o modelo cinemático) com um modelo de infiltração baseado nas equações do movimento vertical da água no solo inicialmente não saturado. Este modelo matemático pode ser utilizado para descrever o escoamento superficial em talhões e bacias hidrográficas de pequenas dimensões. O modelo permite uma análise do escoamento superficial em diferentes superfícies permeáveis. O modelo KININF poderá ser combinado com um modelo de transporte de sedimentos.

Os factores morfológicos a considerar no estudo do escoamento superficial são: inclinação, comprimento, forma e exposição da superfície a ventos predominantes trazendo precipitação. No Capítulo 6 estes factores são analisados através de exemplos de aplicação.

Apesar do seu impacto no escoamento superficial estar fortemente condicionado pelas propriedades do solo, rugosidade hidráulica da superfície, cobertura vegetal e precipitação efectiva, esses factores morfológicos não deverão ser ignorados. A inclinação e o comprimento das superfícies são os factores que mais fortemente condicionam as características do escoamento superficial. A forma das encostas é importante na determinação da forma do ramo ascendente do hidrógrafo de escoamento superficial e do tempo necessário para atingir o pico. A exposição das encostas é também de grande importância no caso de encostas expostas a ventos predominantes fortes.

O efeito do vento não é normalmente considerado em estudos de escoamento superficial e de erosão hídrica. Nos Subcapítulos 7.1 e 7.2 os efeitos da chuva inclinada e da tensão tangencial provocada pelo vento no escoamento superficial são analisados experimentalmente tendo-se usado um túnel aerodinâmico de inclinação variável. Vento soprando de jusante atrasa o início do escoamento superficial e aumenta a espessura da lâmina líquida na superfície impermeável em estudo. Escoamento para montante, na parte superior da superfície inclinada, foi também observado.

A intensidade e duração do vento afectam a precipitação efectiva ao nível do solo e a mecânica do escoamento superficial. O escoamento superficial é afectado da seguinte maneira: forma, dimensão, inclinação e velocidade de impacto das gotas de chuva, forma do rebentamento das gotas e tensão tangencial na superfície do escoamento superficial. Para precipitações de grande intensidade, os efeitos da tensão tangencial e da forma do rebentamento das gotas são pequenos em relação ao efeito do impacto das gotas inclinadas na superfície do escoamento superficial. Contudo, no caso de chuva com baixa energia cinética (chuvas de pequena intensidade ou, no caso de chuva simulada, pouca altura de queda das gotas), e quando a lâmina de escoamento superficial cobre toda a superfície, o efeito da tensão tangencial não deverá ser desprezado.

O modelo matemático WROF estudado nos Subcapítulos 7.1 and 7.2 é um modelo simplificado para a simulação do escoamento superficial sob a acção combinada do vento e da chuva. No entanto acredita-se que este modelo seja suficientemente preciso para utilização na prática, aplicado a problemas de escoamento superficial provocado por precipitação inclinada devido à acção do vento. Considera-se necessário investigar em mais detalhe o efeito combinado da chuva e do vento no escoamento superficial. O efeito da intensidade e frequência dos ventos associados a chuvas em zonas mais afectadas pela erosão hídrica também merece ser estudado em mais profundidade. Acredita-se com interesse a combinação do modelo WROF com um modelo de transporte de sedimentos.

Chuva inclinada pela acção do vento leva a erros na determinação da precipitação efectiva em superfícies inclinadas. Isto tem repercussões em vários estudos como, por exemplo, balanços hidrológicos, erosão hídrica, análise de caudais de cheia, etc. No Subcapítulo 7.3 apresenta-se um ábaco para o factor de correcção de udómetros (C_{gau}). C_{gau} é um factor multiplicativo da quantidade de precipitação registada num udómetro horizontal (P_{gau}) de modo a obter a intensidade real da precipitação numa superfície inclinada ($P_{act} = C_{gau}\ P_{gau}$). O factor de correcção é função da intensidade do vento, tipo de precipitação, e inclinação e orientação da superfície relativamente à chuva inclinada. Contudo, efeitos topográficos podem levar a variações locais da precipitação que poderão causar erros na utilização do ábaco.

O Subcapítulo 7.4 analisa a importância da anisotropia do rebentamento de gotas de chuva em relação à erosão hídrica por impacto. A inclinação da superfície, o vento e a velocidade do escoamento superficial são os factores que contribuem para essa anisotropia. A im-

portância destes factores na forma da coroa foi estudada com a ajuda de meios fotográficos. Só foram estudadas gotas de chuva com diâmetro equivalente de 3.5 mm. A grande maioria dos autores concorda com a importância do papel desempenhado pela inclinação da superfície na assimetria do rebentamento de gotas de chuva. Os resultados experimentais mostram, no entanto, que um modelo para o rebentamento de gotas de chuva não poderá ignorar os efeitos do vento e da velocidade do escoamento superficial. De modo a analisar e quantificar os efeitos acima referidos deverá efectuar-se um estudo experimental mais elaborado (usando, por exemplo, fotografia de alta velocidade).

O autor espera que esta tese contribua para um esclarecimento e melhoramento do conhecimento actual do escoamento superficial sob a acção da chuva.

SAMENVATTING EN CONCLUSIES

Dit proefschrift behandelt verschillende aspecten van de stroming van water over een landoppervlak, veroorzaakt door neerslag:

Hoofdstuk 1 geeft achtergrond-informatie. De afstroming van water over de oppervlakte wordt gedefinieerd en geplaatst in het kader van andere disciplines zoals (agro)hydrologie, erosie door water, waterkwaliteit, oppervlakte-bevloeiing en waterzuivering.

De doel van Hoofdstuk 2 is het geven van een korte inleiding over de mogelijkheden tot wiskundige modellering van het verschijnsel. Daarbij wordt in het bijzonder aandacht besteed aan de theorie van de kinematische afvoergolf, omdat deze de grondslag vormt van de in deze studie gebruikte modellen.

Het proces van stroming over een hellend landoppervlak wordt sterk beïnvloed door de vorm van de helling. Voor een juiste benadering van het verschijnsel is het daarom nodig de aandacht niet te beperken tot oppervlakken met een gelijkmatige helling. Gebruik makend van de theorie van de kinematische afvoergolf en de hypothese van Zarmi betreffende de aard van de stroming kon een analytische oplossing worden verkregen voor stroming over een oppervlak waarvan de vertikale doorsnede een parabolische vorm heeft (covex of concaaf).

De laboratoriumproef beschreven in Hoofdstuk 3 was gericht op het onderzoek naar de invloed van de bovenstroomse randvoorwaarde op de stroming. De experimenten werden uitgevoerd met een regensimulator boven een ondoorlatend hellend oppervlak.

Bij geringe hellingen tonen de uitkomsten van deze proeven aan, dat het nodig is ook andere randvoorwaarden te beschouwen dan de gebruikelijke voorwaarde $h(0,t)=0$ voor $t\geq 0$, waarin $h(x,t)$ de waterdiepte is op tijd t en afstand x van de top van de helling. Bij nietloodrecht vallende neerslag (onder invloed van wind) blijkt er aan de top van de helling een van nul afwijkende waterdiepte op te kunnen treden, afhankelijk van helling, windrichting, windsterkte en neerslagintensiteit (Sectie 7.1 en 7.2). Ook voor deze gevallen is de voorwaarde $h(0,t)=0$ voor $t\geq 0$ niet toepasbaar.

Het aandeel van de oppervlaktespanning, in het bijzonder voor de zeer kleine waterdiepten kort na het begin van de neerslag, verdient nog nadere aandacht. Het in de proeven waargenomen hysteresis-effect wordt door deze oppervlaktespanning veroorzaakt. Aanvullend onderzoek zou gericht moeten zijn op de invloeden van ruwheid en bevochtigbaarheid van het oppervlak op deze verschijnselen. Dit onderzoek valt echter buiten het kader van deze studie.

Een methode om een ruimtelijk gemiddelde te vinden voor de berging van water in ingesloten laagten op bewerkte landbouwgronden wordt voorgesteld in Hoofdstuk 4. Deze werkwijze berust op de kinematische afvoergolf over een hellend oppervlak zoals voorgesteld door Rose et al. (1983). In het laboratorium werden alleen de invloeden van bewerking, regenintensiteit en helling bestudeerd. De volgende oppervlakken -alle ondoorlatend - werden onderzocht: plastic ribbels, betonnen ruggen en heuvels. Een vlak beton-oppervlak diende ter vergelijking.

De methode van de kinematische afvoergolf werd geverifieerd door de voorspelde berging te vergelijken met de berging zoals afgeleid uit de gemeten waterbalans tijdens de proeven. Wij nemen aan dat het model kan worden gebruikt voor een schatting van de berging in afvoerloze depressies, tenminste als de infiltratie in de bodem kan worden geschat of gemeten. Voor het toetsen van deze methode onder praktijk-omstandigheden zullen nadere veldproeven nodig zijn.

Het model KININF, beschreven in Hoofdstuk 5, verenigt een vereenvoudigd stromingsmodel - de kinematische afvoergolf met een infiltratiemodel onleend aan de theorie van de stroming van bodemvocht. Dit model kan worden gebruikt voor het beschrijven van de stroming over het oppervlak van kleine veldjes of "microcatchments". Het geeft inzicht in het optreden van deze stroming op verschillende doorlatende oppervlakken. Een verdere verfijning lijkt mogelijk en ook wenselijk, evenals een koppeling met een model voor het transport van sediment.

Hoewel de invloed van de morfologie van het terrein op de stroming sterk kan worden gewijzigd door de eigenschappen van de bodem - zoals doorlatendheid, ruwheid en bedekking met vegetatie - en door variatie in effectieve neerslag, kan zij toch niet worden verwaarloosd. Hoofdstuk 6 geeft daarom beschouwingen over de invloed van de vorm van de hellingen op het stromingsproces. De uitwerking daarvan is gegeven in de vorm van een aantal voorbeelden.

De belangrijkste morfologische factoren zijn: de gradiënt, de lengte en de vorm van de helling en de expositie ten opzichte van de heersende regen-brengende wind. Gradiënt en helling worden algemeen beschouwd als belangrijkste faktoren.De vorm van de helling blijkt invloed te hebben op de snelheid, waarmede de afvoer reageert op de neerslag ("time to peak") en op de vorm van de rijzende tak van het afvoer-hydrogram. De expositie van de helling is van belang als er tijdens neerslag sprake is van een sterk overheersende windrichting.

Deze wind-invloed is zelden opgenomen in beschouwingen over afstroming en erosie. In de Secties 7.1 en 7.2 zijn de gevolgen van nietloodrecht vallende neerslag en van door de wind op het stromende water uitgeoefende schuifspanningen nader onderzocht. Deze verschijnselen zijn nagegaan in een windtunnel waarvan de helling kon worden veranderd. Helling-opwaarts gerichte winden over een ondoorlatend oppervlak bleken het begin van de afstroming te vertragen en de waterdiepte te vergroten. In sommige proeven werd zelfs opwaarts gerichte stroming waargenomen.

Windsterkte en windrichting bepalen beide de effectieve neerslag en de stroming over het oppervlak. De stroming wordt daarbij beïnvloed door vorm, grootte, invalshoek en valsnelheid van de regendruppels, door de wijze van spatten en door de schuifspanning uitgeoefend op het grensvlak tussen lucht en water. Bij sterke regenval was de invloed van de schuifspanning gering ten opzichte van het effect van de schuin invallende regendruppels. Anderzijds kan de invloed van de schuifspanning belangrijk zijn als het oppervlak geheel wordt bedekt door een dunne waterlaag en de regen een geringe kinetische energie bezit (door een lage intensiteit of, zoals in de beschreven experimenten, door een geringe valhoogte).

Het fysisch-mathematisch model WROF ("Wind, Rain and Overland Flow"), beschreven en getoetst in Secties 7.1 en 7.2 is een vereenvoudigd model, maar is waarschijnlijk nauwkeurig genoeg voor praktische toepassing.

Meer onderzoek is gewenst naar de uitwerking van krachten, uitgeoefend door wind en regen op oppervlakkig afstromend water en over het voorkomen van windsnelheden en windrichtingen tijdens regen in gebieden die gevoelig zijn voor erosie door stromend water. Ook hier zou koppeling met een model voor het transport van sedimenten meer inzicht kunnen verschaffen.

Schuin invallende regen leidt tot fouten in de bepaling van de effectieve neerslag in sterk geaccidenteerde gebieden. Dit kan leiden tot onnauwkeurigheden in studies over watererosie, over het voorkomen van piekafvoeren, over de mogelijkheden tot verbouw van bepaalde gewassen e.d. Sectie 7.3 beschrijft een nomogram waarmede een correctiefaktor voor de gemeten regenval (C_{gau}) kan worden bepaald. De effectieve neerslag P_{act} op het hellende oppervlak kan worden gevonden door de gemeten neerslag (P_{gau}) met deze faktor te vermeningvuldigen ($P_{act}=C_{gau}\ P_{gau}$). De correctiefaktor is een functie van windsnelheid en richting, van het type regenval en van de helling en de oriëntatie van het oppervlak. De lokale topografie kan echter een storende invloed uitoefenen, die niet in het nomogram tot uiting komt.

Sectie 7.4 legt de nadruk op de anisotropie van het uiteenspatten van op een hellend oppervlak vallende neerslag tijdens sterke wind. Helling, windsnelheid enrichting en stroomsnelheid van het water blijken tot deze anisotropie bij te dragen. Met behulp van stroboskopie ("time-lapse photography") kon de anisotropie van de spatkraag worden vastgelegd. Daarbij werd slechts één druppelgrootte (equivalente diameter 3,5 mm) gebruikt. De proeven tonen aan dat in een model voor het spatten van regen niet kan worden voorbijgaan aan de invloeden van de wind en de afstroming op dit verschijnsel. Een verder onderzoek met betere methoden (snelle cinematografie) lijkt noodzakelijk voor het kwantificeren van deze invloeden.

De schrijver hoopt dat dit werkstuk zal bijdragen tot een beter begrip van de afstroming over een landoppervlak onder veld omstandigheden.

NOTATION

In this thesis specific list of symbols are presented per Chapter or symbols are defined in the body of the text. Although most symbols were used in a homogeneous way, attention should be paid to the following symbols and their meanings:

C_{gau} is called a rain-gauge efficiency coefficient in Section 7.1. However this term was considered somehow misleading and C_{gau} was renamed in Section 7.3 to rain-gauge correction factor.

P_{ef} is the effective rainfall in Section 7.1 and P_{act} is the actual rainfall flux in Section 7.3. Both P_{ef} and P_{act} have the same meaning.

P_{act} is the effective rainfall in Section 7.3 and P_{ef} is the actual rainfall flux in Section 7.1. Both P_{ef} and P_{act} have the same meaning.

α is a hydraulic coefficient (of the kinematic wave approximation) in Section 2.4 and Chapters 4 and 5, and the angle of the surface with the horizontal in Chapter 7 (Sections 7.1 to 7.4). β is used instead of α as a hydraulic coefficient in Section 7.1.

β is a hydraulic coefficient (of the kinematic wave approximation) in Section 7.1. α was used instead of β in Section 2.4 and Chapters 4 and 5.

θ is the volumetric soil water content in Chapter 5 and the angle of the rain vector with the vertical in Chapters 6 and 7.

AUTHOR INDEX

APPENDIX A

DERIVATION OF SOME EQUATIONS PRESENTED IN SECTION 7.1

The derivation of some equations presented in Section 7.1 are made in this Appendix for purpose of clarity. The reader is referred to that section, for the meaning of symbols and their units.

Rainfall is assumed to be represented by a vector $\mathbf{r}$ (contained in plane 1, Fig. 1 of Section 7.1) making an angle θ with the vertical and having an azimuth ω. The projection of rainfall vector $\mathbf{r}$ in plane 2 is expressed by:

$$\mathbf{r}_{pl2} = r \sin\theta \cos(\omega-\Omega)\, \mathbf{i} + r \cos\theta\, \mathbf{j} \qquad (A1)$$

where $\mathbf{i}$ and $\mathbf{j}$ are the unit vectors along the horizontal and vertical axis (positive downwards), respectively, in plane 2.

The length of the projection of $\mathbf{r}_{pl2}$ on the perpendicular to the surface (a plane), giving the actual rainfall flux at the surface, P_{ef} (eq. 4 of Section 7.1), is:

$$P_{ef} = r \cos\theta \cos\alpha + r \sin\theta \sin\alpha \cos(\omega-\Omega) \qquad (A2)$$

replacing $\cos(\omega-\Omega)$ by $(\cos\omega \cos\Omega + \sin\omega \sin\Omega)$ and substituting eq. 3 of Section 7.1 ($P_{gau} = r \cos\theta$) in eq. A2 we obtain:

$$P_{ef} = P_{gau} [\cos\alpha + \tan\theta \sin\alpha (\cos\omega \cos\Omega + \sin\omega \sin\Omega)] \qquad (A3=4)$$

The angle that $\mathbf{r}_{pl2}$ makes with the vertical will be:

$$\theta' = \arctan [\tan\theta \cos(\omega-\Omega)] \qquad (A4=9)$$

Rewriting $\mathbf{F_1}$ and $\mathbf{F_2}$ using the unit vectors we obtain:

$$\mathbf{F_1} = F_1\ \mathbf{j} \tag{A5}$$

$$\mathbf{F_2} = F_2 \sin\theta'\ \mathbf{i} + F_2 \cos\theta'\ \mathbf{j} \tag{A6}$$

The sum of the vectors $\mathbf{F_1}$ and $\mathbf{F_2}$ is:

$$\mathbf{F} = F_2 \sin\theta'\ \mathbf{i} + (F_1 + F_2 \cos\theta')\ \mathbf{j} \tag{A7}$$

Thus, the length of vector **F** is:

$$F = (F_1^2 + F_2^2 + 2\ F_1\ F_2 \cos\theta')^{1/2} \tag{A8=10}$$

The angle that **F** makes with the vertical is:

$$\phi = \arcsin (F_2 \sin\theta'/F) \tag{A9=8}$$

F' and ϕ' (equations 18 and 19 in Section 7.2, respectively) can be easilly derived in the same way.

The impulse-momentum principle is used to derive eq. 13:

$$F_2\ \Delta t = (n\ M)\ V^* \tag{A10}$$

where n is the number of raindrops impinging at the time interval Δt on a section Δx of the plane surface, and M is the mass of a raindrop.

The intensity of the impinging raindrops is defined by:

$$P_{ef} = (n\ M)/(\rho\ \Delta t\ \Delta x) \tag{A11}$$

Substituting (A11) in (A10) and considering a as the fraction of F_2 transmitted to the flowing water sheet, we obtain eq. 12 (of Section 7.1):

$$F_2 = \Delta x\ \rho\ P_{ef}\ V^* a \tag{A12=12}$$

APPENDIX B

ADDITIONAL INFORMATION ON THE MODEL WROF

B.1 Basic assumptions

The set of assumptions needed to obtain model WROF is summarized below. Because the derivation of the equations of the model began with the kinematic wave equations, basic assumptions were automatically and tacitly included: for example, the fluid is continuous, incompressible and Newtonian, and hydrostatic pressure distribution in each section is assumed. Also discharge can be expressed as a unique function of the depth of flow. More specific assumptions are as follows:

(1) Surface is a plane forming an angle α with the horizontal.

(2) The width of the slope is infinite and the transverse water surface profile at any x is horizontal.

(3) Unidirectional overland flow process, along the steepest slope of the plane of best fit. The direction of the flow may be or up or down the slope, along the entire length of the slope. This is not true in the case of strong lateral wind (relativelly to the steepest slope of the plane).

(4) "Instantaneous" complete coverage of the ground surface not covered by mounds, by the water sheet.

(5) The friction factor is considered independent of water depth, water velocity, time and space. The Darcy-Weisbach friction coefficient (f) was used to compute the friction slope. Flow can also be considered to begin as laminar flow with a transition to turbulent flow if a transitional Reynolds number (Re) is reached. However, the general shape of the f-Re relationship on an irregular surface is much more complex than on a plane surface (Roels, 1984; Abrahams et al., 1986; and Rauws, 1988). It should also be apparent that raindrop impact will affect the flow characteristics (see Fig. B1).

(6) Considering a constant, time independent, non wave-forming wind velocity profile. This was the case of the laboratory experiment described in Sections 7.1 and 7.2. In reality wind is strongly variable, both in intensity and direction.

(7) Neglection of adhesive and cohesive forces responsable for binding of water in the water-air-surface boundary. This is specially important in the first phase of the overland flow process and for very mild slopes (see Chapter 3 of this thesis).

(8) The inclination of drop trajectories is constant in time (within time intervals), in space, and over the drop spectrum, i.e. rainfall may be represented by a vector.

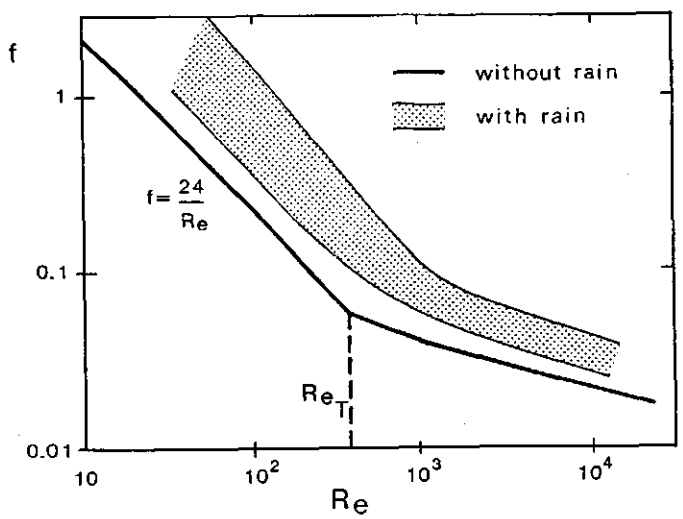

Fig. B1 Typical flow resistance diagram for overland flow on plane surfaces. Modified from Radojković & Maksimović (1987)

B.2 Model inputs and outputs

The model WROF consists of a main program (Fortran 77) and two subroutines. The main program reads the data, and performs a major part of the algorithm. The subroutines solve the Lax-Wendroff scheme and print part of the results.

The input data required to run the program WROF.FOR are:

surface data:

S = steepest slope of the plane of best fit (-)
L = length of the field (m)
W = width of the field (m)
A = area covered by mounds (%)
f = Darcy-Weisbach friction factor (-)
m = parameter for the type of flow (-)
Ω = azimuth of the slope (rad)

rainfall data:

ω = azimuth of the rainfall (rad)
θ = angle of incidence of the rainfall (rad). Only necessary when FLAG3 is 0
V* = terminal vertical velocity of raindrops (m/s)
FLAG1 = type of rainfall data, to be specified with a code: 0 if rainfall data is $P_{eff}(t)$; 1 if rainfall data is $P_{gau}(t)$; and 2 if rainfall data is r(t)
p(1) = rainfall data from time 0 to time t(1) (m/s)
t(1) = end of time interval of p(1) (s)
p(2) = rainfall data from time t(1) to time t(2) (m/s)
t(2) = end of time interval of p(2) (s)
.
.
p(j) = rainfall data from time t(j-1) to time t(j) (m/s)
t(j) = end of time interval of p(j) (s)

splash data:

FLAG2 = code for splash effect: 0 if no splash is to be considered; and 1 if splash effect is to be considered
β* = average angle of elevation of initial velocity of droplets after drop impact (rad)
E = ratio between the splashing mass and the original mass of a rain drop, over n drops (-)
δ = average maximum height of the flight trajectory of the droplets (m)

wind data:

FLAG3 = code for wind shear stress effect: 0 if no wind shear stress is to be considered; and 1 if wind shear stress is to be considered (-)
z_o = hydrodynamic roughness length of the overland flow sheet (m)
V_{10} = average wind speed at 10 m height (m/s)

other data:

i = average (in space and time) infiltration rate (m/s). The program may be adapted for time dependent infiltration rate.
TM = total simulation time (s)
Δt = time increment (s)
Δx = space increment in the x direction (m)
File names

Time and space increments (Δt and Δx) and data file names are asked via the monitor. The remainder of the input data required to run the program are read from a data file.

The program creates two output data files: the first one contains water depth and flow velocity in time (at chosen intervals) and in space (at grid points), and the second one contains the hydrographs of overland flow at the origin (when existing, caused by upslope wind) and at the lower end of the plane.

REFERENCES

Abrahams, A.D., A.J. Parsons and S.H. Luk, 1986. Resistance to overland flow on desert hillslopes. Journal of Hydrology, 88: 343-363.

Radojković, M. and C. Maksimović, 1987. On standardization of computational models for overland flow. IAHS XXII Congress, Fourth International Conference on Urban Storm Drainage, Lausanne, 100-105.

Rauws, O., 1988. Laboratory experiments on resistance to overland flow due to composite roughness, Journal of Hydrology, 103: 37-52.

Roels, J.M., 1984. Flow resistance in concentrated overland flow on rough surfaces. Earth Surf. Process. and Landforms, 9: 541-551.

APPENDIX C

THE EROSION EXPERIMENTAL STATION OF "VALE FORMOSO"

C.1 INTRODUCTION

The erosion experimental station of "Vale Formoso" (Alentejo, Portugal) referred to in Chapter 6 and Section 7.1 is described here.

The erosion research programme related to the experimental station of Vale Formoso was established in 1960 by the "Direcção Geral de Hidráulica e Engenharia Agrícola (DGHEA)" of Portugal. One of the aims is (1) to verify the Universal Soil Loss Equation (USLE) under local conditions, (2) to obtain appropriate values for the factors, and (3) to use the results to design effective conservation techniques in Alentejo.

C.2 LOCATION AND GENERAL DESCRIPTION

The experimental station is situated in the southern part of the Alentejo Region of Portugal, approximately 37° 45' 30'' N and 1° 34' 40'' E (Fig. C1), with mean annual rainfall and mean annual potential evaporation of around 500 mm and 1600 mm, respectively. The surrounding area has been strongly influenced by the proximity of the Guadiana river, and is very dissected, with rather steep slopes and shallow, stony, red soils derived from schists, mainly quartzitic schists (Vx in the portuguese soil classification system - Cardoso, 1965). According to the FAO-Soil map, the area belongs to the I-L 2/3 bc mapping unit corresponding to Lithosols-Luvisols (Lima & Lima, 1988).

The natural vegetation in that region was sparse oak forest and scrub which was largely cleared for cereal production in the nineteen-twenties and thirties. In the Alentejo Region approximately 400 000 ha are planted with winter cereals each year. The traditional, and still by far the most widely-spread, crop rotation is wheat-fallow.

Local practice is to plough deeply in spring, maintain a bare fallow throughout the summer, when no rain falls, and plant in autumn when the wet period begins. This land is therefore unprotected during much of the period October-February when nearly 70% of the average

rainfall is received. This method of soil preparation greatly increases the storage capacity of the cultivated horizon, that overlies a very compact subsoil, with poor permeability (hard rock or plough-pan). When the first winter rains fall no overland flow is generated, and therefore no soil loss occurs until the available storage capacity of the cultivated horizon is filled up. If the initial rainstorms are very heavy and fall on sloping lands, the whole upper layer of soil may be washed off (Ferreira, 1984).

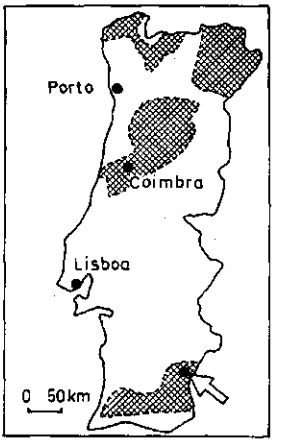

Fig. C1 Location of the experimental station in Portugal (arrow and dot), with areas most liable to water erosion (adapted from Cunha et al., 1980)

C.3 EQUIPMENT

There are 15 standard runoff plots of 20 x 8.33 m^2, or one sixtieth of a hectare, and a half plot of 20 x 4 m^2. The longitudinal slopes vary between 9.9% and 19.9%. The plots are arranged so that their orientation or exposure varies between roughly East and South South West.

Twenty-two crop covers are studied in the different plots of the experimental station, including bare fallow, cereals, stubbles, and pasture crops (Ferreira et al, 1984).

At the lower end of each plot a concrete gutter diverts runoff into a series of three galvanised collecting tanks (1.3x0.7x0.6, 0.8x0.8x0.8 and 0.8x0.8x0.8 m^3). The first two of these tanks are fitted with dividers to allow only an eleventh part of their overflow to pass into the next tank in line. The tanks are equipped with filters, and the first tank has an arrangement to allow the liquid to run off after sampling, so that deposited solid matter can be sampled separately. Photo C1 gives a view of the runoff plots with the tanks.

Photo C1 View of the runoff plots and tanks.

Most of the following data and information are available from 1961/62:

- recording raingauge charts,
- daily rainfall from horizontal and inclined raingauges,
- evaporation from an evaporation pan, a covered evaporation pan, and a Piche evaporimeter,
- wind speed and wind direction,
- amount of runoff and amount of soil loss for each storm or group of storms,
- crop cover,

- notes, varying in detail, on crop and soil conditions, weed infestation, etc., made each time the tanks were emptied,
- type and time of cultivation.

REFERENCES

Cardoso, J.V.J. de C., 1965. Os solos de Portugal, sua classificação, caracterização e génese: 1- A sul do Rio Tejo. Secretaria de Estado da Agricultura - Direcção Geral dos Serviços Agrícolas, Lisboa (in Portuguese).

Cunha, L.V. da, A.S. Gonçalves, V.A. de Figueiredo, and M. Lino, 1980. A gestão da água - princípios fundamentais e sua aplicação em Portugal. Fundação Calouste Gulbenkian, Lisboa (in Portuguese).

Ferreira, I.M.M., A.J.R. Ferreira and D.A. Sims, 1984. Preliminary analysis of runoff plot data from the Vale Formoso research station, for the years 1962/63-1979/80, in terms of the Universal Soil Loss Equation. Drainage and Soil Conservation Project for the Alentejo Region, Direcção Geral de Hidráulica e Engenharia Agrícola, Lisbon.

Ferreira, I.M.M., A.J.R. Ferreira and D.A. Sims, 1985. USLE adapted for use in Portugal. Land and Water (FAO), April 1985, No. 22, 21-24.

Lima, M.I.L.P.P de and J.L.M.P. de Lima, 1988. Report on a visit to Alentejo (Portugal): erosion experimental station of "Vale Formoso". Department of Land and Water Use, Agricultural University Wageningen, Report no. 122.

ACKNOWLEDGEMENT

The author wishes to acknowledge all the help given by Eng. I.M.M. Ferreira and Eng. A.J.R. Ferreira from the "Projecto de Drenagem e Conservação do Solo do Alentejo" (Direcção Geral de Hidráulica e Engenharia Agrícola - DGHEA), in Évora, during his visit to the experimental station of "Vale Formoso".